SÃO PAULO STATE UNIVERSITY – UNESP
JABOTICABAL CAMPUS

ATMOSPHERIC CONCENTRATIONS OF GREENHOUSE GASES IN WILDFIRES AT THE AMAZON BIOME WITH GOSAT

Luciano de Souza Maria
Forest Engineer

2023

SÃO PAULO STATE UNIVERSITY – UNESP

JABOTICABAL CAMPUS

ATMOSPHERIC CONCENTRATIONS OF GREENHOUSE GASES IN WILDFIRES AT THE AMAZON BIOME WITH GOSAT

Luciano de Souza Maria

Advisor: Prof. Dr. Newton La Scala Júnior

Co-advisor: Carlos Antonio da Silva Junior

Thesis presented to the School of Agricultural and Veterinarian Sciences –Unesp, Jaboticabal Campus, as partial fulfillment of the requirements for the degree of Doctor in Science in Agronomy (Plant Production).

2023

M332a

Maria, Luciano de Souza
Atmospheric concentrations of greenhouse gases in wildfires at the amazon biome with GOSAT / Luciano de Souza Maria. -- Jaboticabal, 2023
105 p.

Tese (doutorado) - Universidade Estadual Paulista (Unesp), Faculdade de Ciências Agrárias e Veterinárias, Jaboticabal
Orientadora: Newton La Scala Junior
Coorientadora: Carlos Antonio da Silva Junior

1. Climate change. 2. Fire foci number. 3. Atmospheric concentrations of gases. 4. Remote sensing. 5. Arc of Deforestation. I. Título.

Sistema de geração automática de fichas catalográficas da Unesp. Biblioteca da Faculdade de Ciências Agrárias e Veterinárias, Jaboticabal. Dados fornecidos pelo autor(a).

Essa ficha não pode ser modificada.

UNIVERSIDADE ESTADUAL PAULISTA

Câmpus de Jaboticabal

CERTIFICADO DE APROVAÇÃO

TÍTULO DA TESE: ATMOSPHERIC CONCENTRATIONS OF GREENHOUSE GASES IN WILDFIRES AT THE AMAZON BIOME WITH GOSAT

AUTOR: LUCIANO DE SOUZA MARIA
ORIENTADOR: NEWTON LA SCALA JUNIOR
COORIENTADOR: CARLOS ANTONIO DA SILVA JUNIOR

Aprovado como parte das exigências para obtenção do Título de Doutor em Agronomia (Produção Vegetal), área: Agronomia (Ciência do Solo) pela Comissão Examinadora:

Prof. Dr. NEWTON LA SCALA JUNIOR (Participaçao Virtual)
Departamento de Engenharia e Ciencias Exatas DECEx / FCAV UNESP Jaboticabal

Prof. Dr. RAFAEL COLL DELGADO (Participaçao Virtual)
Departamento de Ciência do Solo-UFRRJ / Seropédica/RJ

gov.br Documento assinado digitalmente
RAFAEL COLL DELGADO
Data: 08/03/2023 10:09:52-0300
Verifique em https://verificador.iti.br

Prof. Dr. ZIGOMAR MENEZES DE SOUZA (Participaçao Virtual)
Faculdade de Engenharia Agrícola / Universidade Estadual de Campinas - UNICAMP

gov.br Documento assinado digitalmente
EDUARDO BARRETTO DE FIGUEIRI
Data: 08/03/2023 09:07:39-0300
Verifique em https://verificador.iti.br

Prof. Dr. EDUARDO BARRETTO DE FIGUEIREDO (Participaçao Virtual)
Departamento de Desenvolvimento Rural / Universidade Federal de São Carlos UFSCAR - São Carlos/SP

Prof. Dr. MARCÍLIO VIEIRA MARTINS FILHO (Participaçao Virtual)
Departamento de Ciências da Produção Agrícola / FCAV UNESP Jaboticabal

Jaboticabal, 16 de fevereiro de 2023

gov.br Documento assinado digitalmente
ZIGOMAR MENEZES DE SOUZA
Data: 08/03/2023 11:17:08-0300
Verifique em https://verificador.iti.br

INFORMATION ABOUT THE AUTHOR

LUCIANO DE SOUZA MARIA – Son of Luiz de Souza Maria and Ana Prata de Abreu Maria, born in Jaboticabal, São Paulo state, on January 3, 1978. In August 2009 he joined the undergraduate course in Forest Engineering at Mato Grosso State University (UNEMAT), in Alta Floresta with completion in February 2015. In March 2016, he joined the master's degree program 'Biodiversity and Amazon Agroecosystems', at Mato Grosso State University (UNEMAT), Alta Floresta Campus, with a scholarship from Foundation for Research Support of the State of Mato Grosso, with completion in October 2018. Since January 2017, he has been part of the Laboratory of Soils and Leaf Analysis - LASAF at Unemat, Alta Floresta. In March 2020, he entered the PhD program in Agronomy (Plant Production) at the São Paulo State University (Unesp), Jaboticabal. In his PhD, he developed the project "Estimation of CO_2 emissions from forest fires in the main Brazilian biomes with OCO-2 satellite" financed with a scholarship by Coordenação de Aperfeiçoamento de Pessoal de Nível Superior - Brasil (CAPES; CAPES – 2020).

“Each season of life is an edition, which corrects the one before and which will also be corrected itself until the definitive edition, (…)” Machado de Assis, Memórias Póstumas de Brás Cubas. São Paulo: Ateliê Editorial, 2001, p.120.

DEDICATION

To my wife ***Maria Inês Lidoino de Souza*** *and daughter* ***Rayssa Camila Lidoino Maria****, for their great affection, understanding, encouragement, and support in this journey. To all my friends for the shared moments.*

ACKNOWLEDGMENTS

First, my wife and daughter, Inês and Rayssa, for the unconditional support and for not giving up on my goals, thank you very much for your dedication and for all the love.

For my mother Ana Prata, who taught me to never give up the fight for knowledge and with her unconditional love inspired me to be a better person.

To my siblings Anésio, Adriano, Andréia, Cristiane, Rodrigo, and Angelo who always inspire me to seek the light of learning in an honest and dignified way, thank you for all the strength.

My advisor, Newton La Scala Júnior, I thank for the friendship and for being largely responsible for structuring and solidifying knowledge, and for all his patience and support in completing this new stage of my life.

To my co-advisor, Carlos Antonio da Silva Junior, for the technical knowledge and support in granting the GAAF infrastructure.

To Professor Alan Rodrigo Panosso, for the dedication and support in the statistical analysis, in addition to the personal teachings and passion for teaching in a humane and very fair way, my immense gratitude.

To my friend Fernando Rossi, always very present and supportive in the most difficult moments, thank you for your friendship.

To my friends Marcelo Odorizzi, Luis da Costa, Adriano Maltezo, and Thiago among so many others who contributed in being on the same journey and same purpose as me, thank you very much.

To Professor Paulo Alexandre, for having granted a teaching internship in his discipline and for the teachings on didactics and tips on how to improve the art of teaching.

The employee Adriana from the Exact Sciences department, for her attention and support, even remotely, thank you very much.

Finally, I would like to thank the São Paulo State University (Unesp), School of Agricultural and Veterinarian Sciences, Jaboticabal Campus, an institution made up of great people who helped me with professional and personal training.

This study was financed in part by the Coordenação de Aperfeiçoamento de Pessoal de Nível Superior - Brasil (CAPES) - Finance Code 001.

Summary

Page

ATMOSPHERIC CONCENTRATIONS OF GREENHOUSE GASES CORRELATED WITH WILDFIRES IN THE AMAZON BIOME WITH GOSAT

ABSTRACT - Understanding the spatio-temporal distribution of greenhouse gases (GHG) in the Amazon biome, as well as the occurrences of fire foci is relevant in the climate change scenario. Therefore, the main objective of the study was to evaluate increase or decrease in atmospheric concentrations of gases (CO_2, CH_4, and CO), as well as the spatio-temporal distribution and possible correlations between gases and fires and other orbital data from the Earth's surface in the time series from 2009 to 2019 for the Amazon biome. For this, we used data from the concentrations in the column-averaged of CO_2 (XCO_2), CH_4 (XCH_4) and carbon monoxide (XCO) based on OCO-2, GOSAT and MERRA satellites. Furthermore, we used the observations of the chlorophyll fluorescence induced by the sun (SIF) by the GOSAT satellite to understand the photosynthetic capacity of the vegetation, in addition to Moderate Resolution Imaging Spectroradiometer (MODIS) products, for example: Enhanced Vegetation Index (EVI), Fire Radiative Power (FRP) and fire foci number. For rainfall information, we used by the Climate Hazards Group Infrared Precipitation with Stations (CHIRPS) and the soil moisture (SM), was obtained by the Soil Moisture Active Passive (SMAP) satellite. Through th trend analysis by the Mann Kendall test, we can observe a monotonic growth trend of XCO, XCO_2 and FRP at the end of the rainy period, as well as the temporal concentrations of gases and other orbital products, in addition to their strong correlation with changes in land use and extreme weather events between 2015 and 2020, for the Amazon biome. With the geostatistical interpolation techniques and methods, it is possible to better understand the spatio-temporal concentrations of CH_4 and its correlation with fire foci number, as well as its strong correlation with soil moisture, especially in the dry period in the Amazon region in the time series (2009-2019). Therefore, gases (CO_2, CH_4 and CO) and their correlations with fire foci number and with biophysical variables can be very important to guide new directions on the effect of anthropic actions and climatic change in the Amazon ecosystem.

Keywords: Climate Change; Forest Degradation; Savanization; Severe Droughts

CONCENTRAÇÕES ATMOSFÉRICAS DE GASES DE EFEITO ESTUFA CORRELACIONADAS COM INCÊNDIOS FLORESTAIS NO BIOMA AMAZÔNIA COM GOSAT

RESUMO – Compreender a distribuição espaço-temporal dos gases de efeito estufa (GEE) no bioma Amazônia, bem como as ocorrências de focos de incêndio são relevantes no cenário de mudanças climáticas. Portanto, o principal objetivo do estudo foi avaliar o aumento ou diminuição das concentrações atmosféricas de gases (CO_2, CH_4 e CO), bem como a distribuição espaço-temporal e possíveis correlações entre gases e incêndios e outros dados orbitais da Terra superfície na série temporal de 2009 a 2019 para o bioma Amazônia. Para isso, utilizamos os dados das concentrações na coluna média de CO_2 (XCO_2), CH_4 (XCH_4) e monóxido de carbono (XCO) com base nos satélites OCO-2, GOSAT e MERRA. Além disso, utilizamos as observações da fluorescência da clorofila induzida pelo sol (SIF) pelo satélite GOSAT para entender a capacidade fotossintética da vegetação, além de produtos Moderate Resolution Imaging Spectroradiometer (MODIS), por exemplo: índice de vegetação aprimorado (EVI), Potência radiativa do fogo (FRP) e número de focos de incêndio. Para as informações pluviométricas, utilizamos o Climate Hazards Group Infrared Precipitation with Stations (CHIRPS) e a umidade do solo (SM), obtida pelo satélite Soil Moisture Active Passive (SMAP). Pela análise de tendência pelo teste de Mann Kendall, podemos observar uma tendência monotônica de crescimento de XCO, XCO_2 e FRP ao final do período chuvoso, assim como as concentrações temporais de gases e outros produtos orbitais, além de sua forte correlação com mudanças no uso da terra e eventos climáticos extremos entre 2015 e 2020, para o bioma Amazônia. Com as técnicas e métodos de interpolação geoestatística, pode-se entender melhor as concentrações espaço-temporais de CH_4 e sua correlação com o número de focos de incêndio, bem como sua forte correlação com a umidade do solo, principalmente no período seco na região amazônica no período série (2009-2019). Portanto, os gases (CO_2, CH_4 e CO) e suas correlações com o número de focos de incêndio e com variáveis biofísicas podem ser muito importantes para orientar novos rumos sobre o efeito das ações antrópicas e mudanças climáticas no ecossistema amazônico.

Palavras-chave: Mudanças Climáticas; Degradação Florestal; Savanização; Secas Severas

CHAPTER 1 – WILDFIRE AND GREENHOUSE GAS CONCENTRATION IN THE AMAZON BIOME

1. Introduction

The occurrence of wildfires increased in several regions of the world, justified by the increase in global temperatures and the extension of drought periods, therefore, highlighting the consequences of climate change (Duane; Castellnou; Brotons, 2021). In addition, in several regions of the world, the inappropriate practice of using fire impacts and affects the regions between deforested and protected forest areas (Pivello et al., 2021). Thus, wildfires lead to economic losses (Campanharo et al., 2019), cause respiratory health problems (Campanharo et al., 2022; Schroeder et al., 2022; Smith et al., 2014), and increase emissions of carbon dioxide (CO_2), methane (CH_4), nitrous oxide (N_2O), and carbon monoxide (CO) (Brando et al., 2020b; Miettinen et al., 2016).

The Amazon is the Brazilian biome with the highest greenhouse gas (GHG) emissions from deforestation or forest degradation, with the land use change sector being the main source of GHG emissions in Brazil, with 1.09 Gt of CO_2 emission in 2021 (SEEG, 2022). This fact does not make the climate agreements signed by Brazil, such as the 26th United Nations Conference on Climate Change (COP 26), for example, unfeasible, but rather more difficult to meet (Da Silva Junior et al., 2022),. Thus, reducing deforestation and GHG emissions is a major challenge for Brazilian society (Deutsch; Fletcher, 2022).

The Amazon biome is highly representative and is considered to contain the largest continuous tropical forest on Earth (Heinrich et al., 2021). It has an immense biodiversity of plants and animals (Antonelli et al., 2018) and the largest carbon pool in the biosphere (Hubau et al., 2020). Therefore, understanding the dynamics of the concentration of GHG such as CO_2, CH_4, N_2O, and CO in the Amazon biome, as well as its correlation with the fire foci number, becomes very relevant in the current scenario due to the notoriety of the theme.

In the same way, it is noted that the high amounts of plumes from the burning of the Amazon rainforest (Yuan et al., 2022) result in high concentrations of aerosol particles and can impact regional and global rainfall regimes (Tosca; Randerson; Zender, 2013). Through this approach, fires in the Amazon in 2019 impacted the region and there was the aerosol radiative forcing equivalent to +26 W m^{-2}, with an increase

of 30% compared to 2018 (Yuan et al., 2022). On the other hand, the indirect effects are changes in the properties and life cycle of clouds, justified by the correlation between the aerosols and the formation of cloud condensation nuclei (Rosenfeld et al., 2014). As aerosols act as condensation nuclei (CCN), there is a direct effect in the alteration of the physics and formation of clouds, and consequently, an alteration in the precipitation patterns in the Amazon region (Artaxo et al., 2022; Machado et al., 2018).

Thus, regional climate projections in southern Amazon have a strong increase in fire foci use activities and have the potential to reach 6.0 Pg CO_2 emissions from forest fires in the 2050s, three times higher when compared to emissions in the 2000s (2.0 Pg CO_2) (Brando et al., 2020b). In this way, the transformation of the Amazon forest into a net source of carbon reduces its capacity as a carbon sink due to changes in temperature and reductions in rainfall regimes (Brando et al., 2020b; Gatti et al., 2014). This forest transition is exacerbated by the climate and releases high amounts of GHGs into the atmosphere, accentuating the Global Warming (GW) effect (Nobre et al., 2016).

That is why several studies indicate that change in land use and occupation is mainly associated with increasing rates of deforestation and the correlation with increased GHG emissions resulting from fires foci number (Amaral et al., 2019; Gatti et al., 2021; Lima et al., 2022; Silva et al., 2021; Touma et al., 2021). However, understanding the temporality and spatialization of these gases to the occurrence of fires, as well as their relationships with terrestrial biophysical variables (temperature, soil moisture, and precipitation) is limited due to the lack of measurements of concentrations across the entire Amazon region.

Within this context, in the last two decades, the launch of several satellites, such as Greenhouse gas Observing SATellite (GOSAT), satellite of the Japanese Space Agency (JAXA) (Kuze et al., 2009), Orbiting Carbon Observatory-2 mission (OCO-2) of the National Aeronautics and Space Administration (NASA) (Crisp et al., 2012; Frankenberg et al., 2015; O'Dell et al., 2012), and the Sentinel-5 satellite, of the European Space Agency (ESA) (Veefkind et al., 2012), among others, made it possible to monitor the atmospheric concentration of GHGs. The sensors used in these satellites characterize the average mole fraction of dry air in the XCO_2, XCH_4, and XCO columns, contributing to studies that seek to understand the sources and identify the drains of GHGs, such as wildfires (Guo et al., 2019, 2017; Li; Wang; Yung, 2019;

Mousavi; Falahatkar; Farajzadeh, 2017).

Thus, the hypothesis tested raised by the study is that there is a correlation between the atmospheric concentration of CO_2, CH_4, and CO with wildfires in the dry season to be observed via remote sensing with the GOSAT, MERRA and OCO-2 satellites, in the Amazon biome, with fire foci number being the main reason.

Therefore, the objective was to verify what the spatio-temporal trends of atmospheric concentrations of gases (CO_2, CH_4, and CO) and possible correlation with fire foci number and data of the biophysical variables (rainfall, temperature, moisture soil) and correlation the photosynthetic capacity of the vegetation (EVI and SIF) in the time series from 2009 to 2019 for the Amazon biome.

1.2 Literature review

1.2.1. The Amazon Forest

The Amazon Biome (Figure 1.1) extends over 4.2 million km² (MapBiomas, 2022), corresponding to 49.29% of the Brazilian territory, encompassing the states of the North Region (Acre, Amapá, Amazonas, Pará, Rondônia, and Roraima), the Center-West Region (Mato Grosso and small Northern part of Tocantins) and the Northwest part of the state of Maranhão. The composition of the biome is classified as a tropical rainforest, with emphasis on the dense ombrophilous forests (IBGE, 2020). In addition, it currently has more than 2,500 native forest species and a third of the world's tropical wood (Da Silva Junior et al., 2020), making it possible to find 300 different forest species in just one hectare (Coutinho, 2016). This highlights the importance of the region due to its high biodiversity, considered one of the highest on the planet (Amaral et al., 2019).

There are several direct and indirect Amazonian ecosystem services provided by nature to society (Ramos et al., 2020), including the storage of biodiversity (Fearnside, 1997), regulation and maintenance of the hydrological cycle (Brando et al., 2019) and GHG mitigation (Strand et al., 2018), among others. That is the reason conservation of the standing forest becomes so valuable when contrasted with the suppression of vegetation, especially if we compare its direct and indirect benefits to society (Nobre et al., 2016). In this scenario, the valorization of ecosystem services still

makes it possible to guide mechanisms for the implementation of forest conservation, such as payments for ecosystem services, in order to protect its rich Amazonian biodiversity (Strand et al., 2018).

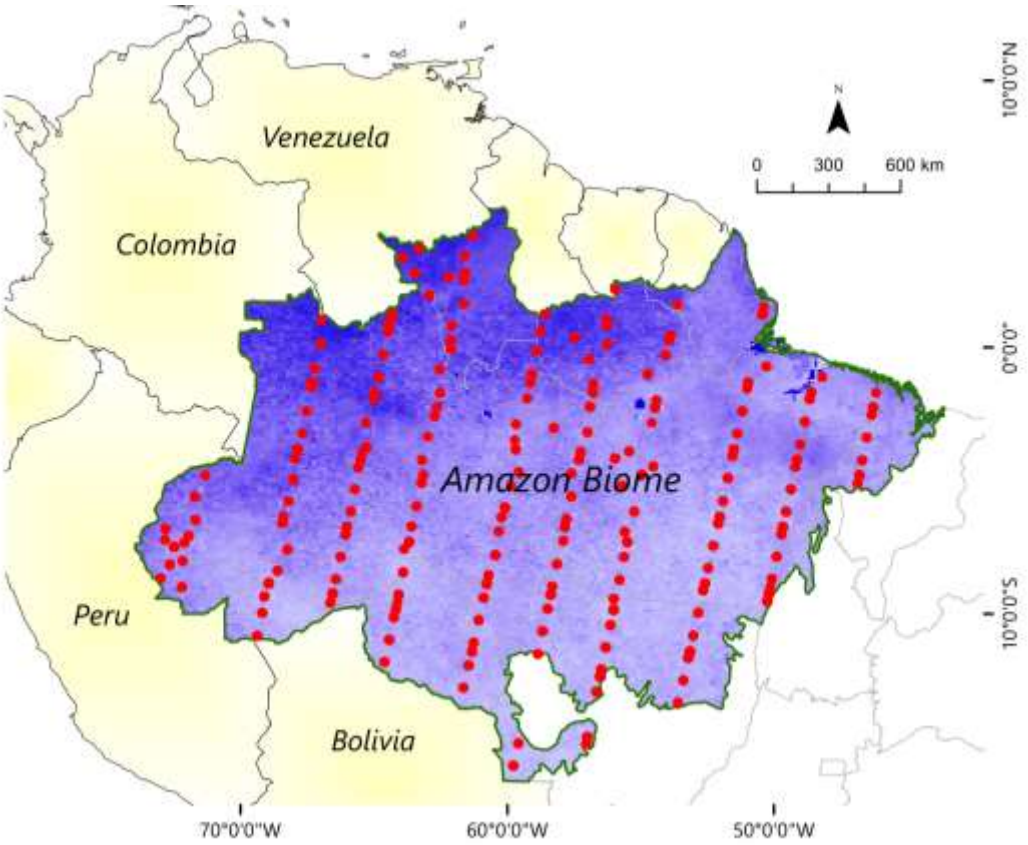

Figure 1.1. Location map of the Brazilian Amazon Forest biome and the XCH_4 GOSAT observations (red circles) in the Amazon biome in 2019, obtained by the University of Leicester GOSAT Proxy with version 9.0 (Parker, R.; Boesch, 2020). Source: Own elaboration (2022)

Since the 1980s, the occurrence of forest fires has shown alarming data. At the same time, it shows high rates of deforestation, in addition to the indiscriminate use of fire resulting in a high fragmentation of forest ecosystems (Mouillot; Field, 2005; Silva et al., 2020). There is concern about the loss of resilience of the Amazon rainforest, facing changes in land use and occupation along with climate change (Boulton; Lenton; Boers, 2022). This reflects directly on the reduction or loss of carbon absorption (Net productivity ecosystem - NPE) in the biome (Figure 1.2),

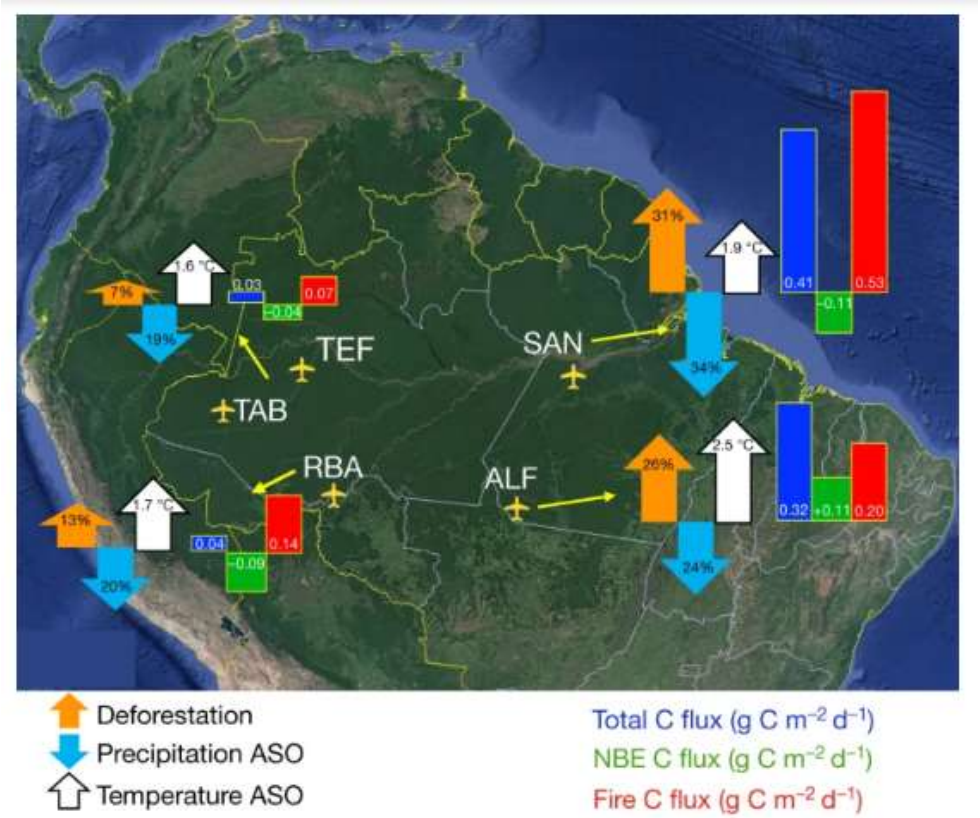

Figure 1.2. Overview of results of deforestation (orange arrows) from 2010 to 2018, rainfall (light blue arrows), temperature (white arrows) and carbon fluxes (total, dark blue bars; NBE - Net biome exchange, with green bars; fire, red bars), at four locations in the Amazon from 2010 to 2018. ALF- Alta Floresta-MT (8.80° S 56.75° W), RBA - Rio Branco-AC (9.38° S 67.62° W), SAN - Santarém-PA (2.86° S 54.95 ° W), TAB – Tabatinga-AM (5.96° S 70.06° W) and TEF - Tefé-AM (3.39° S 65.6° W). Fonte Gatti et al (2021).

resulting mainly in extreme drought events, such as in 2005 and 2010, where the Amazon temporarily became a source of C emission, caused by high tree mortality (Brienen et al., 2015; Feldpausch et al., 2016; Hubau et al., 2020) and east and south of the biome, which saw an increase in deforestation (26 to 31%) and temperature (1.9 to 2.5 ºC), accompanied by a reduction in precipitation (24 to 34%), resulting in higher carbon fluxes from fires (0.20 to 0.53 g C m^{-2} day^{-1}; Gatti et al., 2021), according to figure 1.2). According to Fearnside (2005), the region is known as the “Arc of deforestation”, characterized by the intense conversion of forests into pastures and agricultural crops in recent decades.

There are several direct and indirect Amazonian ecosystem services provided by nature to society (Ramos et al., 2020), including the storage of biodiversity (Fearnside, 1997), regulation and maintenance of the hydrological cycle (Brando et al.,

2019) and GHG mitigation (Strand et al., 2018), among others. That is the reason conservation of the standing forest becomes so valuable when contrasted with the suppression of vegetation, especially if we compare its direct and indirect benefits to society (Nobre et al., 2016). In this scenario, the valorization of ecosystem services still makes it possible to guide mechanisms for the implementation of forest conservation, such as payments for ecosystem services, in order to protect its rich Amazonian biodiversity (Strand et al., 2018).

1.2.2. Main features of the Biome Amazon climate

The main drivers of fires in the Amazon biome are not purely meteorological events, but Amazonian fires are ignited by anthropic action (Berenguer et.al., 2021). On other hand, the meteorological conditions enable us to understand fires interannual variability. For example, the solar radiation that acts as a force in the atmospheric circulation in the Amazon (Marengo et al., 2018) and the variability in precipitation and a rainy season and a dry season observed near the Amazon delta is due to the alternating heating of the two hemispheres and the annual cycle associated with the Seasonal Southern Migration of the Intertropical Region Convergence Zone (ITCZ) (Vera et al., 2006). Similarly, the trade winds act as driver from the tropical North and South Atlantic convergee along the ITCZ (Marengo et al, 2018). Finally, the Hadley cell acts as a driver for the tropical and sub-tropical climates due to its rising motion in equatorial latitudes and broad subsidence in the subtropics (Rao et al., 2022) corroborating with Tsui and Toumi (2021)we found Hadley-type response to fires in the Southern Amazon through a direct thermal circulation.

The Amazon rainforest plays an essential role in the global energy and regional hydrological budgets, mainly role in South American one (Marengo et al., 2018), also playing an essential role in moisture and carbon balances (Phillips and Brienen, 2017). On the other hand, the climate change increases the vulnerability of ecosystem services in the Amazon region (Marengo et al., 2018), affecting the moisture flux (Soares and Marengo, 2009) and altering the hydrological cycle (Jiang et al., 2021). And there is alteration in the forest-atmosphere interactions which regulates the humidity within the region (Marengo et al., 2018). Similarly, among the anthropic actions, deforestation acts as the main driver for the occurrence of fires in the Amazon

(Aragão et at., 2018; Marengo et al., 2018).

1.2.3. Land Use Over the Amazon Region

Changes in land cover and use are one of the main changes in different biogeochemical and climatic processes on a global scale (Armenteras et al. 2019). Consequently, this scenario of changes, whether the suppression of the forest for livestock or agricultural activities tend to increase concentrations of greenhouse gases (GHG) and affect soil carbon sequestration (Verburg et al. 2011).

There is a close correlation between soil and Amazonian vegetation (Moline and Coutinho 2015), justified by the high dependence on nutrient cycling to maintain fertility and biodiversity in these soils, which in turn depends on organic material from vegetation (Chaves et al. 2020). However, the conversion of areas to livestock or agriculture in the Amazon has been the major cause of forest loss, and as a consequence of poor management, it results in soil degradation (Solar et al. 2016; da Cruz et al. 2021).

Recently, the region has become a new agricultural frontier, consequently exacerbating widespread land-cover change (Marengo et al., 2018). In this way, many areas converted into pasture or agriculture in the region have low productivity, continuous deforestation impacts the loss of biodiversity and reverberates in high risks with irreversible alteration of the Amazon biome (Nobre et al., 2016).

The PRODES (Monitoring of Deforestation in the Legal Amazon by Satellite) consists in a program that monitors the annual estimates of deforestation with focus on the Brazilian Amazon after 1988 using 30 meter resolution (INPE, 2022), registered a record in deforestation of 27,772 km^2 in 2004 and a major deforestation drivers was cattle ranching (Marengo et al., 2018), corroborating for an increase rate of deforestation in the last 43 years, resulting in 20% (788,353 km^2) of its territory deforested in the period from 1975–2018 (da Cruz et al., 2021). Many areas were converted to pasture, with emphasis on the state of Para with higher converted area (35.2 %) (Mapbiomas 2022).

1.2.4. Wildfires

Wildfires can be of natural or anthropogenic origin. Larger ones, however, are of anthropic origin and cause a lot of damage and loss (Kalantar et al., 2021; Seydi et al., 2022) and are basically characterized as uncontrolled fires in the understory (Barlow et al., 2020), playing a key role in forest species composition and structure (Ribeiro-Kumara et al., 2020). Similarly, wildfires impact global biogeochemical cycles, atmospheric composition, and terrestrial ecosystem attributes (Williams et al., 2016), releasing GHGs and aerosols while changing the surface albedo (Ward et al., 2012).

The large amounts of aerosols and trace gases from fires influence not only the chemical composition of the atmosphere but also the entire terrestrial climate system (Köster et al., 2017). Combustion is a chemical process resulting from oxidation and degradation of dead organic matter as well as living vegetation (Magro et al., 2021). And this combustion or burning of forest biomass can be complete or incomplete, causing a high increase in GHG (CO_2, CH_4 and N_2O), in addition to photochemically reactive compounds, such as CO (Koch et al., 2019). Different from CO_2 and CH_4, CO does not directly affect global temperature, but has a direct negative effect on the ability of the atmosphere chemistry to purify itself from other polluting gases (Magro et al., 2021). Therefore, the suppression of forests followed by fires has a relevant impact on global climate change (Koch et al., 2019).

Monitoring information on fire foci and their respective impacts while detecting deforestation in real time contributes as efficient measures to combat fire risks (Naus et al., 2022). The efficiency of this monitoring depends on remote sensing products, such as fire counts (Giglio et al., 2003; Wiedinmyer et al., 2011), albedo changes (Van Der Werf et al., 2017), and Fire Radiative Power – FRP (Giglio et al., 2003; Kaiser et al., 2012). In 2019, the rapid detection of fire activity in Brazilian biomes was due to the high processing speed of a large amount of orbital data (Brando et al., 2020a; Lizundia-Loiola; Pettinari; Chuvieco, 2020).

On the other hand, small fires in areas smaller than 25 ha (approximately 1 MODIS 500 m pixel) are likely to go undetected by sensors, as many occur in just a fraction of a pixel in orbital sensors (Ramo et al., 2021). Similarly, monitoring understory fires becomes a great challenge (Morton et al., 2013). In addition, these events favor the fragmentation and mortality of the forest while contributing to the

increase in the vulnerability of the forest (Nepstad et al., 2001); therefore, monitoring active fires and developing knowledge about the loss of carbon to the atmosphere in the Amazon is very relevant (Naus et al., 2022).

Similarly, deforestation, forest fragmentation, illegal logging, and climate are the collective modulators of fires in the Amazon (Cochrane, 2003; Cochrane; Laurance, 2008; Nepstad et al., 1999) and recent events corroborate this, as in the first half of 2022 alone, 3,750 km² were deforested and 2,562 active fires were detected, the highest record for the month of June (2022) in 15 years (INPE, 2022).

In addition, the frequent severe droughts of 2010 and 2015/16 showed the highest biomass burning in the biome (Silva Junior et al., 2019). Adding to the monthly atmospheric distribution of carbon monoxide (XCO) in Brazil, with a direct relationship with fire foci, especially in the dry season (May to October) (Figure 1.3). The highest XCO in the West Amazon are noted in the dry season and the main reason is the expansion of the agricultural frontier in this region, not to mention the period favoring the accumulation of pollutants in the troposphere (Alvim et al., 2021).

And the southern and eastern edges of the Amazon processes of ecosystem alteration are underway that is, a savannization process characterized by the change of the forest vegetation structure to one with lower biomass (savannah) and the constant association with fire in the system (Silvério et al., 2013), supporting the “tipping point” or changing parts of the Amazon rainforest into non-forest ecosystems that could be achieved with 20 to 25% forest clearing (Lovejoy; Nobre, 2019). In the period from 1975–2018, 788,353 km² of native vegetation were suppressed in the biome, resulting in 20% (da Cruz et al., 2021).

According to Aragão et al (2014) carbon emissions in drier years can double emissions (0.24 to 0.46 Pg C y^{-1}) in the Amazon biome. On the other hand, an increase in GHGs intensifies the greenhouse effect that impacts the planet, as well as favors greater occurrences of forest fires (Pablo et al., 2022). Thus, the warming of the global average temperatures and climate change increase the highest occurrences and frequencies of droughts with more severity, resulting in greater forest fires.

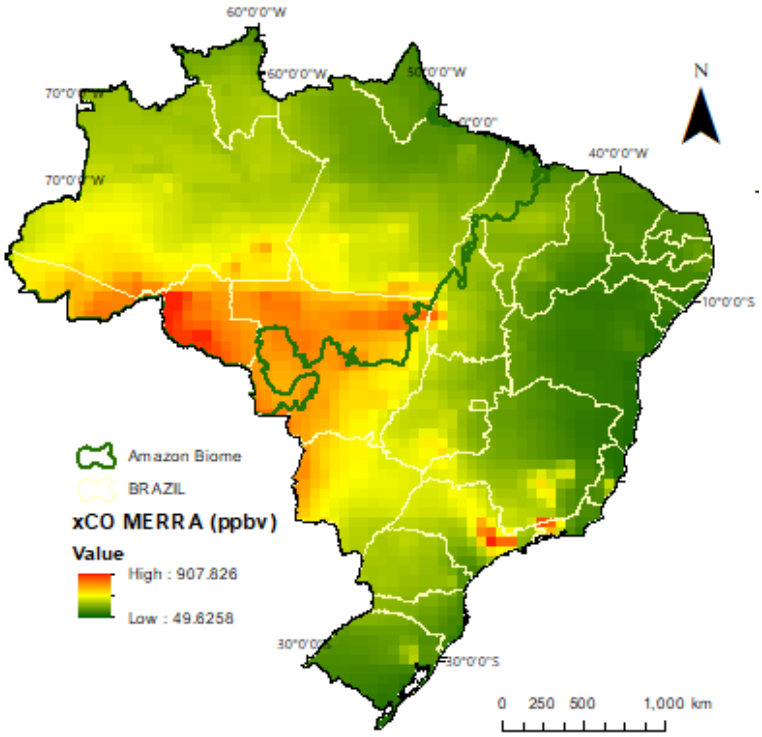

Figure 1.3. Monthly average distribution of atmospheric carbon monoxide (XCO) concentration August 2019 in Brazil. Data Obtained by the Retrospective of the Modern Era for Research and Applications, Version 2 (MERRA-2; GMAO, 2015). Source: Own elaboration (2022).

The complexity in quantifying and explaining the variability of CO and CH_4 gases in forest fires is justified by the heterogeneity of the types of fuels (wood, branches, and leaves) (Magro et al., 2021). The burning of tropical forests has a higher proportion of smoldering combustion (heterogeneous combustion) than flaming combustion (homogeneous combustion), since flaming combustion is more recognized by flames found in environments dominated by fine fuels (pasture) (Santoso et al., 2019). According to Guild et al (2004), a significant presence of latent combustion in fires in the Amazon was observed, and therefore, higher concentrations of CO and CH_4, mainly in the months of August and September.

CH_4 is the second most important anthropogenic GHG in relation to the radiative force effect (IPCC, 2019) and is still considered much more efficient at trapping radiation than CO_2 (Magro et al., 2021), at a rate 28 times higher than CO_2, for a period of approximately 100 years (IPCC, 2022). Additionally, anthropogenic actions are responsible for approximately 60% of total global CH_4 emissions (Saunois et al., 2020;

Tian et al., 2016, 2015), most notably fossil fuel use, livestock activity, and biomass burning. For global CH_4 emissions, agropastoral systems (rice cultivation and livestock) are widely prominent (Dangal et al., 2017). The livestock sector alone accounted for 111 Tg CH_4 $year^{-1}$ between the years 2008 to 2017 of global CH_4 emissions, which demonstrates approximately 30% of the globe's anthropogenic emissions (Saunois et al., 2020).

In Brazil, the sources of CH_4 associated with animal agriculture are mainly attributed to enteric fermentation of ruminants, land use and land cover change (LULC), combustion of agricultural residues, and the management of waste (Mendonça et al., 2020). This scenario of heat trapping caused by GHGs, mainly CO_2 and CH_4 (Magro et al., 2021), associated with land use changes (Carvalho et al., 2021), and indiscriminate practices of the use of fire (Alencar et al., 2015), culminate in greater occurrences of fires. The contribution of fires and agriculture account for 37% (1.7 Tg CH_4 y^{-1}) of the total emission of CH_4 in the Amazon. However, in the Southeast of the Amazon, with increasing deforestation rates as a result of fire use, 48% (21 Tg CH_4 y^{-1}) of the total production of CH_4 in the biome was observed. Therefore, in recent decades these gases have increased at an alarming rate (Lopez et al., 2022).

The Amazon is threatened by land-use change and high conversion of forest, as a consequence of the deforestation, forest fires, and the forest degradation associated with tree deaths from severe drought conditions (Brando et al., 2019) evidence the non-adaptability to fires of any intensity in the biome (Cammelli et al., 2020; Garrett et al., 2021).

1.2.5. Greenhouse Gas Monitoring Satellites

The use of satellites is very important to elucidate both the behavior of fires in time and space (Magro et al., 2021), and GHG concentrations on regional scales with high spatio-temporal resolutions (Mustafa et al., 2021), in addition to the possibility of continuous measurement on a global scale (Alberti et al., 2022). These satellites with their respective embedded sensors enable GHG measurements, for example the SCanning Imaging Absorption spectroMeter for Atmospheric CHartographY (SCIAMACHY) (Bovensmann et al., 1999) was the first satellite monitoring CO_2 and CH_4. Afterward, the Japan Aerospace Exploration Agency (JAXA) launched in 2014

the Greenhouse Gases Observing Satellite (GOSAT) (Kuze et al., 2009). Recently, NASA (National Aeronautics Space Administration) launched the Orbiting Carbon Observatory-2 (OCO-2) (Boesch et al., 2011) and the Ministry of Science and Technology of China (MOST) launched the Chinese Carbon Dioxide Observation Satellite (TanSat) (Liu et al., 2018) and the European Space Agency (ESA) launched the TROPOspheric Monitoring Instrument (TROPOMI) aboard Sentinel-5 Precursor (S5-P) (Landgraf et al., 2016).

The GOSAT mission launched by the Japanese Space Exploration Agency (JAXA) on January 23, 2009 (Kuze et al., 2009), with operating time of more than 9 years, p on January 23, 2009, makes it possible to capture the average mole fraction of dry air in the column of atmospheric concentrations of carbon dioxide (XCO_2) and methane (XCH_4), the two main greenhouse gases, through orbital monitoring (Yoshida et al., 2011). GOSAT allows a revisit at the same location in periods of 3 days (temporal resolution) and was developed in order to characterize emission sources and sinks on a continental scale, having a spatial scale cover of approximately 10 km, in circular pixels separated by about 270 km (Parker et al., 2015, 2020), in addition to having a Sun-synchronous descending orbit with a transit time of 13:00 latitude at the Equator. On board the satellite there is an embedded sensor (Thermal and Near-infrared Sensor for Carbon Observation – Fourier Transform Spectrometer – TANSO-FTS) to GHG observation with a spectral resolution of 0.012 nm (0,2 cm^{-1}). The sensor features three centered near-infrared wavelength (SWIR) bands in 0.76, 1.6 and 2.0 μm and two centered thermal infrared (TIR) bands in 5.56 and 14.3 μm (Kuze et al., 2009).

Figure 1.4. describes the spatial resolution of satellites (GOSAT e OCO-2) and shows the observations of methane (XCH_4) in the Amazon Biome in the period from 2009 to 2019.

Another GHG monitoring satellite is the NASA-developed satellite OCO-2 launched into space on July 2, 2014 to measure XCO_2 on a regional and continental scale (Frankenberg et al., 2015). The use of new technology using satellite data contributes for measurements of the XCO_2, with a temporal resolution of 16 days and a spatial resolution of approximately 3 km^2 (Siabi; Falahatkar; Alavi, 2019). OCO-2 has coupled three high-resolution imaging grid spectrometers, collecting spectra of sunlight reflected from the Earth's surface on molecular oxygen (O_2), being two CO_2 bands at 1.6 and 2.06 μm and one band at 0.76 μm (Osterman et al., 2020).

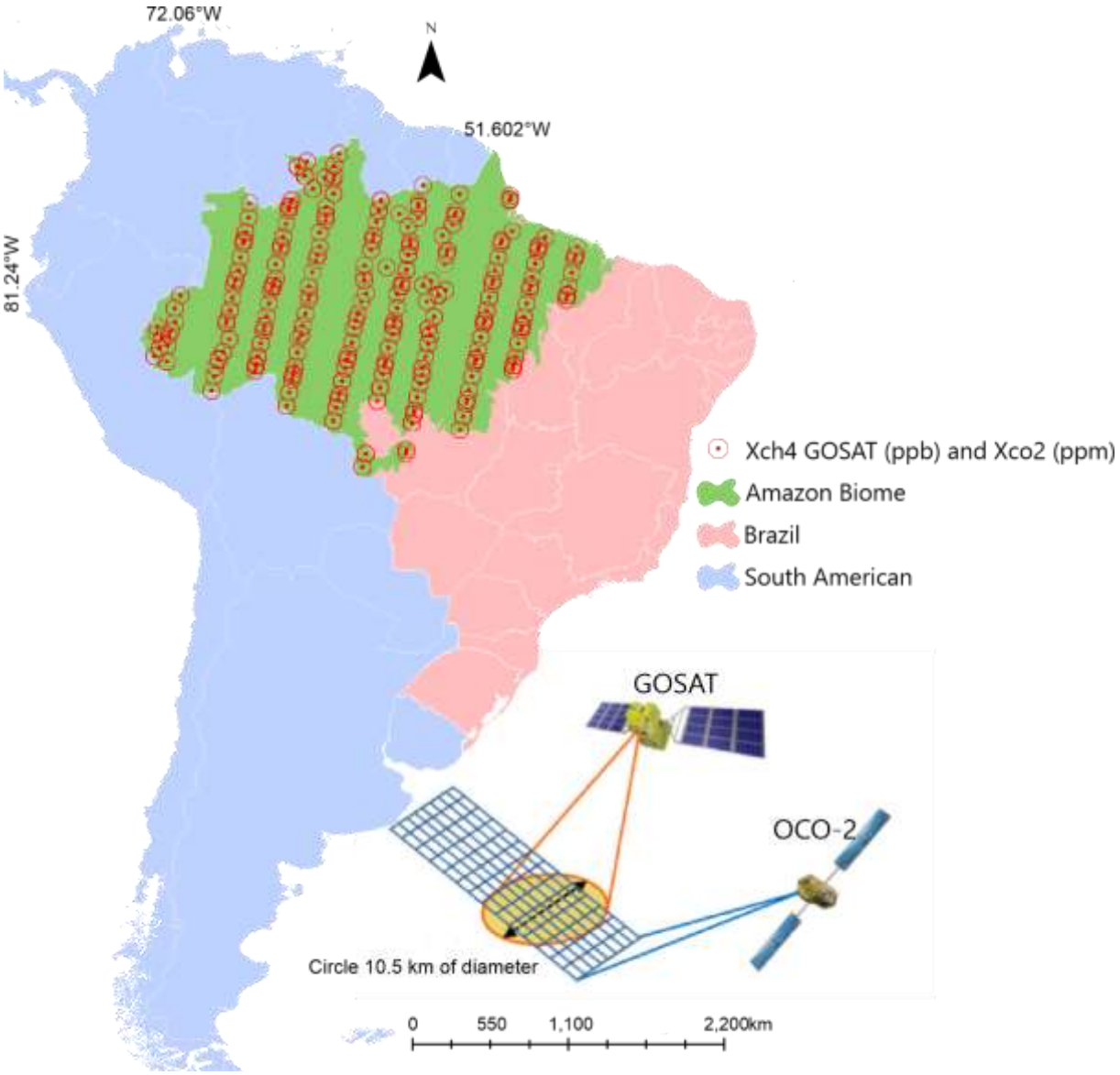

Figure 1.4. Figure with the spatial resolution of the GOSAT and OCO-2 satellites and the XCH_4 observations in the Amazon biome in the time series from 2009 to 2019; the red circles are observed in the biome and obtained by the University of Leicester GOSAT Proxy with version 9.0 (Parker, R.; Boesch, 2020). Source: Own elaboration (2022).

Both GHG monitoring satellites (GOSAT and OCO-2) have two types of observation: thermal infrared (TIR) and short wavelength infrared (SWIR) (Mousavi; Falahatkar; Farajzadeh, 2017; Wang et al., 2014). However, the SWIR, due to the greater sensitivity of the observations in the lower troposphere, becomes more accurate than the TIR, thus making it possible to monitor the main sources and sinks of CO_2 and CH_4 on the Earth's surface (Joiner et al., 2011; Wang et al., 2014).

1.3. References

ARMENTERAS, D., et al. Scenarios of land use and land cover change for NW Amazonia: Impact on forest intactness. **Global Ecology and Conservation** 17, 2019. https://doi.org/10.1016/j.gecco.2019.e00567

ALBERTI, C. et al. Investigation of spaceborne trace gas products over St Petersburg and Yekaterinburg, Russia, by using COllaborative Column Carbon Observing Network (COCCON) observations. **Atmospheric Measurement Techniques**, v. 15, n. 7, p. 2199–2229, 2022.

ALENCAR, A. A. et al. Landscape fragmentation, severe drought, and the new Amazon forest fire regime. **Ecological Applications**, v. 25, n. 6, p. 1493–1505, 2015.

ALVIM, D. S. et al. Evaluating carbon monoxide and aerosol optical depth simulations from cam-chem using satellite observations. **Remote Sensing**, v. 13, n. 11, p. 1–36, 2021.

AMARAL, S. S. et al. CO_2, CO, hydrocarbon gases and PM2.5 emissions on dry season by deforestation fires in the Brazilian Amazonia. **Environmental Pollution**, v. 249, p. 311–320, 2019.

ANTONELLI, A. et al. Amazonia is the primary source of Neotropical biodiversity. **Proceedings of the National Academy of Sciences of the United States of America**, v. 115, n. 23, p. 6034–6039, jun. 2018.

ARAGÃO, L. E. O. C. et al. Environmental change and the carbon balance of Amazonian forests. **Biological Reviews**, v. 89, n. 4, p. 913–931, 1 nov. 2014.

ARAGÃO, L. E. et al. 21st Century drought-related fires counteract the decline of Amazon deforestation carbon emissions. **Nat. Commun**, 12, 2018.

ARTAXO, P. et al. Tropical and Boreal Forest – Atmosphere Interactions: A Review. **Tellus B: Chemical and Physical Meteorology**, v. 74, n. 2022, p. 24–163, 2022.

BARLOW, J. et al. Clarifying Amazonia's burning crisis. **Global Change Biology**, v. 26, n. 2, p. 319–321, 2020.

BERENGUER, E. et al. Improving the spatial-temporal analysis of Amazonian fires. **Glob Change Biol**., 27:469–471, 2021.

BOESCH H., D. B. ; et al. Global Characterization of CO_2 Column Retrievals from Shortwave-Infrared Satellite Observations of the Orbiting. p. 270–304, 2011.

BOULTON, C. A.; LENTON, T. M.; BOERS, N. Pronounced loss of Amazon rainforest resilience since the early 2000s. **Nature Climate Change**, v. 12, n. 3, p. 271–278, 2022.

BOVENSMANN, H. et al. SCIAMACHY: Mission objectives and measurement modes. **Journal of the Atmospheric Sciences**, v. 56, n. 2, p. 127–150, 1999.
BRANDO, P. et al. Amazon wildfires: Scenes from a foreseeable disaster. **Flora: Morphology, Distribution, Functional Ecology of Plants**, v. 268, n. May, p. 151609, 2020a.

BRANDO, P. M. et al. Prolonged tropical forest degradation due to compounding disturbances: Implications for CO_2 and H_2O fluxes. **Global Change Biology**, v. 25, n. 9, p. 2855–2868, 2019.

BRANDO, P. M. et al. The gathering firestorm in southern Amazonia. **Science Advances**, v. 6, n. 2, p. 1–10, 2020b.

BRIENEN, R. J. W. et al. Long-term decline of the Amazon carbon sink. **Nature**, v. 519, n. 7543, p. 344–348, 2015.

CAMMELLI, F. et al. Fire risk perpetuates poverty and fire use among Amazonian smallholders. **Global Environmental Change**, v. 63, n. July 2019, p. 102096, 2020.

CAMPANHARO, W. A. et al. Translating fire impacts in Southwestern Amazonia into economic costs. **Remote Sensing**, v. 11, n. 7, 2019.

CAMPANHARO, W. A. et al. Hospitalization due to fire-induced pollution in the brazilian legal amazon from 2005 to 2018. **Remote Sensing**, v. 14, n. 1, 2022.

CARVALHO, N. S. et al. Spatio-Temporal variation in dry season determines the Amazonian fire calendar. **Environmental Research Letters**, v. 16, n. 12, 2021.

CHAVES, S.F.S., et al. Evaluation of physicochemical attributes of a yellow latosol under agroforestry system as compared to secondary forest in the Eastern Amazon. **Agroforestry Systems** 6, 2020. https://doi.org/10.1007/s10457-020-00513-6

COCHRANE, M. A. Fire science for rainforests. **Nature**, v. 421, n. 6926, p. 913–919, 2003.

COCHRANE, M. A.; LAURANCE, W. F. Synergisms among fire, land use, and climate change in the Amazon. **Ambio**, v. 37, n. 7–8, p. 522–527, 2008.

COUTINHO, L. M. **Biomas brasileiros**. Oficina de ed. São Paulo: 128 p.

CRISP, D. et al. The ACOS CO_2 retrieval algorithm – Part II: Global XCO_2 data characterization. **Atmos. Meas. Tech.**, v. 5, n. 4, p. 687–707, abr. 2012.

DANGAL, S.R.S. et. al. Methane emission from global livestock sector during 1890-2014: Magnitude, trends and spatiotemporal patterns. **Glob. Chang. Biol.** 23, 4147–4161, 2017

DA SILVA JUNIOR, C. A. et al. Persistent fire foci in all biomes undermine the Paris Agreement in Brazil. **Scientific Reports**, v. 10, n. 1, p. 1–14, 2020.

DA SILVA JUNIOR, C. A. et al. Fires Drive Long-Term Environmental Degradation in the Amazon Basin. **Remote Sensing**, v. 14, n. 2, 2022.

DA CRUZ DC, BENAYAS JMR, FERREIRA GC, et al. An overview of forest loss and restoration in the Brazilian Amazon. **New Forests** 52:1–16, 2021.

DEUTSCH, S.; FLETCHER, R. The 'Bolsonaro bridge': Violence, visibility, and the 2019 Amazon fires. **Environmental Science and Policy**, v. 132, n. February, p. 60–68, 2022.

DUANE, A.; CASTELLNOU, M.; BROTONS, L. Towards a comprehensive look at global drivers of novel extreme wildfire events. **Climatic Change**, v. 165, n. 3–4, p. 1–21, 2021.

FEARNSIDE, P. Deforestation in Brazilian Amazonia: History, Rates, and Consequences. Conservation Biology, v. 19, n. 3, p.680–688, 2005

FEARNSIDE, P. M. Serviços ambientais como estrategia para o desenvolvimento sustentavel na Amazonia rural, n. 92, 1997.

FELDPAUSCH, T. R. et al. Amazon forest response to repeated droughts. **Global Biogeochemical Cycles**, p. 964–982, 2016.

FRANKENBERG, C. et al. The Orbiting Carbon Observatory (OCO-2): spectrometer performance evaluation using pre-launch direct sun measurements. **Atmospheric Measurement Techniques**, v. 8, n. 1, p. 301–313, 2015.

GARRETT, R. D. et al. Forests and Sustainable Development in the Brazilian Amazon: History, Trends, and Future Prospects. **Annual Review of Environment and Resources**, v. 46, n. 1, p. 1–28, 2021.

GATTI, L. V. et al. Amazonia as a carbon source linked to deforestation and climate change. **Nature**, v. 595, n. 7867, p. 388–393, 2021.

GATTI, L. V et al. Drought sensitivity of Amazonian carbon balance revealed by atmospheric measurements. **Nature**, v. 506, n. 7486, p. 76–80, 2014.

GIGLIO, L. et al. An Enhanced Contextual Fire Detection Algorithm for MODIS. **Remote Sensing of Environment**, v. 87, n. 2–3, p. 273–282, out. 2003.

GUILD, L. S. et al. MODELING BIOMASS BURNING EMISSIONS FOR AMAZON FOREST AND PASTURES IN RONDÔNIA, BRAZIL. **Ecological Applications**, v. 14, n. sp4, p. 232–246, ago. 2004.

GUO, J. et al. Growth, photosynthesis, and nutrient uptake in wheat are affected by differences in nitrogen levels and forms and potassium supply. **Scientific Reports**, v. 9, n. 1, p. 1–12, 2019.

GUO, M. et al. CO_2 emissions from the 2010 Russian wildfires using GOSAT data. **Environmental Pollution**, v. 226, p. 60–68, 2017.

HEINRICH, V. H. A. et al. Large carbon sink potential of secondary forests in the Brazilian Amazon to mitigate climate change. **Nature Communications**, v. 12, n. 1, p. 1–11, 2021.

HUBAU, W. et al. Asynchronous carbon sink saturation in African and Amazonian tropical forests. **Nature**, v. 579, n. 7797, p. 80–87, 2020.

INPE. **Instituto Brasileiro de Pesquisas Espaciais BDQueimadas.** Available in: <https://queimadas.dgi.inpe.br/queimadas/bdqueimadas> Acess on: July 12 2022.

IPCC. **Intergovernmental Panel on Climate Change2019 Refinement to the 2006 IPCC Guidelines for National Greenhouse Gas Inventories – IPCC, available at:** Available in <https://www.ipcc.ch/report/2019-refinement-to-the-2006-ipcc-guidelines-for-national-greenhouse-gas-inventories/>. Acesso em: 17 mar. 2019.

IPCC (INTERGOVERNMENTAL PANEL ON CLIMATE CHANGE). **Climate Change 2022: Impacts, Adaptation, and Vulnerability. Contribution of Working Group II to the Sixth Assessment Report of the Intergovernmental Panel on Climate Change**. 1st. ed. Cambridge: Cambridge University Press. In Press., 2022.

JIANG, X. et al. Impact of Amazonian fires on atmospheric CO2. **Geophysical Research Letters**, 48, 2021.

JOINER, J. et al. First observations of global and seasonal terrestrial chlorophyll fluorescence from space. **Biogeosciences**, v. 8, n. 3, p. 637–651, 2011.

KAISER, J. W. et al. Biomass burning emissions estimated with a global fire assimilation system based on observed fire radiative power. **Biogeosciences**, v. 9, n. 1, p. 527–554, 27 jan. 2012.

KALANTAR, B. et al. Deep neural network utilizing remote sensing datasets for flood hazard susceptibility mapping in Brisbane, Australia. **Remote Sensing**, v. 13, n. 13, 2021.

KOCH, N. et al. Agricultural Productivity and Forest Conservation: Evidence from the Brazilian Amazon. **American Journal of Agricultural Economics**, v. 101, n. 3, p. 919–940, 2019.

KÖSTER, E. et al. Carbon dioxide, methane and nitrous oxide fluxes from a fire chronosequence in subarctic boreal forests of Canada. **Science of the Total Environment**, v. 601–602, p. 895–905, 2017.

KUZE, A. et al. Thermal and near infrared sensor for carbon observation Fourier-transform spectrometer on the Greenhouse Gases Observing Satellite for greenhouse gases monitoring. **Applied Optics**, v. 48, n. 35, p. 6716, dez. 2009.

LANDGRAF, J. et al. Carbon monoxide total column retrievals from TROPOMI shortwave infrared measurements. **Atmospheric Measurement Techniques**, v. 9, n. 10, p. 4955–4975, 2016.

LI, A. X.; WANG, Y.; YUNG, Y. L. Inducing Factors and Impacts of the October 2017 California Wildfires. **Earth and Space Science**, v. 6, n. 8, p. 1480–1488, 2019.

LIMA, M. et al. The “New Transamazonian Highway”: BR-319 and Its Current Environmental Degradation. **Sustainability**, v. 14, n. 2, p. 823, 12 jan. 2022.

LIU, Y. et al. The TanSat mission: preliminary global observations. **Science Bulletin**, v. 63, n. 18, p. 1200–1207, 2018.

LIZUNDIA-LOIOLA, J.; PETTINARI, M. L.; CHUVIECO, E. Temporal Anomalies in Burned Area Trends: Satellite Estimations of the Amazonian 2019 Fire Crisis. **Remote Sensing**, v. 12, n. 1, p. 151, 2020.

LOPEZ, F. P. A. et al. XCO_2 and XCH_4 Reconstruction Using GOSAT Satellite Data Based on EOF-Algorithm. 2022.

LOVEJOY, T. E.; NOBRE, C. Amazon tipping point: Last chance for action. **Science Advances**, v. 5, n. 12, p. 4–6, 2019.

MACHADO, L. A. T. et al. Overview: Precipitation characteristics and sensitivities to environmental conditions during GoAmazon2014/5 and ACRIDICON-CHUVA. **Atmospheric Chemistry and Physics**, v. 18, n. 9, p. 6461–6482, 2018.

MAGRO, C. et al. Atmospheric trends of CO and CH_4 from extreme wildfires in Portugal using sentinel-5P TROPOMI level-2 data. **Fire**, v. 4, n. 2, p. 1–20, 2021.

MAPBIOMAS - **Coleção 7 (1985-2021) da Série Anual de Mapas de Cobertura e Uso de Solo do Brasil.** Disponível em: https://plataforma.mapbiomas.org/map#coverage. Access on: 02 set 2022.

MARENGO, J. A. et al. Changes in Climate and Land Use Over the Amazon Region: Current and Future Variability and Trends. **Frontiers in Earth Science**, v. 6, n. December, p. 1–21, 2018.

MENDONÇA, A.K. et al. An overview of environmental policies for mitigation and adaptation to climate change and application of multilevel regression analysis to investigate the CO2 emissions over the years of 1970 to 2018 in all Brazilian states. **Sustainability,** 12, 1–18, 2020.

MIETTINEN, J. et al. On the extent of fire-induced forest degradation in Mato Grosso, Brazilian Amazon, in 2000, 2005 and 2010. **International Journal of Wildland Fire**, v. 25, n. 2, p. 129–136, 2016.

MORTON, D. C. et al. Understorey fire frequency and the fate of burned forests in southern Amazonia. **Philosophical Transactions of the Royal Society B: Biological Sciences**, v. 368, n. 1619, 2013.

MOLINE, E.F.V., COUTINHO, E.L.M. Atributos químicos de solos da Amazônia Ocidental após sucessão da mata nativa em áreas de cultivo. **Revista de Ciências Agrarias - Amazon Journal of Agricultural and Environmental Sciences** 58:14–20, 2015. https://doi.org/10.4322/rca.1683

MOUILLOT, F.; FIELD, C. B. Fire history and the global carbon budget: A 1° × 1° fire history reconstruction for the 20th century. **Global Change Biology**, v. 11, n. 3, p. 398–420, 2005.

MOUSAVI, S. M.; FALAHATKAR, S.; FARAJZADEH, M. Assessment of seasonal variations of carbon dioxide concentration in Iran using GOSAT data. **Natural Resources Forum**, v. 41, n. 2, p. 83–91, 2017.

MUSTAFA, F. et al. Validation of GOSAT and OCO-2 against In Situ Aircraft Measurements and Comparison with CarbonTracker and GEOS-Chem over Qinhuangdao, China. **Remote Sensing**, v. 13, n. 5, 2021.

NAUS, S. et al. Sixteen years of MOPITT satellite data strongly constrain Amazon CO fire emissions. **EGUsphere**, v. 2022, p. 1–25, 2022.

NEPSTAD, D. et al. Road paving, fire regime feedbacks, and the future of Amazon forests. **Forest Ecology and Management**, v. 154, n. 3, p. 395–407, 2001.

NEPSTAD, D. C. et al. Large-scale impoverishment of amazonian forests by logging and fire. **Nature**, v. 398, n. 6727, p. 505–508, 1999.

NOBRE, C. A. et al. Land-use and climate change risks in the amazon and the need of a novel sustainable development paradigm. **Proceedings of the National Academy of Sciences of the United States of America**, v. 113, n. 39, p. 10759–10768, 2016.

O'DELL, C. W. et al. The ACOS CO₂ retrieval algorithm – Part 1: Description and validation against synthetic observations. **Atmospheric Measurement Techniques**, v. 5, n. 1, p. 99–121, jan. 2012.

OFFICE, G.-G. M. AND A. **Global Modeling and Assimilation Office (GMAO) MERRA-2 tavgM_2d_chm_Nx: 2d,Monthly mean,Time-Averaged,Single-Level,Assimilation,Carbon Monoxide and Ozone Diagnostics V5.12.4**. Available in <https://disc.gsfc.nasa.gov/datasets/M2TMNXCHM_5.12.4/summary>. Access on: January 31 2022.

OSTERMAN, G., O'DELL, C., ELDERING A., FISHER, B., CRISP, D., CHENG, C., FRANKENBERG, C., LAMBERT, A., GUNSON, M., MANDRAKE, L., AND WUNCH, D. **Orbiting Carbon Observatory-2 and 3 (OCO-2 & OCO-3), Data Product User's Guide, Operational Level 2 Data Versions 10 and Lite File Version 10 and VEarly, Technical Report National Aeronautics and Space Administration, Jet Propulsion Laboratory, California**. Available in <https://docserver.gesdisc.eosdis.nasa.gov/public/project/OCO/OCO2_OCO3_B10_DUG.pdf>. Access on: May 3 2022.

PARKER, R.; BOESCH, H. **University of Leicester GOSAT Proxy XCH_4 v9.0. Centre for Environmental Data Analysis**.

PARKER, R. J. et al. Assessing 5 years of GOSAT Proxy XCH₄ data and associated uncertainties. **Atmospheric Measurement Techniques**, v. 8, n. 11, p. 4785–4801, nov. 2015.

PARKER, R. J. et al. A decade of GOSAT Proxy satellite \chem{CH_4} observations. **Earth System Science Data**, v. 12, n. 4, p. 3383–3412, 2020.

PIVELLO, V. R. et al. Understanding Brazil's catastrophic fires: Causes, consequences and policy needed to prevent future tragedies. **Perspectives in Ecology and Conservation**, v. 19, n. 3, p. 233–255, 2021.

PHILLIPS, O.L.; BRIENEN, R.J.W. Carbon uptake by mature Amazon forests has mitigated Amazon nations' car emissions. **Carbon Balance Manag**, 12, 1, 2017.

RAMO, R. et al. African burned area and fire carbon emissions are strongly impacted by small fires undetected by coarse resolution satellite data. **Proceedings of the National Academy of Sciences of the United States of America**, v. 118, n. 9, p. 1–7, 2021.

RAMOS, D. L. et al. Ecosystem Services Provided by Insects in Brazil: What Do We Really Know? **Neotropical Entomology**, v. 49, n. 6, p. 783–794, 2020.

RAO, V.B. et al. In a changing climate Hadley cell induces a record food in amazon and another recorded drought across South Brazil in 2021. **Natural Hazards**, 12, 2022

RIBEIRO-KUMARA, C. et al. Long-term effects of forest fires on soil greenhouse gas emissions and extracellular enzyme activities in a hemiboreal forest. **Science of the Total Environment**, v. 718, p. 135291, 2020.

SAUNOIS, M. et al. The global methane budget 2000-2017. **Earth System Science Data**, v. 12, n. 3, p. 1561–1623, 15 jul. 2020.

SANTOSO, M. A. et al. Review of the Transition From Smouldering to Flaming Combustion in Wildfires. **Frontiers in Mechanical Engineering**, v. 5, n. September, 2019.

SCHROEDER, L. et al. Fire association with respiratory disease and COVID-19 complications in the State of Pará, Brazil. **The Lancet Regional Health - Americas**, v. 6, n. November 2021, p. 1–14, 2022.

SEEG - **Sistema de Estimativas de Emissões e Remoções de Gases de Efeito Estufa** (2022), Análise das emissões brasileiras de gases de efeito estufa e suas implicações para as metas climáticas do Brasil 1970 – 2020, SEEG, disponível em: https://seegbr.s3.amazonaws.com/DocumentosAnaliticos/SEEG_9/OC_03_relatorio_2021_FINAL.pdf (access on: 19 fev. 2023)

SEYDI, S. T. et al. Fire-Net: A Deep Learning Framework for Active Forest Fire Detection. **Journal of Sensors**, v. 2022, 2022.

SIABI, Z.; FALAHATKAR, S.; ALAVI, S. J. Spatial distribution of XCO_2 using OCO-2 data in growing seasons. **Journal of Environmental Management**, v. 244, n. May, p. 110–118, 2019.

SILVA, C. A. et al. Fire occurrences and greenhouse gas emissions from deforestation in the Brazilian Amazon. **Remote Sensing**, v. 13, n. 3, p. 1–18, 2021.

SILVA, C. V. J. et al. Estimating the multi-decadal carbon deficit of burned Amazonian forests. **Environmental Research Letters**, v. 15, n. 11, 2020.

SILVA JUNIOR, C. H. L. et al. Fire responses to the 2010 and 2015/2016 Amazonian droughts. **Frontiers in Earth Science**, v. 7, n. May, p. 1–16, 2019.

SILVEIRA, M. V. F. et al. Drivers of fire anomalies in the Brazilian Amazon: Lessons learned from the 2019 fire crisis. **Land**, v. 9, n. 12, p. 1–24, 2020.

SILVÉRIO, D. V. et al. Testing the Amazon savannization hypothesis: Fire effects on invasion of a neotropical forest by native cerrado and exotic pasture grasses. **Philosophical Transactions of the Royal Society B: Biological Sciences**, v. 368, n. 1619, p. 12–14, 2013.

SMITH, L. T. et al. Drought impacts on children's respiratory health in the Brazilian Amazon. **Scientific Reports**, v. 4, p. 1–8, 2014.

SOARES, W., and MARENGO, J. A. Assessments of moisture fluxes east of the Andes in South America in a global warming scenario. **Int. J. Climatol.** 29, 1395–1414, 2009.

SOLAR, R.R.C., et al. Biodiversity consequences of land-use change and forest disturbance in the Amazon: A multi-scale assessment using ant communities. **Biological Conservation** 197:98–107, 2016. https://doi.org/10.1016/j.biocon.2016.03.005

STRAND, J. et al. Spatially explicit valuation of the Brazilian Amazon Forest's Ecosystem Services. **Nature Sustainability**, v. 1, n. 11, p. 657–664, 2018.

TOSCA, M. G.; RANDERSON, J. T.; ZENDER, C. S. Global impact of smoke aerosols from landscape fires on climate and the Hadley circulation. **Atmospheric Chemistry and Physics**, v. 13, n. 10, p. 5227–5241, 2013.

TOUMA, D. et al. Human-driven greenhouse gas and aerosol emissions cause distinct regional impacts on extreme fire weather. **Nature Communications**, v. 12, n. 1, p. 1–8, 2021.

TSUI, E.Y.L. and TOUMI, R. Hurricanes as an enabler of Amazon fires, **Scientific Reports**, 11, 16960,2021.

VAN DER WERF, G. R. et al. Global fire emissions estimates during 1997--2016. **Earth System Science Data**, v. 9, n. 2, p. 697–720, 2017.

VEEFKIND, J. P. et al. TROPOMI on the ESA Sentinel-5 Precursor: A GMES mission for global observations of the atmospheric composition for climate, air quality and ozone layer applications. **Remote Sensing of Environment**, v. 120, n. 2012, p. 70–83, 2012.

VERA, C. Et al. Toward a Unified View of the American Monsoon Systems. J Clim, 19: 4977–5000, 2006.

VERBURG, P.H. et al. Challenges in using land use and land cover data for global change studies. **Global Change Biology** 17:974–989, 2011 https://doi.org/10.1111/j.1365-2486.2010.02307.x

WANG, T. et al. Combining XCO_2 Measurements Derived from SCIAMACHY and GOSAT for Potentially Generating Global CO_2 Maps with High Spatiotemporal Resolution. **PLOS ONE**, v. 9, n. 8, p. 1–8, 2014.

WARD, D. S. et al. The changing radiative forcing of fires: global model estimates for past, present and future. **Atmospheric Chemistry and Physics**, v. 12, n. 22, p. 10857–10886, 2012.

WIEDINMYER, C. et al. The Fire INventory from NCAR (FINN): a high resolution global model to estimate the emissions from open burning. **Geoscientific Model Development**, v. 4, n. 3, p. 625–641, 2011.

WILLIAMS, C. A. et al. Disturbance and the carbon balance of US forests: A quantitative review of impacts from harvests, fires, insects, and droughts. **Global and Planetary Change**, v. 143, p. 66–80, 2016.

YOSHIDA, Y. et al. Retrieval algorithm for CO 2 and CH 4 column abundances from short-wavelength infrared spectral observations by the Greenhouse gases observing satellite. **Atmospheric Measurement Techniques**, v. 4, n. 4, p. 717–734, 2011.

YUAN, S. et al. Severe Biomass-Burning Aerosol Pollution during the 2019 Amazon Wildfire and Its Direct Radiative-Forcing Impact: A Space Perspective from MODIS Retrievals. **Remote Sensing**, v. 14, n. 9, 2022.

CHAPTER 2 - FIRE FOCI IN THE AMAZON BIOME RELATED TO A COLUMN-AVERAGED CONCENTRATION OF CO_2, CH_4 AND CO BY REMOTE SENSING

ABSTRACT - The unsuitable use of fires related with human activities in the Amazon biome leads to serious damage, causing reduction of forest areas and related GHG. Our study evaluated an analysis of trends in the time scale of concentrations in the column-averaged of CO_2 (XCO_2), CH_4 (XCH_4) and CO (XCO) in the atmosphere based on GOSAT and MERRA observations satellites data and investigated the possible correlations between the spectral index of the terrestrial surface and the fire occurrences in the Amazon. For this, the Enhanced Vegetation Index (EVI), Fire Radiative Power (FRP), and fire foci number MODIS products were used. Solar-Induced Fluorescence (SIF), XCH_4 and XCO_2 were obtained by GOSAT from 2009 to 2019, as well as MODIS for the Amazon. The correlation between XCO_2 and FRP was linearly expressed by the following equation XCO_2= 381.37 + 0.09 FRP ± 0.09. The annual averages by Mann-Kendall Test from the time series of XCO_2, XCH_4 and XCO did not differ significantly in the time series (2009 to 2019). However, when monthly averages were compared, data from April showed an increase after 2014 for both XCO_2 (2.3-3.03 ppm) and XCO (2.9-5.67 ppb). The FRP showed a monotonic growth for April (3.05-11.25 MW) and July (4.3-9.9 MW) after 2014. However, the higher fire foci related with increments in XCO_2 and XCO indicate that probably human activities related to land use change are responsible for increases in the concentration of GHG observed in the Amazon.

Key words: Climate change, Deforestation, Forest Degradation, Droughts, Wildfires

CAPÍTULO 2 – FOCOS DE INCÊNDIO NO BIOMA AMAZÔNIA RELACIONADOS A CONCENTRAÇÃO MÉDIA DE COLUNA DE CO_2, CH_4 E CO POR SENSORIAMENTO REMOTO

RESUMO – O uso inadequado do fogo relacionadas às atividades humanas no bioma amazônico leva a sérios danos, causando redução de áreas florestais e GEE relacionados. Nosso estudo avaliamos uma análise das tendências na escala de tempo para as concentrações na coluna média de CO_2 (XCO_2), CH_4 (XCH_4) e CO (XCO) na atmosfera com base em satélites de observações GOSAT e MERRA, e estabelecer as possíveis correlações entre o índice espectral da superfície terrestre e a ocorrência de incêndios na Amazônia. Para isso, foram utilizados os produtos do MODIS: Índice de Vegtação Aprimorado (EVI), Poder Radiativo do Fogo (FRP) e Número de focos de fogo. As concentrações de Fluorescência Induzida pelo Sol (SIF), XCH_4 e XCO_2 foram obtidas pelo GOSAT de 2009 a 2019, assim como outras variáveis para a Amazônia. A relação entre XCO2 e FRP foi expressa linearmente pela seguinte equação XCO_2= 381,37 + 0,09.FRP ± 0,09. Ao comparar as médias anuais pelo Teste de Mann-Kendall das séries temporais do XCO_2, XCH_4 e XCO não diferiram significativamente na série temporal. No entanto, ao comparar as médias mensais, abril apresentou um aumento na série de dados após 2014 tanto para XCO2 (2,3-3,03 ppm) quanto para XCO (2,9-5,67 ppb). Da mesma forma, o FRP teve um crescimento monotônico para abril (3,05-11,25 MW) e julho (4,3-9,9 MW) após 2014. No entanto, os maiores focos de fogo com aumentos nas concentrações de CO_2 e CO indicam que provavelmente atividades humanas relacionadas à mudança de uso terra estão relacionadas aos aumentos na concentrações dos GEE's observados na Amazônia.

Palavras-Chaves: Mudanças Climáticas, Desmatamento, Degradação Florestal, Secas, Incêndios

2.1. Introduction

With increase in GHG emissions from fires in tropical forest (Miettinen et al., 2016; Ribeiro et al., 2020; C. H. L. Silva et al., 2018), disturbances in terrestrial ecosystems on regional and global scales can be observed (Koch et al., 2019; Lovejoy and Nobre, 2019; C. H. L. Silva et al., 2018). Therefore, forest fires play a relevant role in global biogeochemical cycles, atmospheric composition, and the attributes of terrestrial ecosystems, with negative impact in the climate system (Williams et al., 2016). Thus, the suppression of forest fires is considered a relevant factor in global environmental changes (Koch et al., 2019).

In 2020, 222,797 fire foci were identified in the whole country, and 46.3% of them were registered in Brazilian Amazon biome (103.161) (INPE, 2022), with a strong representation in the trend of increasing fire foci in the Amazon biome (Amigo, 2020; C. A. Silva et al., 2021). Higher fire foci number can be related to a much warmer climate, more severe and frequent droughts, and continuous changes in land use and occupation of forest areas in this region (Oliveira et al., 2022). Most fires in the Amazon are intentional, promoted by farmers to clear forest areas for cattle ranching (Brando et al., 2020; C. A. Silva et al., 2021). We also emphasize that the lack of strategic actions to fight fire foci strongly affects the biomes and protected areas observed throughout the country (Oliveira et al., 2022).

Under the Paris climate agreement, established between countries to reduce GHG emissions, the Brazilian government pledged to restore 120,000 km² of forests by 2030 (Lovejoy and Nobre, 2019). However, between 2019 and 2020, there was an increase of 9.5% in deforested areas (10,129 to 11,008 km²) in the legal Amazon (INPE, 2022). The deforestation in the Brazilian Amazon results in emissions of approximately 200 t ha^{-1} of CO_2 from biomass (C. V. J. Silva et al., 2020; Soares Neto et al., 2009).

There are several techniques to measure GHG emissions (ships, balloons, towers, and aircraft), but these methods provide several gaps in the spatio-temporal concentrations of atmospheric carbon dioxide (CO_2) data, often due to the cost of these techniques (Gloor et al., 2000). Additionally, there are many uncertainties in the estimation of CO_2 concerning sources and sinks (Mousavi et al., 2017; Yoshida et al., 2011), and orbital observations can contribute to the gaps and increase the real sources and sinks of CO_2 (Wecht et al., 2014).

The Japanese Space Agency (JAXA) GOSAT mission (Kuze et al., 2009), the OCO-2 mission (NASA) (C Frankenberg et al., 2015), and other satellites allow the use of average mole fraction of dry air from CO_2 and methane (CH_4) (XCO_2 and XCH_4) (Mousavi et al., 2017). The GOSAT satellite is equipped with TIR/SWIR sensors - Fourier Transform Spectrometer (TANSO-FTS) and the Cloud and Aerosol Imager (TANSO-CAI) and with OCO-2 satellite, it is possible to measure XCO_2 in the Short Waves InfraRed (SWIR) band (Kuze et al., 2009).

Remote sensing allows to estimate CO_2 emissions from fires in boreal forests (J. Guo et al., 2019), tropical forests (Heymann et al., 2017; Jiang et al., 2021; Liu et al., 2017; Yin et al., 2018), and arid regions (Li et al., 2019). Thus, our objective was to investigate the temporal variability of GHGs over the Brazilian Amazon and its relationship with vegetative aspects and fire foci that occurred in the region between 2009 and 2019.

The hypothesis tested in the present study is that there is a tendency for higher concentrations of CO, CH_4, and CO_2, due the anthropogenic changes carried out in the region. Therefore, the present study aims to answer the following questions:

(i) Are there correlations between the direct GHG (XCO_2 and XCH_4) and indirect GHG (XCO) orbital data and the Enhanced Vegetation Index (EVI), Rainfall and Solar-Induced Fluorescence (SIF) and the occurrence of fire (Fire foci and Fire Radiative Power (FRP))? (ii) What are the temporal trends of the orbital data (XCH_4, XCO_2, and XCO), due to human activities, in the Amazon biome from 2009 and 2019?

2.2. Material and Methods

2.2.1. Study area

The study area comprises the Brazilian Amazon Forest biome (Figure 2.1). Territorial representation represents 4.2 million km^2, covering nine Brazilian states: Acre, Amapá, Amazonas, Para, Roraima, Rondônia and parts of the states of Maranhão, Mato Grosso and Tocantins (IBGE 2020).

Figure 2.2-1. Location map of the Brazilian Amazon Forest biome. Source: Google Earth Pro, 2020.

The Brazilian Amazon Forest stands out for its importance for several ecosystem services such as high biodiversity, climate regulation, and freshwater reservoirs (Strand et al., 2018). However, there was an increased rate of deforestation in the last 43 years, resulting in 20% (788,353 km²) of its territory deforested in the period from 1975–2018 (da Cruz et al., 2021). Many areas were converted to pasture, with emphasis on the state of Para, with higher converted area (35.2 %) (Mapbiomas 2022).

According to the Koppen Climate classification, 3 climate types are predominant: Af (no dry season), Am (monsoon) and Aw (with dry winter). Average

annual rainfall can eXCeed 1,900 mm, reaching up to 4,000 mm, with average temperature of 26.8°C in the Brazilian Amazon biome (Alvares et al., 2013). The wet or rainy period extends from October to April, while the dry period extends from May to September (Zemp et al., 2017).

2.2.2. Data Acquisition of Fire Radiative Power and Fire foci

Active fire or fire foci number remote sensing data were used to identify the timing, location, and radiative force (Fire Radiative Power - FRP) of fires that are actually consuming vegetation in the Amazon Forest. FRP can be a good driver to estimate biomass burning, initially described by Kaufman et al. (1998) and later refined by Wooster et al. (2003). In this way, the FRP is equivalent to the total radiative power of the fire, as described by the Stefan-Boltzmann law and usually measured in megawatts (MW). Thus, the FRP data of all fire pixels detection was carried out using an algorithm that characterizes or detects high emissions of average infrared radiation from fires (Giglio et al., 2003). Archival quality MODIS products (MYD14 and MOD14) data from the Fire Information System for Resource Management (Fire Information for Resource Management System - FIRMS) website (https://earthdata.nasa.gov/firms; accesson 2 October 2021). The Terra/Aqua satellite has moderate resolution imaging spectroradiometer sensor termed MODIS (Moderate Resolution Imaging Spectroradiometer) onboard. FIRMS enable real-time data acquisition of fire foci with a temporal resolution of every 3 hours of observation and a spatial resolution of 1 km. The data was aggregated into monthly averages from May 1, 2009, to December 31, 2019.

2.2.3. Acquisition Enhanced Vegetation Index Data

Enhanced Vegetation Index (EVI) was proposed by Huete et al (1997), which minimizes the effect of the ground and atmosphere considering the blue spectral band. The images used were retrieved from the MOD13Q1 product of collection 6 from the MODIS sensor, with an aggregation of 16 days and 250 m of spatial resolution, where the EVI value, were estimated by Equation 1 (Huete et al., 2002). The retrieval and processing of the data was made in Google Earth Engine for the time series of the study. The images obtained were multiplied by their scale factor of 0.0001 and thus their values range from -1 to 1.

$$EVI = g\frac{\rho IVP - \rho V}{\rho IVP + (c1 * \rho V) - (c2 * \rho A) + L}$$ Equation (1)

Where: EVI- Enhanced Vegetation Index; g is the gain factor (2.5); ρIVP, ρV, and ρA are the reflectance in the near-infrared spectral range, red and blue, respectively, c1 and c2 are the correction coefficients for the atmospheric effects of red (6) and blue (7.5), respectively and L is the factor of the correction for soil interference (1).

2.2.4. Rainfall Data

The data of Climate Hazards Group Infrared Precipitation with Stations (CHIRPS) was obtained through the Google Earth Engine platform, using JavaScript codes for image acquisitions '.TIFF' format, with a spatial resolution of 0.05° for the dataset since 1981 from the collection ("UCSB-CHG/CHIRPS/DAILY"; Funk et al., 2015). In the time series of the images, an annual precipitation sum was made in each pixel for each year of the study.

2.2.5. Acquisition of data from the average column of carbon monoxide (XCO)

Retrospective Analysis of the Modern Era for Research and Applications, version 2 (MERRA-2) enables the acquisition of meteorological, atmospheric, and geological data collected since 1980, within a global climate model framework and with a latitudinal spatial resolution of 50 km (Gelaro et al., 2017; Herrera Estrella et al., 2021). Trace gas concentrations near the surface, such as carbon monoxide in part per billion (XCO; M2TMNXCHM v5.12.4) were obtained from NASA Giovanni system (GMAO 2015), and the data was aggregated in monthly averages for the time series.

2.2.6. Acquisition of XCO_2 and XCH_4 data from the GOSAT satellite

On January 23, 2009, the GOSAT satellite was launched in Japan. It is important to highlight the two main instruments on board: 1) a thermal sensor (TIR) and a near-infrared sensor (SWIR) for GHG monitoring (TANSO), with the Fourier Transform Spectrometer technique (FTS), 2) Cloud and Aerosol Imager (CAI), respectively. The TANSO-FTS sensor has four bands: three being SWIR bands (in the spectral range of 760, 1600, and 2000 nanometers -nm) used in estimating the average CO_2 column concentrations (XCO_2) and a TIR band (5500-14300 nm), used

to describe the vertical profile of CO_2 concentration in the upper troposphere. The images from the TANSO-CAI sensors have four bands (380, 675, 870, and 1600 nm) providing a spatial resolution of 500 m, with application primarily for mapping the properties of clouds and aerosols in the atmosphere (Guerlet et al., 2013; Ross et al., 2013).

The main objective of the GOSAT mission was to assess the sources and sinks of GHGs, mainly to estimate the concentrations of carbon dioxide and methane (XCO_2 and XCH_4, in part per million), on a regional and global scale. In this way, it contributes to environmental managers and researchers on the understanding of the carbon cycle of ecosystems (Guo et al., 2017, 2012; Oguma et al., 2011).

The XCO_2 data was taken from Earthdata (NASA), from the site <htts://oco2.gesdisc.eodisc.nasa.gov/data/GOSAT_TANSO_Level2/ACOS_L2_Lite_FP.9r/> with files in nc format.

Total methane column data (XCH_4) was obtained from the University of Leicester GOSAT Proxy, with version 9.0. It is important to note that they are in the public domain (https://data.ceda.ac.uk/neodc/gosat/data/ch4/nceov1.0/CH4_GOS_OCPR/), with files in nc format (Parker, R.; Boesch, 2020). The average dry air column methane mole fractions (XCH_4) were derived using the proxy method of using the CO_2 emission models, so the method multiplies the ratio XCH_4/XCO_2 by a model of in situ observations XCO_2 (Parker et al., 2011, 2015). The XCO_2 model was based on local measurements of land surfaces using the median metric of the global models: GEOS-Chem (Feng et al., 2011), Carbon Tracker (Peters et al., 2007), and LMDZ (Chevallier et al., 2010). This GOSAT Proxy product has been validated with aircraft measurements in the Amazon region (Tunnicliffe et al., 2020; Wilson et al., 2020).

2.2.7. Sun-induced chlorophyll fluorescence (SIF757) from GOSAT

The sun-induced chlorophyll fluorescence (SIF) is the emission of photons by the chlorophyll molecules during the photosynthetic process of the plant, and in the two photosystems (I and II) the emission ranges are from 600 to 850 nanometers (Castro et al., 2020). The SIF data enables the tracking of photosynthetic activity in the ecosystem in regional and global scale (Drusch et al., 2017; Porcar-Castell et al., 2014). Phenological seasonality in Amazonian ecosystems is conditioned by climatic drivers. Thus, the seasonality of the SIF in the Amazon biome is answered with 76%

of the variation of radiation, while on the other hand, 13% and 11% are answered by rainfall and a combination of both (radiation + rainfall) (Bertani et al., 2017).

The first satellite observations of global SIF came from GOSAT (Frankenberg et al., 2011; Joiner et al., 2011). Thus, data from SIF of 755 nanometers level 2 with GOSAT Lite version 9 (v9; Frankenberg, 2022) was obtained in netCDF format files found in: https://data.caltech.edu/records/8771 (Last access: April 22, 2022).

Summary information for the different variables used to identify the tendency of greenhouse gases and the fire foci, their source, and their temporal and spatial resolution was described in table 1.

Table 1. Summarizes the main information for the different variables used to identify the correlations of greenhouse gases and the fire foci, their source, and their temporal and spatial resolution in this study.

Category	**Variable**	**Source**	**Temporal resolution**	**Spatial resolution**
Indirect GHG	XCO	Column-averaged of CO in the atmosphere (Gelaro et al., 2017)	Hourly	50 km
Direct GHG	XCO_2	Column-averaged of CO_2 in the atmosphere (Kuze et al., 2009)	3 days	10.5 km
	XCH_4	Column-averaged of CH_4 in the atmosphere (R. J. Parker et al., 2020)	3 days	10.5 km
Vegetation	SIF	Sun-induced chlorophyll fluorescence (Frankenberg 2022)	3 days	10.5 km
	EVI	MOD13C2-Enhanced Vegetation Index (A. Huete et al., 2002)	16 days	1 km
Climatic	Rainfall	Precipitation data from CHIRPS (Funk et al., 2015)	Daily	~ 5 km
Burning vegetation	Fire foci	MYD14/MOD14 - Fire pixel location (Giglio et al., 2003)	Daily	1 km
	FRP	MYD14/MOD14 - Fire Radiative Power (Giglio et al., 2003)	Daily	1 Km

2.2.8. Statistical analysis

To understand the natural and regional variability of XCO_2 and XCH_4 and their relationships with biophysical variables, we used regression to subtract the background of the greenhouse gases (XCO_2 and XCH_4) removing the growth trend from the data. For statistical analysis, we used a monthly time scale from 2009 to 2019, which made it possible to describe the atmospheric concentrations of gases as well as the other variables obtained by remote sensing. The monthly average data correspond to each geographic coordinate at the centroid of each pixel (0.1° x 0.1°) and for rainfall and fire foci the accumulated sum for each month in the study area were used. On the other hand, data for all variables were identified and outlines removed by Interquartile Range (IQR) technique.

Monthly and annual distribution graphs were constructed for XCO_2 data, XCH_4, and XCO and SIF data associated with the Amazon biome in the time series (2009-2019). Subsequently, Spearman's correlation (r) was performed with the annual means of the variables over the time series. For the variables that correlated significantly with the gas variables (XCO_2, XCH_4 and XCO), linear regression analysis was performed between the variables, as it presents analytical estimates of confidence intervals and robustness to outliers in seasonal data.

Finally, the application of the Mann-Kendall test (MK) (Kendall, 1948; Mann, 1945) made it possible to verify if there is a significant trend for the data of the annual and monthly averages of XCO_2, XCH_4, XCO, SIF, and Fire foci, FRP, EVI and Rainfall in the Amazon biome, as described by Equation 2:

$$S = \sum_{i=0}^{n-1} \sum_{j=i+1}^{n} sgn\left(x_j - x_i\right) \qquad \text{Equation (2)}$$

Where: S is the Kendall sum statistic; x_i of n-terms with the variation (1 ≤i ≤ n); x_j corresponds to the estimated value of n. The trend test is applied to a time series x_j which is classified from i=1,2,..n-1 and x_j, which is classified j = i + 1,2,...n. Each of the data points x_j is taken as a reference point that is compared to the rest of the data points x_j so that Equation 3:

$$Sgn\,(x_j - x_i) \begin{cases} 1 for\,(x_j) - (x_i) > 0 \\ 0\ for\,(x_j) - (x_i) = 0 \\ -1\ for\,(x_j) - (x_i) < 0 \end{cases} \quad \text{Equation (3)}$$

For the series x = x_1, x_j ..., x_n with n > 4 according to the null trend hypothesis (H0), S will demonstrate a normal distribution with variance Var(S), described according to Equation 4:

fcd

$$\mathrm{Var}\,(\mathrm{S}) = \frac{\mathrm{n(n-1)(2n+5)} - \sum_{i=1}^{m} t_i \mathrm{(i-1)(2i+5)}}{18} \quad \text{Equation (4)}$$

Where: n is the number of observations in a dataset; t_i is the number of observations in a dataset containing identical values from the set in i and m is the dataset number, including equivalent values in the group i from the series. The second term demonstrates a fit in the data. Where t_i is shown as the number of equal data up to the sample i .

For the significance test S, a two-tailed test was used, in which H0 must be rejected for higher values of Zc (Equation 5):

$$Zc = \begin{cases} \frac{S-1}{\sqrt{Var\,(S)}}, S > 0 \\ 0, S = 0 \\ \frac{S+1}{\sqrt{Var\,(S)}}, S < 0 \end{cases}$$ Equation (5)

Where: Zc standardized test statistic; S - standardized test statistic; t_i is the number of observations in a dataset containing identical values from the set in i and m is the dataset number, including equivalent values in the group i from the series. The second term demonstrates a fit in the data. Where t_i is shown as the number of equal data up to the sample i.

For the significance test S, a two-tailed test was used, in which H_0 must be rejected for higher values of Zc (Equation 5):

$$K_t = max\left|U_{t,T}\right|$$ Equation (6)

Where:

$$U_{t,T} = \sum_{i=1}^{t} \sum_{j=t+1}^{T} sgn\left(X_j - X_i\right)$$ Equation (7)

Where: K_t is the location of the change point in the case of probability level of significance (p), which is approximately less than or equal to 5%, described by equation 8:

$$p \approx 2 \exp\left(\frac{-6K_t^2}{T^3 - T^2}\right)$$ Equation (8)

The analyses were performed using the statistical software R version 4.1.2. R is a free access software, thus democratizing the access to statistical analysis (R Core Team, 2022).

2.2. Results

2.3.1. Annual and monthly averages of XCO_2, XCO and XCH_4

The annual distributions of XCO_2, XCO, and XCH_4 for the Brazilian Amazon biome showed distinct characteristics in the analyzed time series (Figure 2.2 a, b and

c).

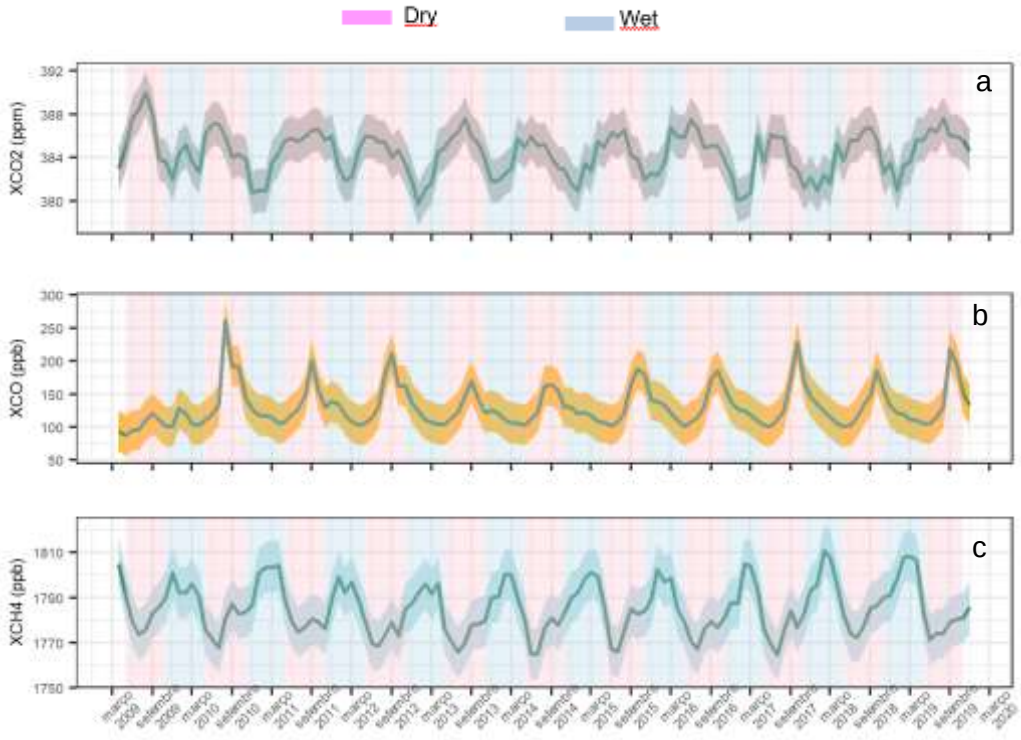

Figure 2.2. XCO_2, XCO and, XCH_4 annually for the Amazon biome. Data from orbital observations of the variables were 668 (2009), 1464 (2010), 1135 (2011), 1223 (2012), 890 (2013), 726 (2014), 971 (2015), 1708 (2016), 1172 (2017), 1063 (2018) and 761 (2019). Pink rectangle is dry period and blue rectangle is wet period. XCO_2 data was obtained by the Japanese Space Agency - JAXA (Kuze et al. 2009) (a). Yearly average XCO data was obtained by NASA Giovanni (GMAO 2015) (b).). XCH_4 GOSAT Proxy data obtained from the University of Leicester (Parker, R.; Boesch, 2020) (c).

The outliers were removed from all variables, but there were occurrences of outliers more frequently for lower values in XCO_2 and higher values in XCO. Therefore, it is very important to note that there were outlines for some variables, even after the IQR technique was used.

Based on data acquired from the present study, XCO_2 data presented annual average values below the mean CO_2 concentration (384.31 ± 2.05 ppm) of the period of 2014 and 2017 (Figure 2.2 a). On the other hand, we noticed that the annual average of XCO data, for the years 2009, 2013 and 2014 showed values below the XCO average (131.07 ± 30.79 ppb), while for the years 2010 and 2016, we noticed a decrease and the XCO values stayed above average (Figure 2.2 b). It is important to note that the years 2010 and 2016 had the most intense droughts in the region, which increased the risk of fires (Marengo et al., 2018) and consequently increased the sources of XCO emissions.

The annual average of XCH_4 data presented values above the average of the

studied period (1785.18 ± 11.31 ppb) for 2018 and 2019 (Figure 2.2 c).

For the monthly distribution, we observed that the period of May to October showed XCO_2 values above the average (384.31 ± 2.05 ppm) of the studied period, and the other months were below the average (384.31 ± 2.05 ppm) (Figure 2.3 a). The monthly distribution of XCO_2 is inversely proportional to the monthly rainfall volume; that is, lower values of XCO_2 were observed for the months from November to March when the highest rainfall occurred in the studied region (Fig.2 S1.). The monthly distribution presented values below the average for the months of May to October (Figure 2.3 a) dry period, when there was a reduction in monthly rainfall volume (Fig.2 S1.).

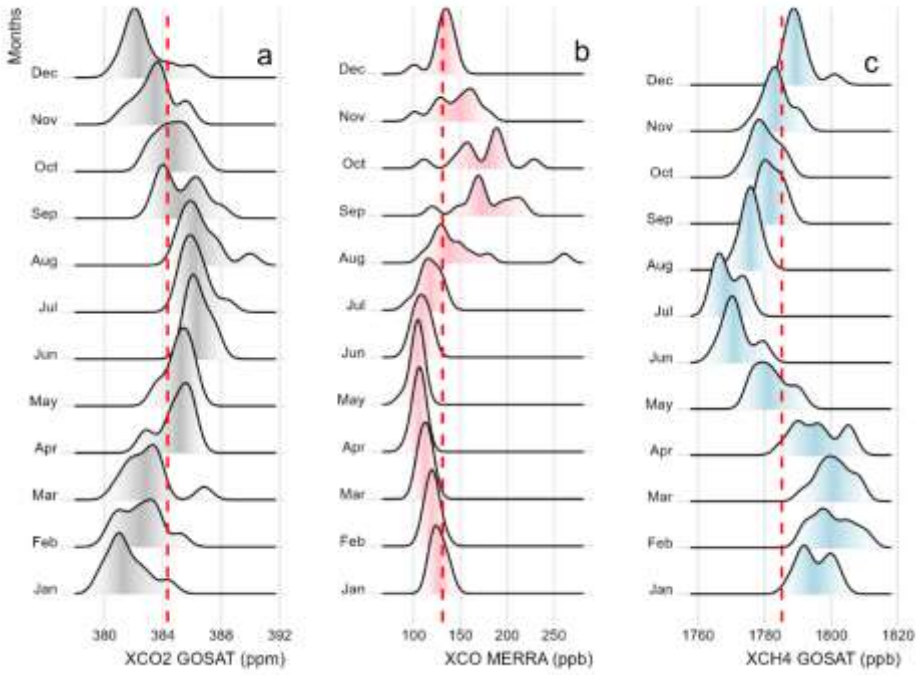

Figure 2.3. Monthly distribution of XCO_2, XCH_4 and, XCO monthly for the Amazon biome. XCO_2 data was obtained from the Japanese Space Agency - JAXA (Kuze et al. 2009) (a). XCH_4 GOSAT Proxy data obtained from the University of Leicester (Parker, R.; Boesch, 2020) (b). Monthly average XCO data obtained from NASA Giovanni (GMAO 2015) (c).

We observed that the monthly distribution of XCO presented higher values in the months of August to November (Figure 2.4 b), the driest period of the year and when there is a greater occurrence of fires (Fig.2 S1.). Mainly, in recent years, an increase in the fire foci number due to extreme climate events, such as ENSO (EL Niño).

On the other hand, we observed that the monthly distribution of CH_4 presented

values below the XCH_4 average (1785.18 ± 11.31 ppb) for the months of May to October (Figure 2.3. c) dry period when there was a reduction in monthly rainfall volume (Figure 2 A1.). In a study of emission distributions of CH_4 in the Amazon basin, between 2009 and 2018, we could observe a tendency for higher CH_4 emissions during the wet season (Wilson et al., 2020).

2.3.2. Annual and monthly averages of SIF, Fire foci number and Fire Radiative Power

Based on data acquired from the present study, the variable SIF recorded values below the annual average in the period studied (1,12 ± 0.16 W m^{-2} sr^{-1} μm^{-1}) for 2016, 2018 and 2019 (Figure 2.4 a). We noticed that the fire foci number and Fire Radiative Power was similar to the distribution of XCO for the monthly distribution (Figure 2.5 b e c).

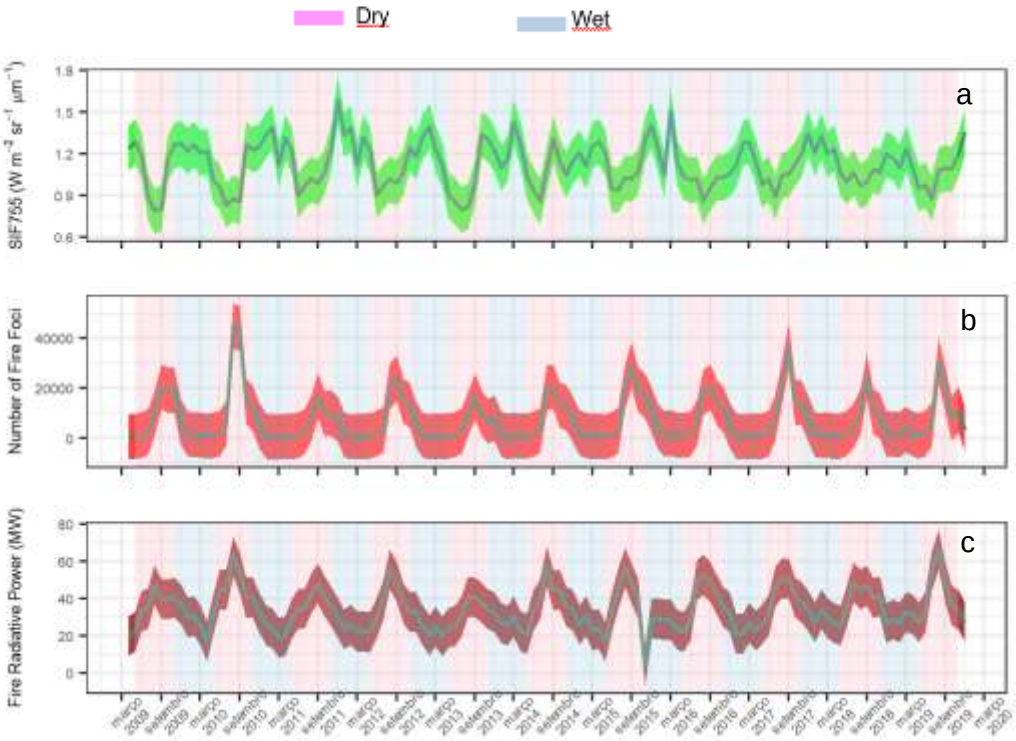

Figure 2.4. SIF755 GOSAT, Fire foci number, Fire Radiative Power (FRP) and annually for the Amazon biome. Pink rectangle is dry period and blue rectangle is wet period. Annual mean Sun-Induced Chlorophyll Fluorescence Data (SIF 755) obtained by the GOSAT satellite (Frankenberg, 2022) (a). Fire foci number (b) and Fire Radiative Power (c) data obtained by Moderate Resolution Imaging Spectroradiometer- MODIS (Giglio et al., 2003).

For the SIF data, we noticed that the monthly distribution also follows the

rainfall patterns, as the months from May to October record SIF values below the average (1.12 ± 0.16 W m^{-2} μm^{-1} sr^{-1}) (Figure 2.5 c). Based on our results, SIF value (Figure 2.5 c) were the highest in the Amazon basin during wet season. Similarly, this period (wet) there was the high rainfall volume and soil moisture.

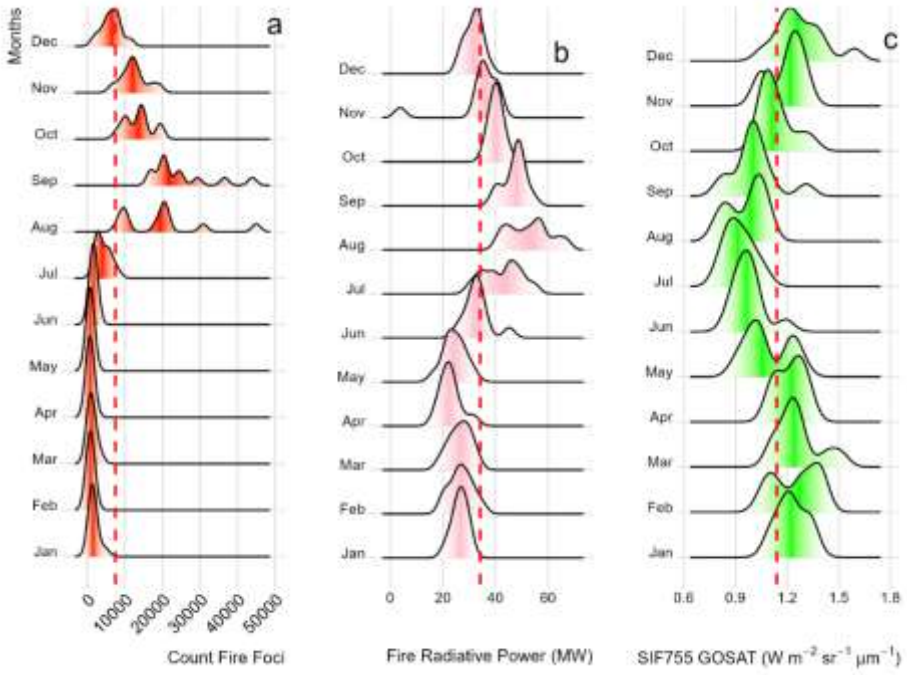

Figure 2.5. Monthly distribution of Fire foci number, Fire Radiative Power (MW) and SIF GOSAT monthly for the Amazon biome. Data from mean annual Sun-Induced Chlorophyll Fluorescence Data (SIF) obtained by the GOSAT satellite (Frankenberg, 2022) (a). Fire foci number (b) and Fire Radiative Power (c) obtained by Moderate Resolution Imaging Spectroradiometer- MODIS (Giglio et al., 2003).

2.3.3. Correlations between the variables

Spearman's temporal correlation analysis indicates positive interactions among variables XCO_2, XCO, Fire foci number, and FRP. However, we noticed that variables XCH_4, SIF, EVI, and Rainfall showed a negative linear correlation with variables XCO_2, XCO, Number of ire foci, and FRP for the time series (2009 to 2019).

The XCO_2 variable is negatively correlated to the EVI ($r=-0.71$ and $p<0.001$), rainfall ($r=-0.62$ and $p<0.001$), XCH_4 ($r=-0.66$ and $p<0.001$), and SIF ($r=-0.57$ and $p<0.001$) variables. On the other hand, there was a significant and positive correlation ($p<0.05$) of intermediate force between XCO_2 and FRP ($r=0.40$ and $p<0.001$) (Figure 2.6). As expected, the variable XCO had a positive correlation ($p<0.05$) with FRP ($r=0.54$ and $p<0.001$) and fire foci ($r=0.72$ and $p<0.001$) (Figure 2.6). Conversely,

XCH_4 was strongly correlated to rainfall (r=0.81 and p<0.001); however, it showed a significant positive correlation (p<0.05) of intermediate strength with variables SIF (r=0.71 and p<0.001) and EVI (r=0.64 and p<0.001) (Figure 2.6).

According to the blue lines, it may be possible to delimit the degree of positive interactions between the variables, for example, XCO_2 and FRP are more closely related than XCO (Figure 2.6). However, the red lines, delimiting the degree of negative interactions, and XCH_4 and the SIF greater degree of approximation, as shown in figure 2.6.

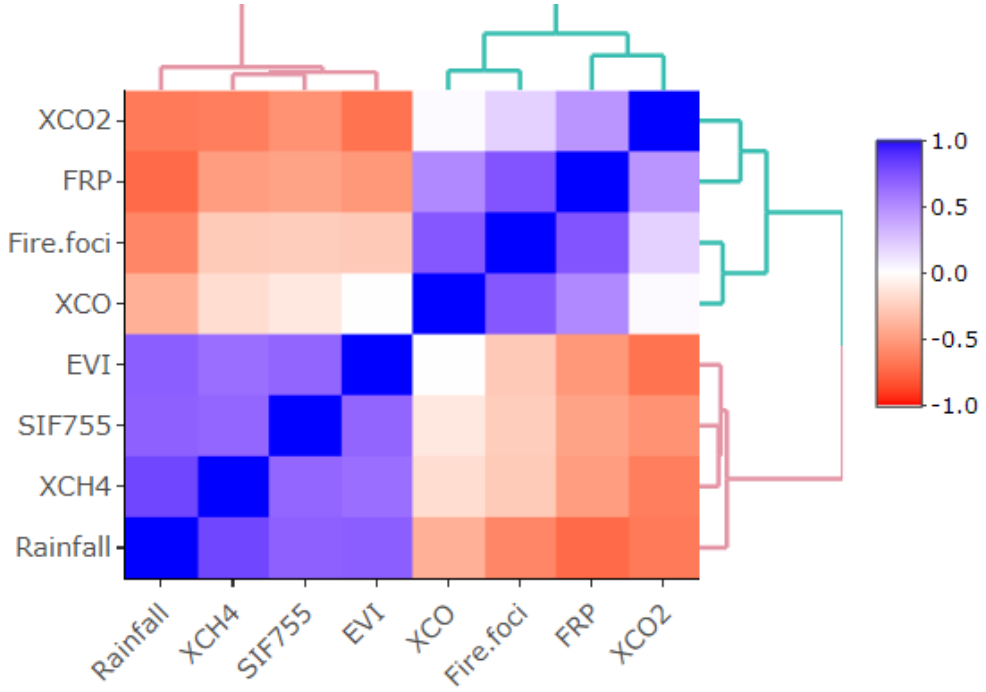

Figure 2.6. Correlation of variables XCO_2, XCH_4, XCO, SIF755, Rainfall, EVI, FRP and Fire Foci evaluated between the years 2009 to 2019 for the Brazilian Amazon biome. Red means a negative correlation (0 to 1) and blue means a positive correlation (0 to -1).

There were two significant correlations when the linear correlation method was applied, we could observe a positive linear correlation between XCO_2 and FRP and a second negative correlation between XCO_2 and SIF (Figure 2.7).

The analysis of standardized residuals indicates perceptible normality in the distribution of 95% of the residuals in the range of -2.5 and +2.5 to XCO_2 data. Thus, it was evidenced that the errors were approximately normally distributed with constant variance (Fig.2 S2).

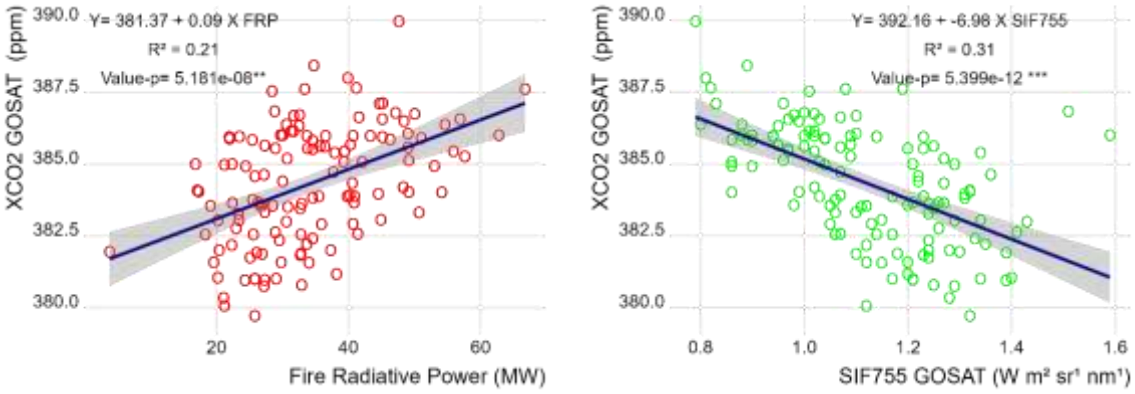

Figure 2.7. Linear regression between Fire Radiative Power (MW), Solar-Induced Fluorescence -SIF755 GOSAT (W m² sr¹ µm¹) and XCO_2 GOSAT (ppm) variables.

2.3.4. Results of the trend analysis

The Mann-Kendall test was not statistically significant ($p<0.05$), at the 5% probability level, statistically corroborating the confirmation of the absence of increasing or decreasing monotonic behavior in the annual average for the variables XCO_2, XCH_4, XCO, SIF, EVI, rainfall, FRP, and fire foci number analyzed in the time series (Table S1). Therefore, the Pettit test was deemed unnecessary, justified by the absence of a trend in the annual averages in the time series.

For trend analysis of monthly averages, XCO_2 and XCO applying the Mann-Kendall test were significant at the 5% probability level ($p<0.001$) (Table S2), indicating the presence of an increase for April along the time series, and the Pettit test was significant at the 5% probability level ($p<0.005$) (Table S3), indicating monotonic growth after 2014 to XCO_2 (Figure 2.8 A and Table S2). For the other months, this trend was not observed. Thus, there was increase of 0.30 ppm for XCO_2 (Figure 2.8 A and Table S2) and 1.6 ppb for XCO (Figure 2.8 B and Table S2) for the period of the time series.

Similarly, our results for the trend of monthly averages, the variable FRP (Mann-Kendall test), was significant ($p<0.001$) (Table S2), indicating the presence of increase FRP values for the month of April along the time series. In the same way, the FRP variable was also significant ($p<0.001$) (Figure 2.9 and Table S2) for the month of July. Thus, the Pettit test was significant for the month of April ($p<0.005$) (Figure 2.9 A and Table S3) and for the month of July ($p<0.005$), indicating continuous increase after 2014 (Figure 2.9 B and Table S3). For the other months, this trend was not observed.

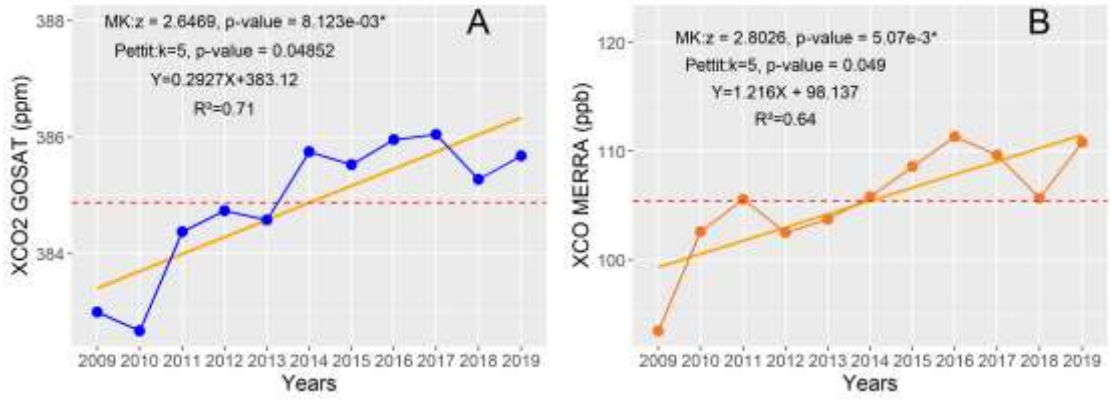

Figure 2.8. Trend for the monthly averages of April for XCO_2 GOSAT (ppm) (A) and XCO MERRA (ppb) (B) to MK-Mann Kendall Test, k- Change point at time. Red dashed line is the monthly average of April in the period from 2009 to 2019.

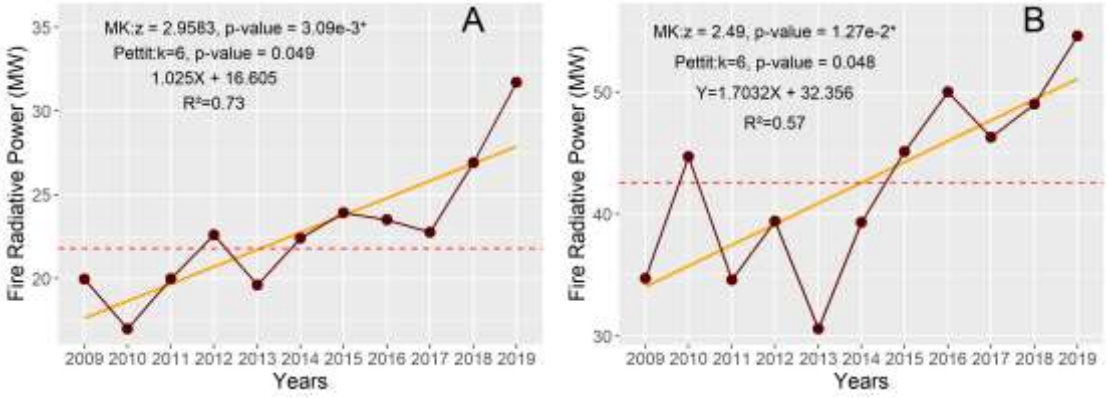

Figure 2.9. Trend for the monthly averages of April for Fire Radiative Power – FRP (Mw) (A) and July for FRP (B) para o MK-Mann Kendall Test, k- Change point at time. Red dashed line are the monthly average of April and July in the period from 2009 to 2019.

2.4. Discussion

2.4.1. XCO_2, EVI, SIF and Rainfall

In the time series from 2009 to 2019, our results showed the highest concentrations of CO_2 (XCO_2) and the lowest precipitation, as well as a reduction in the photosynthetic process of vegetation during the dry period in the Amazon (Figure 2.3 a and Figure 2 A1), suggesting that these combined factors can be leading the forest to lose its capacity to sequester carbon, justified by the lower availability of water and lower photosynthetic rate of the vegetation. It is worth noting that in 2009 and 2015, the lowest rainfall occurred, El Niño-Southern Oscillation (ENSO) (Pontes-Lopes et al., 2021) (Figure2 A1); on the other hand, the highest rainfall was observed in 2011, 2013, 2014, 2018 and 2019.

Thus, we also observed thatthe reduction in SIF and EVI variables was positively correlated to the XCO_2 increase. In the Amazon, low SIF values in the dry period indicate lower photosynthetic activity during the dry period than during the wet period, justified by the limitation of water (Albright et al., 2022; Wu et al., 2017), corroborated by the negative temporal correlation ($r = -0.62$ and $p<0.001$) between XCO_2 and rainfall (Figure 2.6). Similarly, the negative temporal correlation between EVI ($r=-0.71$ and $p<0.001$) and XCO_2 and SIF ($=-0.71$ and $p<0.001$) and XCO_2 (Figure 2.6).

2.4.2. XCO_2 and FRP

Our results pointed out that for the dry period, there is a higher occurrence of fire foci number and higher FRP values with a positive correlation with an increase in XCO_2 and XCO. This indicates a contribution of biomass burning emissions on the higher XCO_2 observed during this period in addition to the uptake reduction by photosynthesis (Figure 2.5 a e b). The most severe droughts caused by the El Niño-Southern Oscillation (ENSO) and the Atlantic Mutidecadal Oscillation (AMO) in the Amazon region (Marengo et al., 2018) GHG concentrations (XCO_2, XCH_4 and xN_2O) in the Amazon environment. The reduction of precipitation in the Amazon (L V Gatti et al., 2014), the intensification of land use change (C. V. J. Silva et al., 2020), and the flammability of the forest (Nepstad et al., 2004) are impacted by these more extreme weather events affecting the regional carbon cycle (Aragão et al., 2014).

2.4.3. XCH_4 and numbe of fire foci

Values of XCH_4 collected during the time series 2009 to 2019, did not positively correlate with the FRP and Fire foci number, however, there was a positive correlation ($p<0.005$) with Rainfall. Thus, it demonstrates that the most important factors impacting CH_4 concentrations in the atmosphere could be the higher soil moisture during the rainy season, and that soil moisture is a strong indicator of greater or lesser concentrations for the biome. In addition, the emissions from flooded areas are the largest source of methane (more than 70% of the total emission) and between years of 2014 to 2018 were estimated at 33.9 ± 10.8 Tg CH_4 y^{-1} in wetlands in the Amazon region (Basso et al., 2021). The La Niña events caused increase in the precipitation in the basin of the Amazon, which could increase wetland emissions (Nisbet et al., 2014). In the same way, escalating biomass burning emissions during the wet season,

mainly in 2019 (Silva Junior et al. 2019) and intensification of agricultural activities in the Amazon region were observed (Crippa et al., 2021).

2.4.4. XCH_4 and Rainfall

Values of XCH_4 collected during the time series 2009 to 2019, showed a positive correlation between XCH_4 and Rainfall (Figure 2.6). Similarly, Wilson et al. (2020) found a strong correlation between rainfall and methane and found that emissions increased during the rainy season (December-March). Therefore, our results pointed out that higher XCH_4 in the atmosphere during rainy season were observed between November and April (Figure 2.3 c), validating the strong positive correlation ($r=0.81$ and $p<0.001$) with rainfall, and suggesting that wet season in addition to flooded areas can be a more import source of CH_4 in the Amazon biome than CH_4 emission promoted by fires.

A study investigating the impact of rainfall from East Africa showed that the main sources of methane were wetlands, due to the decomposition of organic matter under anaerobic conditions (Mark F. Lunt et al., 2021). It is important to note that CH_4 emissions represent 65% of global emissions, together with emissions from agriculture and waste (Saunois et al., 2016) and this CH_4 emission can be explained by temperature, carbon availability and groundwater depth (Bloom et al., 2012; Lunt et al., 2019). Similarly, rainfall anomalies contribute to altering the water table, directly affecting CH_4 emissions in the wetlands (Pandey et al., 2017).

2.4.5. Correlations between variables

Considering the slope of the linear regression of XCO_2 against SIF, this regression has a slope of − 6.98 ppm (W m^{-2} sr^{-1} μm^{-1}). Costa et al. (2021), in a study in sugarcane-producing areas in São Paulo, found a lower angular coefficient of – 4.754 ppm (W m^{-2} sr^{-1} μm^{-1}), and there was a shorter period of evaluation of four years (2015 to 2018), which possibly contributes to the lower value of the coefficient.

On the other hand, the coefficient of determination of R^2 was 0.31, which indicates that the data established a relationship between the variables XCO_2 and SIF. It is worth noting that in the annual cycle, SIF increase is strongly related to precipitation, while CO_2 concentrations are related to the balance of photosynthesis and respiration (soil and plant) (Albright et al., 2022), highlighting that SIF is sensitive to incident dry periods in vegetation (Da Costa et al., 2021). For example, during the

2015-2016 El Niño events, which caused reduction in precipitation, corroborating with our study period of 2009 to 2019, when we observed high XCO_2 and lower SIF and lower photosynthetic activities and lower SIF values and high XCO_2 even in the rainy season (Liu et al., 2017; Yang et al., 2018). And this increase of the suppression of Gross Production Primary (GPP) and an increase of respiration over tropical forest consequently lower SIF values (Koren et al., 2018).

Based on our results, for the years 2009 to 2019, the values of FRP were positively correlated with XCO_2, acting as a driver in increasing the concentration of CO_2 in the atmosphere. Additionally, fire foci promote the highest concentrations of CO in the Brazilian Amazon biome, especially in the period of lower precipitation from the period of May to October, and greater occurrence of fires. The FRP is a rate of thermal release radiation from a fire and is highly correlated with the rate of fuel consumption, making it an excellent indicator of emission of gases (CO_2 and CO) to the atmosphere (Freeborn et al., 2008; Wooster et al., 2005).

2.4.6. Trend analysis for variables

Our results showed a monotonic growth for the month of April in the XCO_2 and XCO observed for the time series (2009 to 2019). As the Amazon rainforest is not tolerant of fire (Bush, 2017), our results can support the concern because there could be an increase in the dry period in the south region and a reduction in the rainy season in the north, considering the month of April. Even though there was no reduction trend for rainfall in this month (April). Similarly, rainfall volume and temperature can cause possible changes in vegetation, from forest to savanna in the Amazon, but other factors, such as increased occurrence of fire foci number (Bush, 2017; Nobre et al., 2016).

Our study showed that there was an increase of XCO_2 showing a correlation between the variables of atmospheric concentrations of gases (XCO_2 and XCO) and fire foci number in the Brazilian Amazon biome. The Amazon biome is considered the largest tropical forests on Earth, therefore showing high relevance as an essential carbon sink in recent decades (Maia et al., 2020). However, this carbon sink could possibly be in decline by the increase of land use change, fires, and droughts in the biome (Gatti et al., 2021).

Based on our results, fires increase the concentrations of direct GHG (XCO_2) and indirect GHG (XCO) and reverse the role of the Amazon Forest from a sink to a

source of CO_2 and CO to the atmosphere. This is worrisome from a climate point of view, as it shows that the Amazon biome may be very close to the “tipping point” (Lovejoy and Nobre, 2018), in addition to directing discussions on the processes of savannization of the biome (Nobre et al., 2016), mainly the southern and eastern portion of the Amazon biome. Thus, understanding GHG emissions and their dynamics can be important and essential for better targeting firefighting policies.

2.5. Conclusion

Thus, the main hypothesis of the present study emphasizes that there is a tendency for growth in the concentrations of gases, especially CO and CO_2 due to natural or anthropogenic changes carried out in the region. Our objective was to investigate the temporal variability of GHs over the Brazilian Amazon and its correlation with vegetative aspects and fire foci number that occurred in the region between 2009 and 2019. Therefore, the present study aims to answer the following questions: (i) Was there a correlation between the GHG (CO_2) and SIF (Vegetation) and FRP (Power fire)? (ii) Similarly, was there an increase (trend) in the concentration of CO and CO_2 gases? The monthly averages of XCO_2 and XCO presented increase for the month of April, after 2014, with FRP indicating continuous increase for the months of April and July. This increase of gases (CO_2 and CO) and fire occurrence (FRP) for the months of April and July was not related to rainfall in this period but possibly to anthropic activities, such as the use of fire and deforestation in the biome. Additionally, correlations and regression analysis corroborated with the establishment of positive drivers between XCO_2 and FRP, that is, a relationship with the occurrence of fires in the biome. Therefore, our results evidenced an early fire occurrence and the increase of atmospheric gases (XCO and XCO_2) in the Amazon biome, possibly due to more intense and severe droughts as a result of climate change, especially in recent years, which contributes to increasing the occurrence of fires, making the Amazon biome vulnerability increase and reducing its capacity as a global carbon sink.

2.6. Acknowledgment

The study was funded by the Coordenação de Aperfeiçoamento de Pessoal de Nível Superior (CAPES). I am grateful to the group Geotechnology Applied in Agriculture and Forestry (GAAF) and SojaMaps and to the University of the State of

Mato Grosso (UNEMAT) for the infrastructure of this study.

2.7. References

ALBRIGHT, R. et al. Seasonal Variations of Solar-Induced Fluorescence, Precipitation, and Carbon Dioxide Over the Amazon. **Earth and Space Science**, v. 9, n. 1, p. 1–11, 2022.

ALVARES, C. A. et al. Köppen's climate classification map for Brazil. **Meteorologische Zeitschrift**, v. 22, n. 6, p. 711–728, 1 dez. 2013.

AMIGO, I. The Amazon's Fragile Future. Nature, v. 578, n. February, p. 505–507, 2020.

ARAGÃO, L. E. O. C. et al. Environmental change and the carbon balance of Amazonian forests. **Biological Reviews**, v. 89, n. 4, p. 913–931, 1 nov. 2014.

BERTANI et al. Chlorophyll fluorescence data reveals climate-related photosynthesis seasonality in Amazonian forests. **Remote Sens.**, 9, 1275, 2017.

BRANDO, P. M. et al. The gathering firestorm in southern Amazonia. **Science Advances**, v. 6, n. 2, p. 1–10, 2020.

CASTRO, A.O. et al. OCO-2 Solar-Induced Chlorophyll Fluorescence Variability across Ecoregions of the Amazon Basin and the Extreme Drought Effects of El Niño (2015–2016). **Remote Sens.** 12, 1202, 2020.

CHEVALLIER, F. et al. On the impact of transport model errors for the estimation of CO_2 surface fluxes from GOSAT observations. **Geophysical Research Letters**, v. 37, n. 21, 2010.

CRIPPA, M. et al. GHG emissions of all world countries -Report, EUR 30831 EN, Publications Office of the European Union, Luxembourg, 2021, 12 p.

DA COSTA, L. M. et al. Spatiotemporal variability of atmospheric CO_2 concentration and controlling factors over sugarcane cultivation areas in southern Brazil. **Environment, Development and Sustainability**, n. 0123456789, 2021.

DA CRUZ DC, BENAYAS JMR, FERREIRA GC, et al. An overview of forest loss and restoration in the Brazilian Amazon. New Forests 52:1–16, 2021

DRUSCH, M. et al. The fluorescence explorer mission concept—ESA's earth explorer

8. IEEE Trans. Geosci. Remote Sens. , 55, 1273–1284, 2017

FENG, L. et al. Evaluating a 3-D transport model of atmospheric CO_2 using ground-based, aircraft, and space-borne data. **Atmospheric Chemistry and Physics**, v. 11, n. 6, p. 2789–2803, 2011.

FRANKENBERG, C. et al. New global observations of the terrestrial carbon cycle from GOSAT: Patterns of plant fluorescence with gross primary productivity. **Geophysical Research Letters**, v. 38, n. 17, p. 1–6, 2011.

FRANKENBERG, C. **GOSAT Solar-Induced Chlorophyll Fluorescence Datasets** 2009-2020 (Version 1.0). Available in <https://data.caltech.edu/records/8771>. Acess on: March 12 2021.

FREEBORN, P. H. et al. Relationships between energy release, fuel mass loss, and trace gas and aerosol emissions during laboratory biomass fires. Journal of **Geophysical Research**, v. 113, n. D1, p. D01301, 5 jan. 2008.

GATTI, L. V et al. Drought sensitivity of Amazonian carbon balance revealed by atmospheric measurements. **Nature**, v. 506, n. 7486, p. 76–80, 2014.

GELARO, R. et al. The Modern-Era Retrospective Analysis for Research and Applications, Version 2 (MERRA-2). **Journal of Climate**, v. 30, n. 14, p. 5419–5454, 2017.

GIGLIO, L. et al. An Enhanced Contextual Fire Detection Algorithm for MODIS. **Remote Sensing of Environment**, v. 87, n. 2–3, p. 273–282, out. 2003.

GUERLET, S. et al. Reduced carbon uptake during the 2010 Northern Hemisphere summer from GOSAT. **Geophysical Research Letters**, v. 40, n. 10, p. 2378–2383, 2013.

GUO, M. et al. The effects of sand dust storms on greenhouse gases. International **Journal of Remote Sensing**, v. 33, n. 21, p. 6838–6853, 2012.

GUO, M. et al. CO_2 emissions from the 2010 Russian wildfires using GOSAT data. **Environmental Pollution**, v. 226, p. 60–68, 2017.

HERRERA ESTRELLA, E. et al. Quantifying vegetation response to environmental

changes on the Galapagos Islands, Ecuador using the Normalized Difference Vegetation Index (NDVI). **Environmental Research Communications**, v. 3, n. 6, p. 065003, 2021.

IBGE - **INSTITUTO BRASILEIRO DE GEOGRAFIA E ESTATÍSTICA.** Conheca cidades e Estados do Brasil.

INPE. **Instituto Brasileiro de Pesquisas Espaciais BDQueimadas.** Available in: <https://queimadas.dgi.inpe.br/queimadas/bdqueimadas> Acess on: July 17 2022.

JOINER, J. et al. First observations of global and seasonal terrestrial chlorophyll fluorescence from space. **Biogeosciences**, v. 8, n. 3, p. 637–651, 2011.

KENDALL, M. G. **Rank correlation methods**. Oxford, England: Griffin, 1948.

KOCH, N. et al. Agricultural Productivity and Forest Conservation: Evidence from the Brazilian Amazon. **American Journal of Agricultural Economics**, v. 101, n. 3, p. 919–940, 2019.

KOREN G. et al. Widespread reduction in sun-induced fluorescence from the Amazon during the 2015/2016 El Niño. **Phil. Trans. R. Soc.** v.373, n1, 2018.

KUZE, A. et al. Thermal and near infrared sensor for carbon observation Fourier-transform spectrometer on the Greenhouse Gases Observing Satellite for greenhouse gases monitoring. **Applied Optics**, v. 48, n. 35, p. 6716, dez. 2009.

LIU, J. et al. Contrasting carbon cycle responses of the tropical continents to the 2015–2016 El Niño. **Science**, v. 358, n. 6360, 2017.

LOVEJOY, T. E.; NOBRE, C. Amazon tipping point. **Science Advances**, v. 4, n. 2, p. 1–2, 2018.

LOVEJOY, T. E.; NOBRE, C. Amazon tipping point: Last chance for action. **Science Advances**, v. 5, n. 12, p. 4–6, 2019.

MANN, H. B. Nonparametric Tests Against Trend Author (s): Henry B . Mann Published by : The Econometric Society Stable. **Econometrica**, v. 13, n. 3, p. 245–259, 1945.

MARENGO, J. A. et al. Changes in Climate and Land Use Over the Amazon Region: Current and Future Variability and Trends. **Frontiers in Earth Science**, v. 6, n. December, p. 1–21, 2018.

Mapbiomas - **Coleção 7 (1985-2021) da Série Anual de Mapas de Cobertura e Uso de Solo do Brasil.** Disponível em: https://plataforma.mapbiomas.org/map#coverage. Acesso em: 02 set 2022.

MIETTINEN, J. et al. On the extent of fire-induced forest degradation in Mato Grosso, Brazilian Amazon, in 2000, 2005 and 2010. **International Journal of Wildland Fire**, v. 25, n. 2, p. 129–136, 2016.

NEPSTAD, D. et al. Amazon drought and its implications for forest flammability and tree growth: a basin-wide analysis. **Global Change Biology**, v. 10, n. 5, p. 704–717, 2004.

NISBET, E. G. et al. Very Strong Atmospheric Methane Growth in the 4 Years 2014–2017: Implications for the Paris Agreement. **Global Biogeochemical Cycles**, v. 33, n. 3, p. 318–342, 1 mar. 2019.

NOBRE, C. A. et al. Land-use and climate change risks in the amazon and the need of a novel sustainable development paradigm. P**roceedings of the National Academy of Sciences of the United States of America**, v. 113, n. 39, p. 10759–10768, 2016.

OFFICE, G.-G. M. AND A. **Global Modeling and Assimilation Office (GMAO)** MERRA-2 tavgM_2d_chm_Nx: 2d,Monthly mean,Time-Averaged,Single-Level,Assimilation,Carbon Monoxide and Ozone Diagnostics V5.12.4. Available in <https://disc.gsfc.nasa.gov/datasets/M2TMNXCHM_5.12.4/summary>. Acess on: January 31 2022.

OGUMA, H. et al. First observations of CO2 absorption spectra recorded in 2005 using an airship-borne FTS (GOSAT TANSO–FTS BBM) in the SWIR spectral region. **International Journal of Remote Sensing**, v. 32, n. 24, p. 9033–9049, 2011.

OLIVEIRA, U. et al. Determinants of Fire Impact in the Brazilian Biomes. Frontiers in **Forests and Global Change**, v. 5, n. March, p. 1–12, 2022.

PARKER, R.; BOESCH, H. **University of Leicester GOSAT Proxy XCH_4 v9.0**. Centre for Environmental Data Analysis.

PARKER, R. et al. Methane observations from the Greenhouse Gases Observing SATellite: Comparison to ground-based TCCON data and model calculations. **Geophysical Research Letters**, v. 38, n. 15, ago. 2011.

PARKER, R. J. et al. Assessing 5 years of GOSAT Proxy XCH₄ data and associated uncertainties. **Atmospheric Measurement Techniques**, v. 8, n. 11, p. 4785–4801, nov. 2015.

PETERS, W. et al. An atmospheric perspective on North American carbon dioxide exchange: CarbonTracker. **Proceedings of the National Academy of Sciences**, v. 104, n. 48, p. 18925–18930, 2007.

PETTITT, A. N. A Non-Parametric Approach to the Change-Point Problem Published by : Wiley for the Royal Statistical Society A Non-parametric Approach to the Change-point Problem. J**ournal of the Royal Statistical Society. Series C (Applied Statistics)**, v. 28, n. 2, p. 126–135, 1979.

PONTES-LOPES, A. et al. Drought-driven wildfire impacts on structure and dynamics in a wet Central Amazonian forest. Proceedings of the Royal Society B: **Biological Sciences**, v. 288, n. 1951, 2021.

Porcar-Castell, A. et al. Linking chlorophyll a fluorescence to photosynthesis for remote sensing applications: Mechanisms and challenges. J. Exp. Bot., 65, 4065–4095, 2014.

R Core Team. R: A language and environment for statistical computing. **R Foundation for Statistical Computing**, Vienna, Austria, 2022.

RIBEIRO, T. M. et al. Fire foci assessment in the Western Amazon (2000–2015). **Environment, Development and Sustainability**, v. 23, n. 2, p. 1485–1498, 2020.

ROSS, A. N. et al. First satellite measurements of carbon dioxide and methane emission ratios in wildfire plumes. **Geophysical Research Letters**, v. 40, n. 15, p. 4098–4102, ago. 2013.

SILVA, C. A. et al. Fire occurrences and greenhouse gas emissions from deforestation in the Brazilian Amazon. **Remote Sensing**, v. 13, n. 3, p. 1–18, 2021.

SILVA, C. H. L. et al. Deforestation-induced fragmentation increases forest fire

occurrence in central Brazilian Amazonia. **Forests**, v. 9, n. 6, 2018.

SILVA JUNIOR, C. H. L.. et al. Fire Responses to the 2010 and 2015/2016 Amazonian Droughts. **Front. Earth Sci.**, v. 7, n3, 2019.

SILVA, C. V. J. et al. Estimating the multi-decadal carbon deficit of burned Amazonian forests. **Environmental Research Letters**, v. 15, n. 11, 2020.

TUNNICLIFFE, R. L. et al. Quantifying sources of Brazil's \chem{CH_4} emissions between 2010 and 2018 from satellite data. **Atmospheric Chemistry and Physics**, v. 20, n. 21, p. 13041–13067, 2020.

WILLIAMS, C. A. et al. Disturbance and the carbon balance of US forests: A quantitative review of impacts from harvests, fires, insects, and droughts. **Global and Planetary Change**, v. 143, p. 66–80, 2016.

WILSON, C. et al. Large and increasing methane emissions from Eastern Amazonia derived from satellite data, 2010--2018. **Atmospheric Chemistry and Physics Discussions**, v. 2020, p. 1–38, 2020.

WOOSTER, M. J. et al. Retrieval of biomass combustion rates and totals from fire radiative power observations: FRP derivation and calibration relationships between biomass consumption and fire radiative energy release. **Journal of Geophysical Research**, v. 110, n. D24, p. D24311, 2005.

WU, J. et al. Partitioning controls on Amazon forest photosynthesis between environmental and biotic factors at hourly to interannual timescales. **Global Change Biology**, v. 23, n. 3, p. 1240–1257, 2017.

YANG, J. et al. Amazon drought and forest response: Largely reduced forest photosynthesis but slightly increased canopy greenness during the extreme drought of 2015/2016. **Global Change Biology**, v. 24, n. 5, p. 1919–1934, 2018.

ZEMP, D. C. et al. Self-amplified Amazon forest loss due to vegetation-atmosphere feedbacks. **Nature Communications**, v. 8, n. 1, p. 14681, 2017.

CHAPTER 3 - SPATIOTEMPORAL ANALYSIS OF ATMOSPHERIC XCH_4 AS RELATED TO FIRES IN THE AMAZON BIOME DURING 2015–2020

ABSTRACT - Studies that focus on the concentration of methane and its correlation with the fire foci number in the Amazon become relevant in the current scenario, especially due to the increasing environmental degradation associated with climate change. Thus, we investigated the patterns of spatio-temporal variability in the atmospheric concentration of CH_4 and the relationships with fire foci number, land surface temperature, CO_2 anomalies, and soil moisture under the Amazon biome between January 2015 and December 2020. For this, we used the active fires foci (Fire foci number) and Land Surface Temperature (LST) obtained through the Moderate Resolution Imaging Spectroradiometer (MODIS) sensor, and the atmospheric column-averaged of methane (XCH_4) and carbon dioxide (XCO_2) obtained by the GOSAT satellites and Orbiting Carbon Observatory-2 (OCO-2), respectively. After we obtained XCO_2 data, we calculated the individual value of XCO_2 observed by the OCO-2 and the background of the daily median of XCO_2 over an area of Brazilian territory. For the Soil Moisture (SMAP), we used orbital data from satellite Soil Moisture Active Passive (SMAP). Our results originate from the dry and wet seasons, and the XCH_4 presented as annual average of 1794 ± 5.3 ppb for the rainy season, while for the dry period, the XCH_4 was 1789±5.6 ppb. For the spatial distribution of XCH_4, we noticed a significant correlation ($r = 0.53$ and $p < 0.05$) between XCH_4 and XCO_2 Anomaly in the dry season, possibly justified by the increase in fire foci number umber. Additionally, in the dry period, we noticed that XCH_4 was significantly correlated with SMAP ($r = 0.97$, $p< 0.01$), validating the hypothesis of a strong relationship between the variables. The temporal variability of XCH_4 was significant for SMAP ($r = 0.65$ and $p < 0.01$), similar to the significance of the LST ($r = 0.66$ and $p < 0.01$). Thus, the temporal distribution of XCH_4 was positively correlated to both biophysical variables (soil moisture and land surface temperature). Therefore, considering more frequent droughts and the predominance of fires in the region, as well as the increase in global average temperature, there will be an increase in greenhouse gas (GHG) emissions, especially methane, further impacting the Amazonian ecosystem, because the biome is vulnerable to climate change.

Key words: Arc of Deforestation; Climate Changes; Fire Foci; Methane; Soil Moisture

CAPÍTULO 3 - VARIAÇÕES ESPAÇO-TEMPORAL DE XCH_4 ATMOSFÉRICO E RELACÕES COM FOGO NO BIOMA AMAZÔNIA DURANTE 2015-2020

RESUMO - Estudos que enfocam a concentração de metano e a correlação com número de focos de incêndios na Amazônia tornam-se relevantes no cenário atual, especialmente devido à crescente degradação ambiental associada às mudanças climáticas. Então, investigamos com os padrões espaciais e variabilidade temporal de XCH_4 em períodos secos e úmidos, relacionando esses com os focos de incêndios, temperatura da superfície terrestre, as anomalias de CO_2 e a umidade do solo sob no bioma Amazônico, entre Janeiro 2015 a Dezembro 2020. Para isto, utilizamos os focos ativos de incêndios (Fire Foci) e Land Surface Temperature (LST) obtidos por meio do sensor Moderate Resolution Imaging Spectroradiometer (MODIS), os dados de concentrações atmosféricas da coluna média de metano (XCH_4) e de dióxido de carbono (XCO_2) obtidos pelos satélites GOSAT e o Orbiting Carbon Observatory-2 (OCO-2), respectivamente. Após obtermos os dados de XCO_2 calculamos o valor valor individual observado de XCO_2 pelo OCO-2 e o background da mediana diária de XCO_2 sobre a area do território brasileiro. Para a umidade do solo (SMAP) usamos dados orbitais do satélite Soil Moisture Active Passive (SMAP). Nossos resultados apontam que no período úmido e período, o XCH_4 apresentou uma média anual de 1794 ± 5.3 ppb para período chuvoso, enquanto XCH_4 apresentou uma média anual de 1789±5.6 ppb para período seco. Para a distribuição espacial do XCH_4 notamos uma correlação significativa ($r=0.53$ e $P<0.05$) de forma intermediária entre XCH_4 Dry e a Anomaly XCO_2, possivelmente justificado pelo incremento dos focos de incêndios. Adicionalmente, no periodo seco, observou-se que o XCH_4 Dry se correlacionou significativamente com SAMP ($r=0.97$, $p< 0,01$), validando a hipótese da forte relação entre as variáveis. A variabilidade temporal de XCH_4 foi também significativa com SMAP ($r=0.65$ e $p < 0,01$) tendo significativa similar ($r=0.66$ e $p < 0,01$) com a variável LST. Assim, a distribuição temporal de XCH4 foi positivamente correlacionada com ambas as variavéis biofísicas (umidade do solo como a temperatura da superfície terrestre). Portanto, considerando as secas mais frequentes e a predominância de incêndios na região, bem como o aumento da temperatura média global, haverá um aumento das emissões de gases de efeito estufa (GEE), principalmente o metano, impactando ainda mais o ecossistema amazônico, isso porque o bioma é vulnerável às mudanças climáticas.

Palavras-chave: Arco do desmatamento; Mudanças climáticas; Focos de incêndios; Metano; Umidade do Solo

3.1. Introduction

The Brazilian Amazon biome has a high environmental representation due to its great biodiversity of plants and animals and is therefore considered the largest continuous tropical forest on Earth, occupying 3% of the terrestrial territory (Heinrich et al., 2021). It stands out especially for its capacity as a carbon sink (C) and consequent mitigation of the greenhouse effect (Antonelli et al., 2018; Brienen et al., 2015; Heinrich et al., 2021).

However, there is high vulnerability of this biome due to changes in land use and climate (Marengo et al., 2018; Nobre et al., 2016), mainly in areas where forests are most degraded (Saatchi et al., 2021), which are threatened by deforestation and fire (da Silva Junior et al., 2022; Eufemia et al., 2022; Le Roux et al., 2022; Teodoro et al., 2022). In addition, this biome has been affected by increasingly frequent and extreme droughts, which tend to negatively modify the equilibrium state of humid tropical forests in the coming decades (Anderson et al., 2018; Nobre et al., 2016; Silva et al., 2018).

According to the Intergovernmental Panel on Climate Change (IPCC) report (IPCC, 2022), current atmospheric GHG levels expose the human inability to reduce their impact on the climate. Currently, the atmospheric concentration of methane has reached 1877.3±3.3 ppb (IPCC, 2019), an increment of 2.6 times greater than the concentrations prior to the preindustrial revolution period (Nisbet et al., 2019; Saunois et al., 2020). In addition to alarming atmospheric levels, methane has a heating potential 28 times greater (100 years) than CO_2 (IPCC, 2019). According to the sixth assessment report (AR6) of the IPCC, despite the shorter length of stay (~10 years), methane contributed to approximately 16% (0.54 Wm^{-2}) of the total effective radiative forcing (ERF) among the GHGs for the period 1750-2019.

Regarding the emission sources, wetlands stood out among the interannual variability of CH_4 sources (Bousquet et al., 2006) and, to a lower extent, emissions from incomplete combustion of biomass and soil carbon during foci of forest fires (Kirschke et al., 2013). The frequency and severity of droughts increase the occurrence of fire foci in the in Amazon biome (Anderson et al., 2018; Basso et al., 2021; Morgan et al., 2019), which consequently increase CH_4 emissions, especially in areas with large amounts of biomass, mainly in the tropics, where tropical forests

(Amazon Forest) are burned (Saunois et al., 2020), and emit high amounts of CH_4 into the atmosphere due to incomplete burning of forest biomass (Basso et al., 2021).

The GOSAT mission aimed to assess the sources and sinks of GHGs to estimate atmospheric concentrations of CH_4 (XCH_4) at regional and global scales. Therefore, it sought to contribute to the generation of information and better management of environmental resources, in addition to assisting research aimed at understanding the global ecosystem carbon cycle, through the observation of the averaged atmospheric column CO_2 (XCO_2) (Guo et al., 2017; Oguma et al., 2011).

Similarly, the OCO-2 mission launched in July 2014 by NASA also makes it possible to observe XCO_2 from space (Frankenberg et al., 2015). Thus, CO_2 emissions from forest fires have been contemplated by several studies, whether in boreal forests (Guo et al., 2019, 2017) or rainforests (Heymann et al., 2017; Jiang et al., 2021; Yin et al., 2018). However, it is worth noting that fires in tropical forests can produce more carbon monoxide (CO) and CH_4 per unit of fuel burned (Webb et al., 2016; Wecht et al., 2014; Wilson et al., 2020). The frequency and severity of droughts accentuate the occurrence of fires, which consequently increase CH_4 emissions (Anderson et al., 2018; Basso et al., 2021; Morgan et al., 2019).

Despite the importance of the topic, there are several gaps in the understanding of the temporal distribution and spatialization of fires and their relationship with CH_4 emissions, especially for those occurring in the Amazon biome. Geostatistical interpolation methods, such as kriging, are important ways to relate the distribution of XCH_4 in space and over the years of study (Li et al., 2022). This method has been used to fill important gaps in regard to GHG, especially in the period of greater occurrence of fires and when comparing dry and wet periods (Devkota, 2021; Falahatkar et al., 2017; Li et al., 2022).

This study aimed to test 2 main hypotheses: (i) is the spatialization of XCH_4 seasonality related to fire foci? and (ii) are there any correlation between XCH_4 and soil moisture for the dry and wet periods under the Amazon? Thus, the objective of the study was to investigate the patterns of spatio-temporal variability of the atmospheric concentration of CH_4 and the correlations with the MODIS products (Fire foci number and LST), XCO_2 anomalies, and the product of Soil Moisture Active Passive (soil moisture) in the Brazilian Amazon.

3.2. Material and methods

3.2.1. Study area

The study area comprises the Brazilian Amazon Forest biome (Figure 2.1.), with a territorial extension of 4.2 million km², covering the states of Acre, Amapá, Amazonas, Pará, Roraima, Rondônia and partially the state of Maranhão, Mato Grosso and Tocantins (IBGE, 2020).

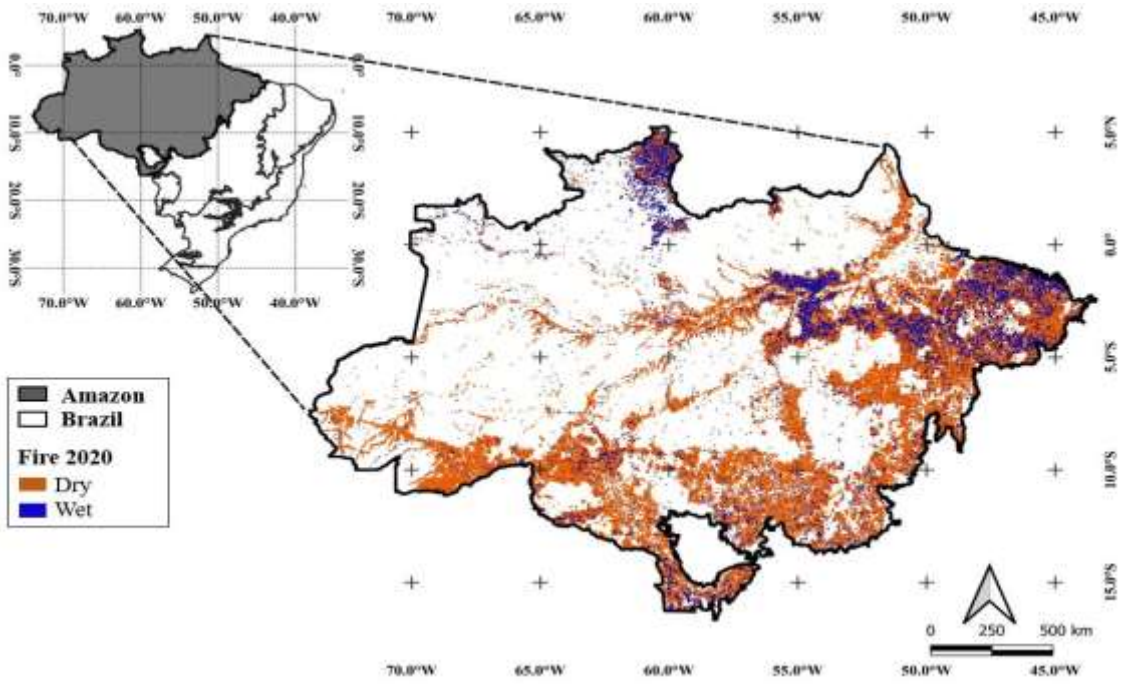

Figure 3.1. The study area in the Brazilian Amazon Forest Biome with fire foci during Dry (Orange) and Wet (Blue) period in 2020 obtained from Moderate Resolution Imaging Spectroradiometer (MODIS) data using swath products (MOD14/MYD14; FIRMS, 2022; Giglio et al., 2003).

According to the Koppen climate classification of the Amazon forest, the predominance of climate classes Am (monsoons) and Aw (with dry winters) occurs under the studied area. The annual precipitation varies from 1800 to 4000 mm, and the average temperature is 26.8°C in the Amazon region (Alvares et al., 2013). The dry period is evidenced from May to October, and the rainy season extends from November to April each year (Zemp et al., 2017).

3.2.2. Land Surface Temperature Data

In Land Surface Temperature (LST) analysis, daytime and nighttime data from the MOD11A2 V006 product from several regions worldwide was used (Wan, Z. et al., 2015), which were produced by NASA (National Aeronautics and Space Administration) from the MODIS (Moderate-Resolution Imaging Spectroradiometer) sensor with 8 days with a spatial resolution of 1 km^2, in which images with fewer invalid pixels were chosen.

The annual average of the MOD11A2 product data was calculated using the Raster Calculator tool of the QGIS 3.16.4-Hannover software. Additionally, the results of calculating the surface temperature without units were multiplied by a scale factor of 0.02 to obtain Kelvin (K) degrees, then converted to Celsius (°C; Equation 1) and divided by 8 to obtain daily values (Wan, Z., Hook, S., & Hulley, 2015).

$$\text{LST\_Celsius\_Day} = \frac{(LST_Day_1 km * 0.02) - 273.25}{8} \quad \text{Equation (1)}$$

3.2.3. Fire Foci Number Data

The daily data of fire foci number of the time series was obtained between 2015 and 2020. Data was obtained directly from the Atmosphere Near real-time Capability for EOS (LANCE) Fire Information for Resource Management System (FIRMS; https://firms.modaps.eosdis.nasa.gov/), calculated through the product obtained by the Moderate Resolution Imaging Spectroradiometer (MODIS) sensor onboard the TERRA/AQUA satellites. Additionally, for data processing, the daily averages of the daily observations of Fire foci number were calculated for each pixel (1 km). Then, the number of points (n) of fire foci number greater than 8 in each pixel was considered. It is worth mentioning that the amount of number of observations (n) influences the construction of better estimates of the parameters of fires.

3.2.4. Orbiting Carbon Observatory 2 (OCO-2) Data

The Orbiting Carbon Observatory-2 (OCO-2) satellite was launched by NASA in July 2014 and has contributed with information about the atmospheric concentration of carbon dioxide (CO_2) available as a primary product since September 2014 (Crisp et al., 2017). According to Crowell et al (2019), this tool made it possible to estimate CO_2 sinks and sources on regional scales. The average concentration of CO_2 in a column of dry air (XCO_2) extends from the Earth's surface to the top of the

atmosphere, approximately 740 km (Crisp et al., 2012; O'Dell et al., 2012).

The data is made available by the OCO-2 (NASA) platform: https://oco2.gesdisc.eosdis.nasa.gov/data/OCO2_DATA/. The XCO_2 values (version V9r) are retrieved using the algorithm of O'Dell et al (2012); therefore, OCO-2 enables products to have a spatial resolution of 2.25 × 1.29 km and a temporal resolution of 16 days. Furthermore, the observations that have the best visibility and the lowest level of uncertainty were considered (quality flag = 0 and alert level < 12) (Costa et al., 2022; Nikitenko et al., 2020; Rossi et al., 2022).

Therefore, the XCO_2 increase trend for the time series studied (2015-2020) was corrected to make it possible to cover the entire territory of Brazil. Thus, this work evaluates CO_2 concentration and its correlation among fire foci in Dry and Wet periods.

3.2.5. Anomaly XCO_2 data from the Amazon biome, 2015-2020, with OCO-2

Due to the long lifetime of CO_2 in the atmosphere, the high difficulty of extracting information from the spatial distributions of the emission areas from XCO_2 satellite measurements, with the averages for each year, becomes evident. Thus, the accumulation of CO_2 in the atmosphere demonstrates a growth rate of approximately 2-3 ppm per year (Hakkarainen et al., 2016). It currently has a general background level of approximately 418 ± 0.2 ppm (NOAA, 2022).

Therefore, to extract the information from the anthropogenic signatures of orbital recoveries (OCO-2 satellite), the XCO_2 concept was used (Hakkarainen et al., 2016). In the present study, the difference between the individual value of XCO_2 observed by the OCO-2 satellite and the background (the daily median of XCO_2 over an area of Brazilian territory) was calculated according to equation 2.

$XCO_2(\text{anomaly}) = XCO_2(\text{individual}) - XCO_2(\text{daily median from Brazil})$ Equation (2)

The result of the equation displays XCO_2 Anomaly values for each pixel (~3 km) of the OCO-2 data. Using the daily background facilitates the removal of seasonal variability and the upward trend of XCO_2. After calculating the XCO_2 anomaly, we defined a spatial grid (0.1° × 0.1°) and averaged each pix during the time series from 2015 to 2020. Positive XCO_2 anomaly in the areas represents CO_2 emissions to the

atmosphere and negative CO_2 anomaly represents CO_2 sinks.

3.2.6. XCH_4 data from the Amazon biome, 2015-2020, with GOSAT satellite

The GOSAT satellite stands out for two main onboard sensors: The Thermal and Near Infrared Sensor for Carbon Observations - Fourier Transform Spectrometer (TANSO-FTS) and the Cloud and Aerosol Imager (TANSO-CAI). It is worth noting that TANSO-FTS has four bands, one related to the Thermal Infrared - TIR (5500-14300 nm), used in the description of the vertical profile of the CO_2 concentration in the upper troposphere and another three for Short-Wave Infrared (SWIR) in the spectral range of 760, 1600 and 2000 nm, used in estimating the average CO_2 column concentrations (XCO_2). The images generated through the TANSO-CAI sensors occur in four bands (380, 675, 870 and 1600 nm) capable of offering spatial resolutions of 500 m, not to mention assisting applications in mapping clouds and atmospheric aerosols (Guerlet et al., 2013; Ross et al., 2013).

Total methane column data was obtained from the University of Leicester GOSAT Proxy with version 9.0. The data is public, available at https://data.ceda.ac.uk/neodc/gosat/data/ch4/nceov1.0/CH4_GOS_OCPR/ (Parker, R.; Boesch, 2020). The average dry air column methane mole fractions (XCH_4) were derived using the proxy method from CO_2 emission models (Parker et al., 2011, 2015). Thus, the method multiplies the ratio $\frac{\mathrm{XCH_4}}{\mathrm{XCO_2}}$ by a model of in situ observations XCH_4, considering the average of each year (Parker et al., 2011, 2015).

The XCO_2 models were based on local measurements of land surfaces using the median metric from the global models GEOS-Chem (Feng et al., 2011), Carbon Tracker (Peters et al., 2007) and LMDZ (Chevallier et al., 2010). It is worth noting that the GOSAT Proxy product was validated through measurements on aircraft in the Amazon region (Tunnicliffe et al., 2020; Wilson et al., 2020).

3.2.7. Soil Moisture Active Passive (SMAP) data

NASA's mission for the Soil Moisture Active Passive (SMAP) satellite enables observations of soil moisture in orbit. The SMAP carries L-band radiometry instruments capable of measuring the surface brightness temperature, thus providing the dimensioning of soil surface moisture with a resolution of approximately 5 cm from the soil (Cui et al., 2018; Ju Hyoung, 2021).

The equipment has a spatial resolution of approximately 9 km and a daily temporal resolution (Entekhabi et al., 2010). To enable the desired relationships and analysis, monthly averages were used for the time series from 2015 to 2020. Therefore, the data was obtained through R software (R Core Team, 2022) using the "rgee" package (Aybar et al., 2020).

3.2.8. Geostatistical Analysis

The XCH_4 (GOSAT) time series data between 2015 and 2020 were subjected to experimental variogram analysis (Webster and Oliver, 1990) and then ordinary kriging for the estimation of the variable in unsampled locations. The sampling grid was determined in grids spaced between 0.5° and 3-day intervals for the entire historical series. Thus, the entire Brazilian territory was considered due to the greater number of data collection points, as well as the low number of points in the sample area in the Amazon biome.

The data used came from two periods: the first for the humid period (Wet), delimited for the months of November, December, January, February, March, and April; and the second for the dry period (Dry), delimited for the months of May, June, July, August, September, and October. Therefore, it was possible to establish patterns of spatial variability of XCH_4 for the two periods studied and then estimate the semivariance at a given distance. The semivariance was estimated by equation 3:

$$\hat{\gamma}(h) = \frac{1}{2\,N\,(h)} \times \sum_{i=1}^{N(h)} [Z(x_i) - Z(x_i + h)]^2 \qquad \text{Equation (3)}$$

Where: h is the distance between pairs of points; $N\,(h)$ is the number of pairs of points separated by distance h; Zx_i is the value of XCH_4 at point x_i; and Zx_i +h is the value of XCH_4 at point $x_i + h$.

To determine the model that best fits the experimental variogram, the cross-validation technique was used. This technique consists of removing each observation belonging to the data set and estimating the value by the interpolation method (ordinary kriging). Thus, the model becomes more capable of estimating the observed values. According to Isaaks and Srivastava (1989), the use of the linear regression equation between predicted and observed values will depend on the estimated values closest to the bisector – intercept equal to zero and slope equal to unity. Therefore, to

better expose the theoretical models used, these were demonstrated in equations 4 (Spherical Model) and 5 (Gaussian Model):

$$\hat{\gamma}(h) = C_0 + C_1 \left[\frac{3}{2}\left(\frac{h}{a}\right) - \frac{1}{2}\left(\frac{h}{a}\right)^3 \right] \quad \text{Equation (4)}$$

Where: 0 < h < d, $\hat{\gamma}(h) = C_0 + C_1$, and h > a.

$$\hat{\gamma}(h) = C_0 + C_1 \left\{ 1 - exp\left[-3\left(\frac{h}{a^2}\right) \right] \right\} \quad \text{Equation (5)}$$

Where: 0 < *h* < *d* , and *d* is the maximum distance at which the variogram was defined. The nugget (C0), sill (C0+C1), and range (a) are important parameters for the variogram (Freitas et al., 2018).

The ratio between nugget and sill makes it possible to infer it as an indicator to classify the spatial dependence of the data set (Cambardella et al., 1994). Therefore, a ratio greater than 0.75 provides a high spatial dependence of the data.

Among the various models tested, for example: logarithm, generalized linear, exponential, Gaussian, and spherical models. However, Spherical and Gaussian models were better to estimate XCH_4 values. Like this, the parameters of the best curve adjustments for the experimental variograms were possible to estimate in unsampled locations in the Amazon biome. In the elaboration of maps with the spatial patterns of CH_4 for the wet and dry periods, the ordinary kriging technique was used, described by equation 5:

$$Z*(x_o) = \sum_{\{i=1\}}^{N} \lambda\, Z(x_i) \quad \text{Equation (6)}$$

Where: *Z**, is the value to be estimated for the unsampled data of xo, the number of measured values Zxi involved in the estimate and i is the weights associated with the measured value of Zxi.

For the descriptive statistics, with the calculation of the semivariance and the appropriate adjustments of the models, software R (R Core Team, 2022) was used.

After adjusting the models, the estimated values in unsampled areas in the Amazon biome were determined by the ordinary kriging interpolation method (Isaaks and Srivastava, 1989; Trangmar et al., 1986). QGIS software was used (QGIS Development Team, 2019) for the elaboration of the spatial maps of the wet and dry

periods.

For the wet period of the 2015 and 2018 time series, the IDW methods were used, justified by the nugget and sill values being equal to 3.34 (2015) and 5.55 (2018); therefore, there is no spatial dependence through the experimental variogram; however, this approach was also used for the spatialization of GHGs in recent studies (da Costa et al., 2021). The description of the model used is shown in equation 7:

$$Z_j = \frac{\sum_{i=1}^{n} = \frac{Z_i}{h_i j \beta}}{\sum_{i=1}^{n} = \frac{1}{h_i j \beta}} \qquad \text{Equation (7)}$$

where Zj = estimated value for location j; Zi = sample value measured for sample i; hij β = distance between Zj and Zi; and β = weighting power.

3.3. Results

3.3.1. Temporal

For the XCH_4 time series, it was observed that for the dry period (May to October), the lowest values were recorded (close to 1,765 ppb), while the highest values (1,809 ppb) were observed in the wet period (November to April; Figure 3.2).

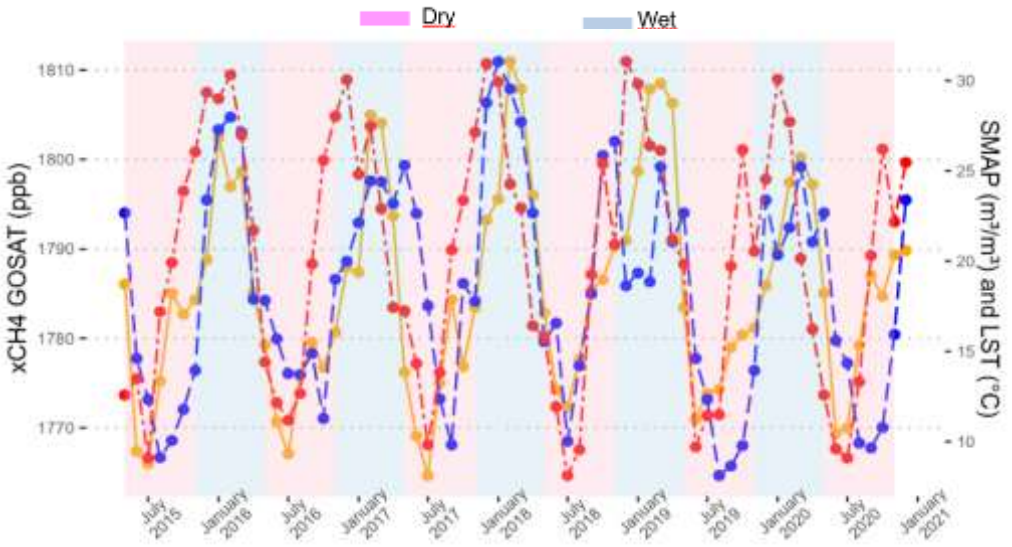

Figure 3.2. Time series of XCH_4 GOSAT (orange line and solid), Soil Moisture Active Passive (SMAP; blue line and long dash) and Land Surface Temperature (LST; red line and two-dash) of monthly averages over the Amazon biome. Units for XCH_4 GOSAT, SMAP and LST are ppb, $m^3\ m^{-3}$ and °C. Pink area is to dry period and blue area is to wet period.

On the other hand, the rainy season provided the highest values of XCH_4 from GOSAT with an increase in amplitude, in SMAP and LST (Figure 3.2). However, the correlation between XCH_4 and XCO_2 Anomaly presented an inverse amplitude with peak concentrations for methane concentrations in January and February for XCH_4, and for Anomaly, variable XCO_2 peaks were observed in July and August (Figure 3.3).

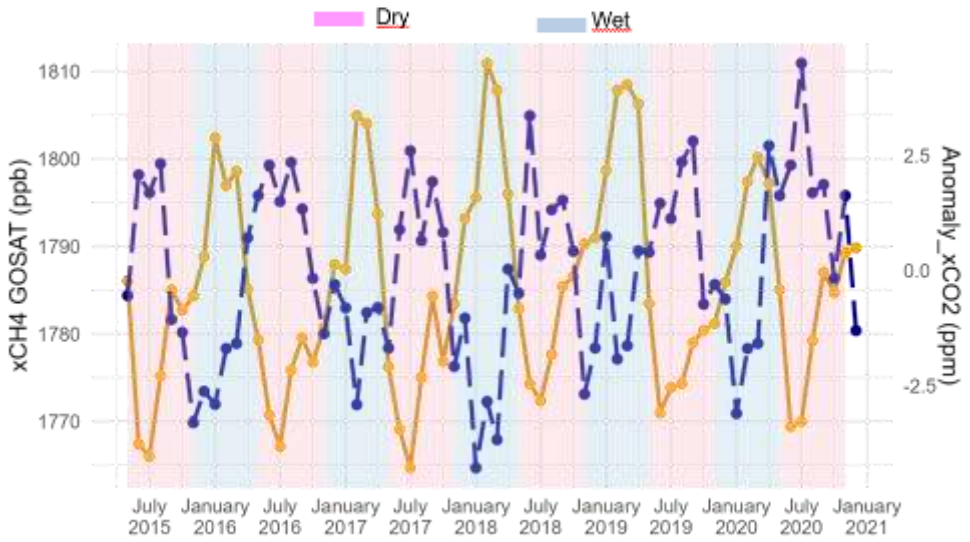

Figure 3.3. Time series of the XCH_4 GOSAT (orange line and solid) and XCO_2 Anomaly (blue line and long dash) of monthly means in the Amazon biome. The units for XCH_4 GOSAT and Anomaly are ppb e ppm. Pink rectangle is dry period and blue rectangle is wet period.

Pearson's correlation coefficient of XCH_4 GOSAT by temporal distribution between SMAP and LST variables was an intermediate positive correlation for the monthly means ($p < 0.05$). On the other hand, a significant ($p < 0.05$) negative intermediate strength between XCH_4 GOSAT and XCO_2 Anomaly ($r = -0.648$) was noted. The XCO_2 anomaly also relates negatively to LST ($r = -0.66$) and SMAP ($r = -0.59$; Figure 3.4).

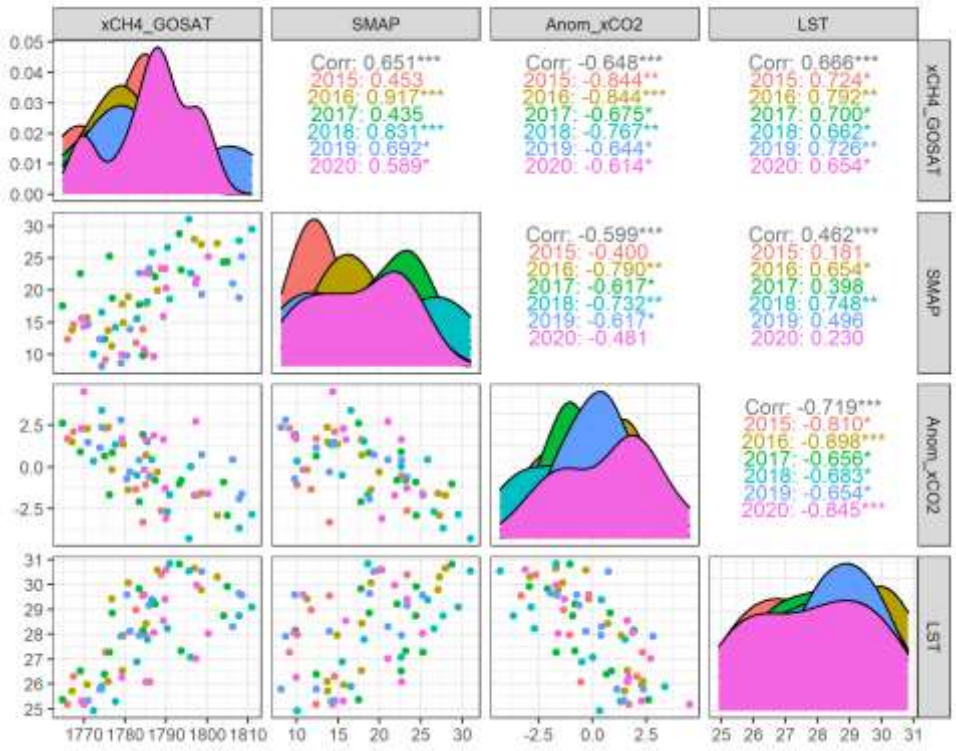

Figure 3.4. Heatmap of the Pearson's temporal correlation matrix for the studied variables XCH_4 GOSAT, Anom (XCO_2 Anomaly), Land Surface Temperature (LST) and Soil Moisture Active Passive (SMAP).

Figure 3.5 illustrates the average daily XCO_2 anomaly obtained by OCO-2 from 2015 to 2020. It is worth noting that the largest XCO_2 anomalies were observed for 2018. For the period between 2019 and 2020, 388,288 fire foci were observed in the Brazilian territory, while 49.5% (192,337) were observed in the Amazon biome during the period (Figure 3.4; INPE, 2022).

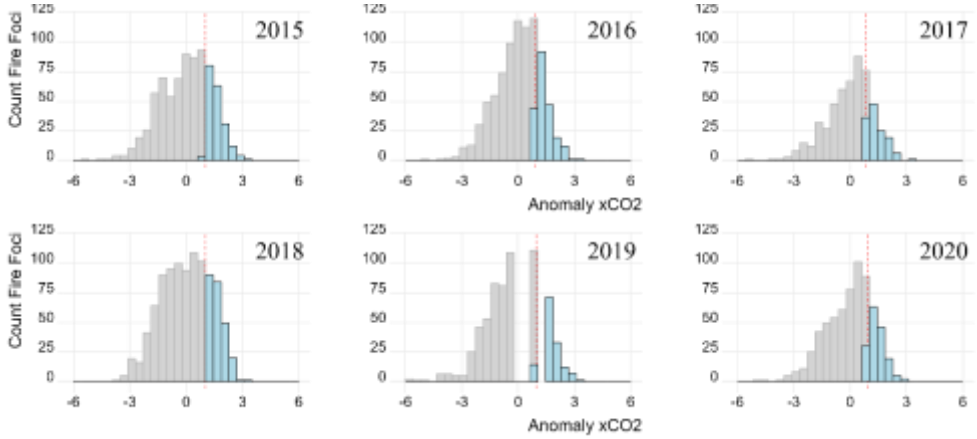

Figure 3.5. Histograms of the relationships between the fire foci number and the anomalous atmospheric concentrations of the average column of carbon dioxide (XCO_2), highlighted in blue histograms.

3.3.2. Spatial

For the analysis of the spatial variability of XCH_4 GOSAT, the parameters of the experimental semivariograms were initially established (Table 3.1). For the wet season, in relation to the degree of spatial dependence (GSD), in 2015 and 2018 (nugget = sill), there was no spatial dependence. However, for 2020 (< 0.25), there was also a strong spatial dependence for the wet season. For the dry period, all years presented moderate GSD (0.25 to 0.75).

The spherical and Gaussian models showed good fits for the experimental semivariograms for the XCH_4 variable (Table 3.1), and they described spatial patterns in the dry and wet periods in the areas inserted in the Amazon biome. Thus, it is worth noting that the Gaussian models allowed the use in regular and continuous phenomena, while the spherical models explained the variables with high continuity, or less erratic in small distances (Isaaks and Srivastava, 1989).

Table 3.1. Models and semivariogram parameters for XCH_4 GOSAT in wet and dry periods for 2015-2020 in areas in the Amazon.

Year	Model	Nugget	Sill	A(m)	SRS	SDD
			Wet			
2015	-	3.34	3.34	0.00	-	-
2016	Gau	9.55	23.68	25.73	225.20	0.40
2017	Sph	3.73	7.72	13.50	32.32	0.48
2018	-	5.55	5.55	0.00	-	-
2019	Gau	6.65	8.50	12.03	82.47	0.78
2020	Sph	0.03	84.74	13.48	500.35	<0.01
			Dry			
2015	Sph	6.17	11.16	13.52	367.43	0.55
2016	Gau	7.71	13.37	13.80	223.88	0.57
2017	Gau	9.00	15.00	20.78	684.25	0.60
2018	Sph	7.73	14.36	20.68	1755.05	0.54
2019	Sph	8.00	15.00	16.00	1899.23	0.53
2020	Sph	5.66	8.61	2.33	87.49	0.66

SDD Spatial dependence degree = nugget/sill, Strong for the values lower than 0.25; moderate for the values between 0.25 and 0.75; weak for the values higher than 0.75 (Cambardella et al., 1994); SRS sum of residue squares; Sph spherical; Gau Gaussian.

The results of Pearson's linear correlation were developed to understand the strength and proportionality between the variables in the spatial distribution (Figure 3. A4). In general, the most correlations observed between the variables were positive

and therefore directly proportional. The fire foci number showed a correlation ($p<0.05$) with the variable XCH_4 for the wet period (XCH_4 Wet). During Wet period there were no correlations ($p>0.05$) between XCO_2 Anomaly (Anom) and XCH_4 (XCH_4 Wet).

Based on our data, CH_4 concentration for the dry and wet periods showed a significant correlation ($p<0.05$) of intermediate strength between the variables, with emphasis on XCH_4 Wet between SMAP (0.65), XCH_4 Dry (0.46) and Fire Foci (0.50). The variable XCH_4 in dry period also showed a significant correlation ($p<0.05$) in an intermediate way with XCO_2 Anomaly (0.53); however, it showed a strong correlation with SMAP (0.89), the highest among the comparisons (Figure 3.6).

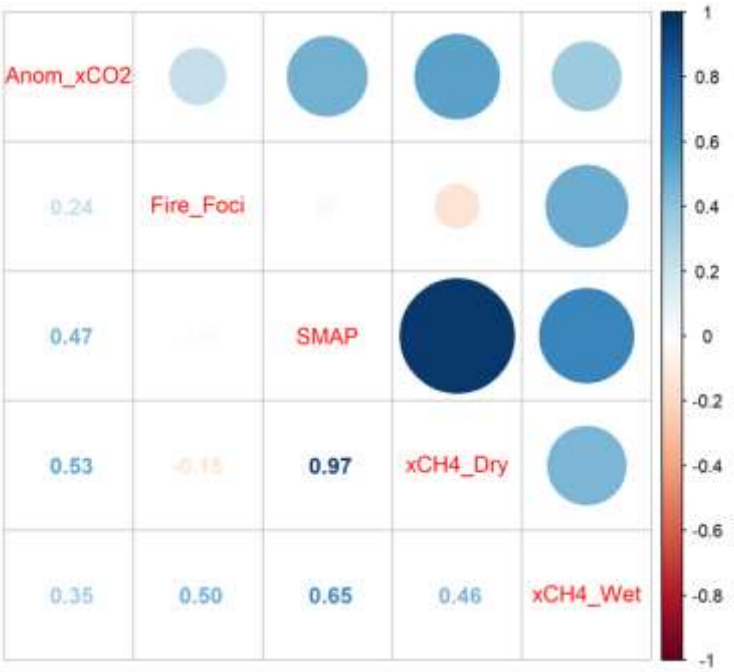

Figure 3.6. Heatmap of the Pearson's correlation matrix for the studied variables XCH_4 (Wet and Dry), Anom (XCO_2 Anomaly), Fire Foci and Soil Moisture Active Passive (SMAP).

The maps of the spatial patterns of XCH_4 in the dry period showed, for 2015, 2016, 2018, and 2019, the largest observations in the southeastern portion of the Amazon biome (Figure 3.7). However, for 2017, it was found that the central Amazon region had the highest observations, and for 2020, there was no pattern, possibly due to a lower number of observation points (<450).

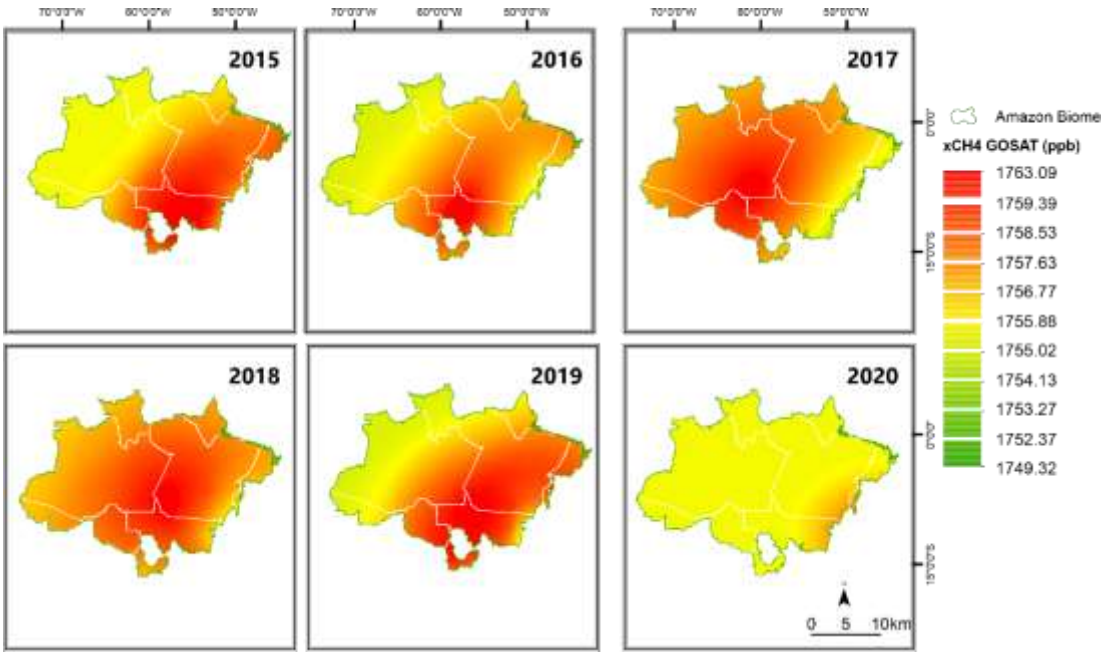

Figure 3.7. Maps of XCH_4 for dry period in the Amazon biome from the period of 2015-2020 applying kriging methodology.

In Figure 3.8, it was observed that the SMAP (m^3 m^{-3}) presented the highest observations in the northwest portion, justified by the highest average annual rainfall for the region. On the other hand, in the southeast and northeast portions, the lowest humidity values were observed for areas inserted in the Amazon biome in the analyzed time series (2015 to 2020; Figures 3.7 and 3.8).

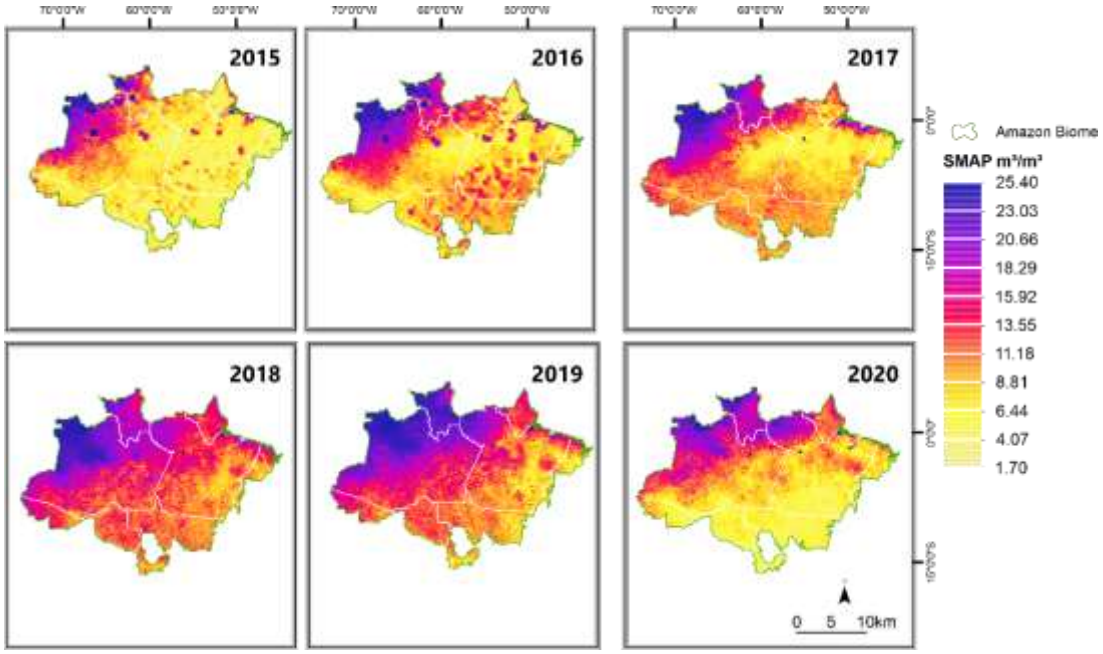

Figure 3.8. Maps of Soil Moisture Active Passive – SMAP (m^3 m^{-3}) from the dry period for 2015-2020 in the Amazon biome

For the wet period, there was no pattern in the spatialization of XCH_4 for the Amazon biome (Figure 3.9). The period of high precipitation for the entire Amazon region, with high cloudiness, reduces the number of significant points for the period. It is also worth noting that the period provides the greatest uncertainties in orbital observations for greenhouse gas monitoring satellites, especially for methane.

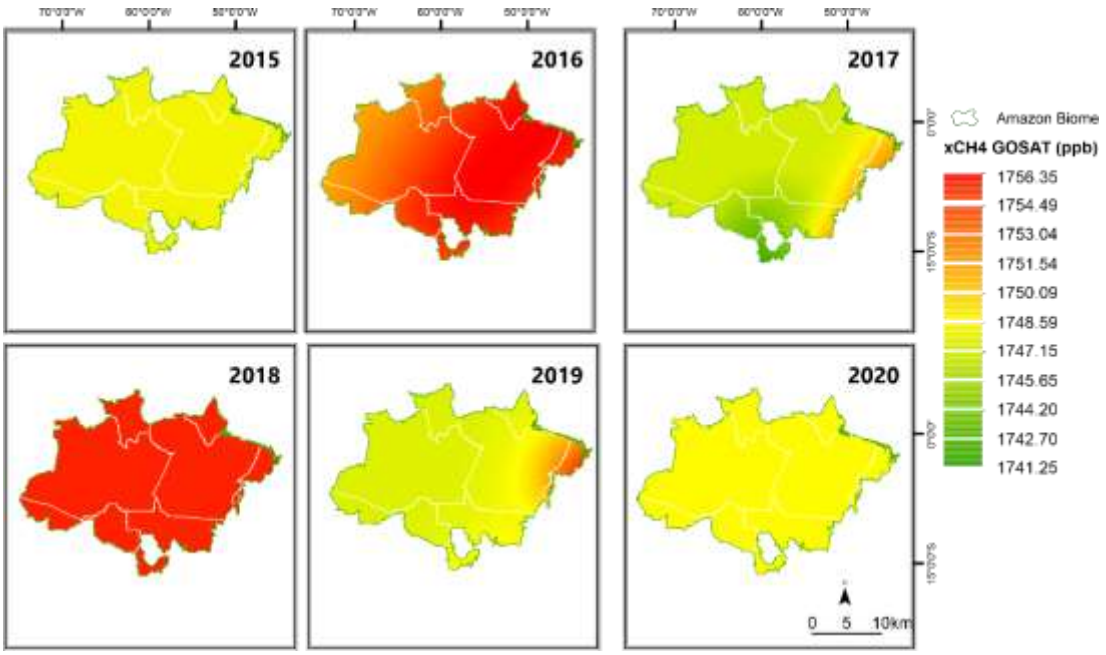

Figure 3.9. Maps of XCH_4 for wet period in the Amazon biome from the period of 2015-2020 applying kriging methodology.

The distribution of soil moisture for the wet season was consistent with the spatial distribution of XCH_4, especially for 2016 (Figure 3.10.). The northern portion of the Amazon biome also had lower soil moisture for 2016, differing from the other years analyzed in the time series.

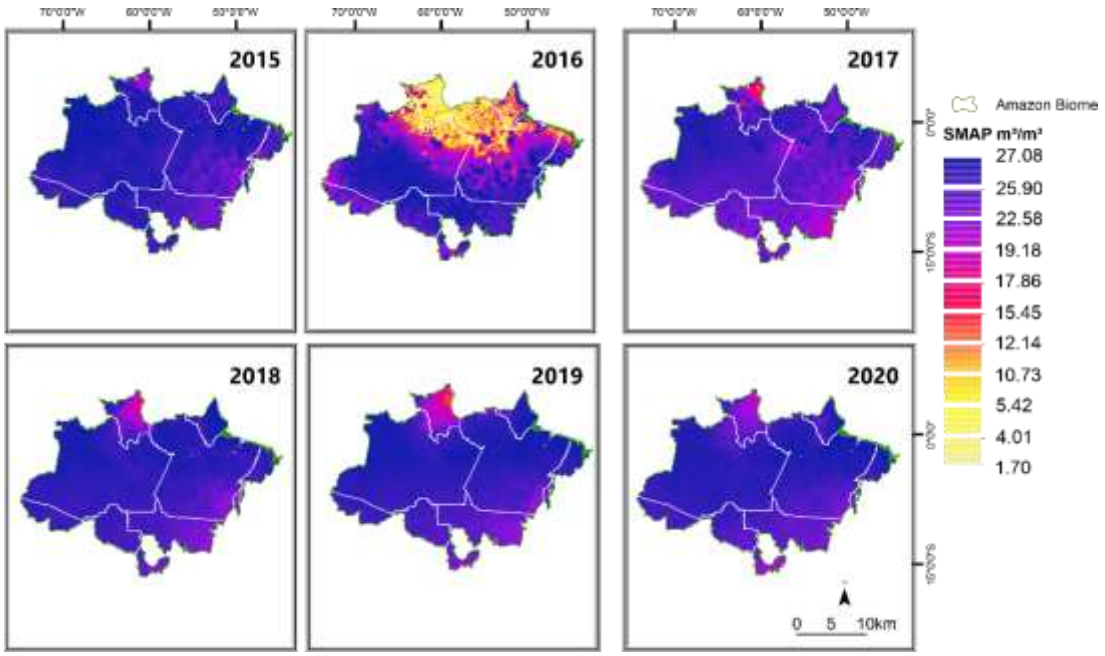

Figure 3.10. Maps of Soil Moisture Active Passive – SMAP (m^3 m^{-3}) from the wet period for 2015-2020 in the Amazon biome.

3.4. Discussion

3.4.1. Temporal

For a temporal CH_4 concentration, we can suggest that some CH_4 peaks during the rainy season (January and March) can support the highest values observed in the time series. Thus, it is important to highlight that SMAP and LST are positively correlated with the XCH_4 in the Amazon. We also observed a strong positive relationship between the XCH_4 and SMAP variables. However, in the rainy season, the highest the XCH_4 were observed in the period from January to March, with lower XCO_2. The negative values of CO_2 anomalies are explained by greater photosynthetic activity of plants and greater availability of water in the rainy season (Albright et al., 2022). Likewise, this justifies higher amplitudes with lower rainfall in July and August, coinciding with higher occurrences of fires (Carvalho et al., 2021; Pontes-Lopes et al., 2021).

Another highlight is that the variability of positive XCO_2 anomaly can be driven by the increase in fire foci (Detmers et al., 2015). Hence, a relationship between the increase in XCO_2 Anomaly and fire foci was observed (Figure 3.5). Thus, it was also observed that the spatial distribution of XCH_4 and the XCO_2 Anomaly for the dry period was significant ($r=0.53$, $p<0.05$) with moderate strength between the variables (Figure 3. A4), possibly justified by the occurrence of fire foci in the period.

On the other hand, there was a significant and positive correlation (r=0.97, p<0.05) between XCH_4 and SMAP, mainly in the dry period for the spatial distribution of XCH_4. Based on our results of spatial and temporal distribution of XCH_4, a strong relationship was observed for variables LST and SMAP. Therefore, a pattern of spatial distribution of the variable XCH_4 was observed for the dry period that matches the pattern of spatialization of the SMAP, except for 2020.

The southeastern and northwestern portions of the Amazonian territory presented the highest XCH_4 (Figures 3.7). This result can be explained by the agricultural activity in the region and mainly by the intense burning of local biomass (Wilson et al., 2021; Kroeger et al., 2021). According to Fearnside (2005), the region is known as the “Arc of deforestation”, characterized by the intense conversion of forests into pastures and agricultural crops in recent decades.

Crippa et al (2021) highlight that the methane emissions in Brazil from biomass burning were 1.4 Tg between 2015 and 2018. The MapBiomas (2022) platform showed that 31 million hectares were burned between 2015 and 2020 in the Amazon biome, occurring mainly in the “arc of deforestation”. During this period, the fires were concentrated in the months of August, September, and October (INPE, 2022). This period falls within the final dry months, when the vegetation is under stress conditions due to lack of rain (Alvares et al., 2013; Zemp et al., 2017).

3.4.2. Spatial

The impact of fire foci on XCH_4 Wet was significant in Pearson's correlation analysis (p<0.05), demonstrating that it contributed positively to higher the XCH_4 in the wet season (Figure 3.6). On the other hand, XCH_4 Dry did not correlate with fire foci. According to Andersen et al (1998), no flooded Tropicalforest soils become sources of CH_4 when devoid of vegetation, especially in the wet season.

The exposure of forest soil caused by the burning of aerial biomass favors solar incidence, consequently impacting the temperature and humidity of the soil, especially close to the surface (Acero and González-Asensio, 2018). As described by MapBiomas (2022), the period of intense fires occurs mostly at the end of the dry season in the Amazon region; therefore, the beginning of the wet season occurs with little or no vegetation on the ground. According to Andersen et al (1998), bacteria responsible for methane oxidation located on the surface are directly affected by periods of water stress. In addition, in periods of drought, methanogenic bacteria

remain protected within the anaerobic interior of soil aggregates, being little or later impacted by water scarcity (Andersen et al., 1998; Acero et al., 2018).

For the wet period, no pattern was observed in the distribution with XCH_4. In 2015 and 2018, there was no spatial dependence observed by the experimental variogram. It is worth noting that in larger observations, XCH_4 tends to be more uniform or homogeneous and consequently reduces the forecast uncertainty. The uncertainty of determining a pattern for the wet season is associated with greater cloudiness for the region of the areas inserted in the Amazon biome, which makes it difficult for satellite observation (Parazoo et al., 2013).

Our results showed that XCH_4 can be derived from the Brazilian territory from orbital data to understand the areas inserted in the Amazon biome. However, interesting alternatives in this context use high-resolution atmospheric transport modeling or local terrestrial observation towers, mainly for humid periods, to reduce the uncertainties in the observations (Feng et al., 2017; Webb et al., 2016).

According to Wilson et al (2020), the increase of CH_4 from eastern Amazon are greater in the wet season, directing an increase in the flow of sources from wetlands as possible drivers of the increase in total methane emissions. However, for the present study, no similar patterns were found that emphasize the same results.

The moderate correlation between Fire Foci and XCH_4 for the wet period suggests biomass burning outside the dry season (June and September). In the case of the exceptional droughts in the Amazon in 2015-2016, they are possibly able to explain the relationship between fire foci and XCH_4 (Marengo et al., 2022).

Taking the Pantanal biome as an example, in the months of January and February during the rainy season, there were unprecedented foci of forest fires (INPE, 2022) heavily reported by international media, mostly in late 2019 and 2020 (Marengo et al., 2021). According to L. Tunnicliffe et al (2020), climate change can be the main driver of emissions for the wet season, mainly due to the rise in surface temperature, thus boosting methane emissions.

3.5. Conclusions

For the period evaluated in this study, XCH_4 showed an increase due to higher SMAP in wet period, as well as XCH_4 was higher LST, validated by positive correlation

in temporal distribution of XCH_4 with SMAP and LST. The spatial distribution of XCH_4 was correlated with the XCO_2 Anomaly but only for the dry period. On the other hand, a spatial distribution pattern of XCH_4 was observed for the dry period, consistent with the spatial pattern of SMAP evidenced by the strong positive correlation between XCH_4 and SMAP. This confirmed the hypothesis that XCH_4 shows a positive relationship with SMAP, both for the dry and wet periods under the Amazon biome and corroborates the positive relationship between the variables. Nonetheless, no pattern was observed in the spatial distribution for XCH_4 for the wet season, with a moderately positive correlation between XCH_4 and SMAP. This shows that the issue of climate change and the change in land use and occupation significantly interfered as drivers of higher methane emissions in the Amazon biome. Regarding fire foci, there was a moderate correlation between the XCH_4 variable, especially for the wet season. This made it possible to validate hypothesis “i” and helped to foster new scientific studies on GHG emissions for the Amazon biome, especially considering the seasonality of dry and wet periods and the contribution of Fire foci number.

3.6. Acknowledgments

The study was funded by Coordenação de Aperfeiçoamento de Pessoal de Nível Superior - Brasil (CAPES). I am grateful to the Geotecnologia Aplicada em Agricultura e Floresta (GAAF) and SojaMaps of the Universidade do Estado de Mato Grosso (UNEMAT) for infrastructure for the present study.

3.7. References

ACERO, J. A.; GONZÁLEZ-ASENSIO, B. Influence of vegetation on the morning land surface temperature in a tropical humid urban area. **Urban Climate**, v. 26, n. August 2017, p. 231–243, 2018.

ALBRIGHT, R. et al. Seasonal Variations of Solar-Induced Fluorescence, Precipitation, and Carbon Dioxide Over the Amazon. **Earth and Space Science**, v. 9, n. 1, p. 1–11, 2022.

ALVARES, C. A. et al. Köppen’s climate classification map for Brazil. **Meteorologische Zeitschrift**, v. 22, n. 6, p. 711–728, 1 dez. 2013.

ANDERSEN, B. L. et al. A new method to study simultaneous methane oxidation and

methane production in soils. **Global Biogeochemical Cycles**, v. 12, n. 4, p. 587–594, 1998.

ANDERSON, L. O. et al. Vulnerability of Amazonian forests to repeated droughts. Philosophical Transactions of the Royal Society B: **Biological Sciences**, v. 373, n. 1760, 2018.

ANTONELLI, A. et al. Amazonia is the primary source of Neotropical biodiversity. **Proceedings of the National Academy of Sciences of the United States of America**, v. 115, n. 23, p. 6034–6039, jun. 2018.

AYBAR, C. et al. rgee: An R package for interacting with Google Earth Engine. **Journal of Open Source Software**, v. 5, n. 51, p. 2272, 2020.

BASSO, L. S. et al. Amazon methane budget derived from multi-year airborne observations highlights regional variations in emissions. **Communications Earth & Environment**, v. 2, n. 1, p. 1–13, 2021.

BOUSQUET, P. et al. Contribution of anthropogenic and natural sources to atmospheric methane variability. **Nature**, v. 443, n. 7110, p. 439–443, 2006.

BRIENEN, R. J. W. et al. Long-term decline of the Amazon carbon sink. **Nature**, v. 519, n. 7543, p. 344–348, 2015.

CAMBARDELLA, C. A. et al. Field-Scale Variability of Soil Properties in Central Iowa Soils. **Soil Science Society of America Journal**, v. 58, n. 5, p. 1501–1511, 1994.

CARVALHO, N. S. et al. Spatio-Temporal variation in dry season determines the Amazonian fire calendar. **Environmental Research Letters**, v. 16, n. 12, 2021.

CHEVALLIER, F. et al. On the impact of transport model errors for the estimation of CO_2 surface fluxes from GOSAT observations. Geophysical Research Letters, v. 37, n. 21, 2010.

COSTA, L. M. DA; et al. An empirical model for estimating daily atmospheric column - averaged - concentration above São Paulo state, Brazil. **Carbon Balance and Management**, p. 1–11, 2022.

CRIPPA, M. et al. GHG emissions of all world countries -Report, EUR 30831 EN,

Publications Office of the European Union, Luxembourg, 2021, 12 p.

CRISP, D. et al. The ACOS CO_2 retrieval algorithm – Part II: Global XCO_2 data characterization. **Atmos. Meas. Tech.**, v. 5, n. 4, p. 687–707, abr. 2012.

CRISP, D. et al. The on-orbit performance of the Orbiting Carbon Observatory-2 (OCO-2) instrument and its radiometrically calibrated products. **Atmospheric Measurement Techniques**, v. 10, n. 1, p. 59–81, 2017.

CROWELL, S. et al. The 2015--2016 carbon cycle as seen from OCO-2 and the global in situ network. **Atmospheric Chemistry and Physics**, v. 19, n. 15, p. 9797–9831, 2019.

CUI, C. et al. Soil moisture mapping from satellites: An intercomparison of SMAP, SMOS, FY3B, AMSR2, and ESA CCI over two dense network regions at different spatial scales. **Remote Sensing**, v. 10, n. 1, 2018.

DA SILVA JUNIOR, C. A. et al. Persistent fire foci in all biomes undermine the Paris Agreement in Brazil. **Scientific Reports**, v. 10, n. 1, p. 1–14, 2020.

DA SILVA JUNIOR, C. A. et al. Fires Drive Long-Term Environmental Degradation in the Amazon Basin. **Remote Sensing**, v. 14, n. 2, 2022.

DETMERS, R. G. et al. Anomalous carbon uptake in Australia as seen by GOSAT. Geophysical Research Letters, v. 42, n. 19, p. 8177–8184, 2015.
DEVKOTA, J. U. Statistical analysis of active fire remote sensing data: examples from South Asia. **Environmental Monitoring and Assessment**, v. 193, n. 9, p. 1–14, 2021.

ENTEKHABI, D. et al. The Soil Moisture Active Passive (SMAP) Mission. **Proceedings of the IEEE**, v. 98, n. 5, p. 704–716, 2010.

EUFEMIA, L. et al. Fires in the Amazon Region: Quick Policy Review. **Development Policy Review**, n. November 2021, p. 1–15, 2022.

FALAHATKAR, S.; MOUSAVI, S. M.; FARAJZADEH, M. Spatial and temporal distribution of carbon dioxide gas using GOSAT data over IRAN. **Environmental Monitoring and Assessment**, v. 189, n. 12, 2017.

FEARNSIDE, P. Deforestation in Brazilian Amazonia: History, Rates, and

Consequences. **Conservation Biology**, v. 19, n. 3, p.680–688, 2005

FENG, L. et al. Evaluating a 3-D transport model of atmospheric CO_2 using ground-based, aircraft, and space-borne data. **Atmospheric Chemistry and Physics,** v. 11, n. 6, p. 2789–2803, 2011.

FENG, L. et al. Consistent regional fluxes of CH_4 and CO_2 inferred from GOSAT proxy XCH_4:XCO_2 retrievals, 2010-2014. **Atmospheric Chemistry and Physics**, v. 17, n. 7, p. 4781–4797, 2017.

FIRMS. **FIRMS-Fire Information for Resource Management System.** Available in: <https://firms.modaps.eosdis.nasa.gov/>. Access on: 1 Apr 2022

FRANKENBERG, C. et al. The Orbiting Carbon Observatory (OCO-2): spectrometer performance evaluation using pre-launch direct sun measurements. **Atmospheric Measurement Techniques**, v. 8, n. 1, p. 301–313, 2015.

GIGLIO, L. et al. An Enhanced Contextual Fire Detection Algorithm for MODIS. **Remote Sensing of Environment**, v. 87, n. 2–3, p. 273–282, out. 2003.

GUERLET, S. et al. Reduced carbon uptake during the 2010 Northern Hemisphere summer from GOSAT. **Geophysical Research Letters**, v. 40, n. 10, p. 2378–2383, 2013.

GUO, M. et al. CO2 emissions from the 2010 Russian wildfires using GOSAT data. **Environmental Pollution**, v. 226, p. 60–68, 2017.

GUO, M. et al. Estimation of CO_2 emissions from Wildfires using OCO-2 data. **Atmosphere**, v. 10, n. 10, p. 1–16, 2019.

HAKKARAINEN, J.; IALONGO, I.; TAMMINEN, J. Direct space-based observations of anthropogenic CO_2 emission areas from OCO-2. **Geophysical Research Letters**, v. 43, n. 21, p. 11,400-11,406, 2016.

HEINRICH, V. H. A. et al. Large carbon sink potential of secondary forests in the Brazilian Amazon to mitigate climate change. **Nature Communications**, v. 12, n. 1, p. 1–11, 2021.

HEYMANN, J. et al. CO_2 emission of Indonesian fires in 2015 estimated from satellite-derived atmospheric CO_2 concentrations. **Geophysical Research Letters**, v. 44, n.

3, p. 1537–1544, 2017.

IBGE **- INSTITUTO BRASILEIRO DE GEOGRAFIA E ESTATÍSTICA**. Conheca cidades e Estados do Brasil. Available in: < https://www.ibge.gov.br/ > Access on: March 12 2022.

INPE. **Instituto Brasileiro de Pesquisas Espaciais BDQueimadas**. Available in: <https://queimadas.dgi.inpe.br/queimadas/bdqueimadas> Access on: July 17 2022.

IPCC. **Intergovernmental Panel on Climate Change 2019 Refinement to the 2006 IPCC Guidelines for National Greenhouse Gas Inventories – IPCC**, Available at: Available in: <https://www.ipcc.ch/report/2019-refinement-to-the-2006-ipcc-guidelines-for-national-greenhouse-gas-inventories/>. Access on: March 17 2019.

IPCC (INTERGOVERNMENTAL PANEL ON CLIMATE CHANGE**). Climate Change 2022: Impacts, Adaptation, and Vulnerability. Contribution of Working Group II to the Sixth Assessment Report of the Intergovernmental Panel on Climate Change.** 1st. ed. Cambridge: Cambridge University Press. In Press., 2022.

ISAAKS, E.H. AND SRIVASTAVA, R. M. **An Introduction to Applied Geostatistics**. 1. ed. Oxford: Oxford University Press, 1989.

JIANG, X. et al. Impact of Amazonian Fires on Atmospheric CO_2. **Geophysical Research Letters**, v. 48, n. 5, p. 1–10, 2021.

JU HYOUNG, L. Prediction of Large-Scale Wildfires with the Canopy Stress Index Derived from Soil Moisture Active Passive. **IEEE Journal of Selected Topics in Applied Earth Observations and Remote Sensing**, v. 14, p. 2096–2102, 2021.

KIRSCHKE, S. et al. Three decades of global methane sources and sinks. **Nature Geoscience**, v. 6, n. 10, p. 813–823, 2013.

L. TUNNICLIFFE, R. et al. Quantifying sources of Brazil's CH_4 emissions between 2010 and 2018 from satellite data. **Atmospheric Chemistry and Physics**, v. 20, n. 21, p. 13041–13067, 7 nov. 2020.

LE ROUX, R. et al. How wildfires increase sensitivity of Amazon forests to droughts. **Environmental Research Letters**, v. 17, n. 4, p. 044031, 2022.

LI, L. et al. Spatiotemporal Geostatistical Analysis and Global Mapping of CH_4 Columns from GOSAT Observations. **Remote Sensing**, v. 14, n. 3, 2022.

MARENGO, J. A. et al. Changes in Climate and Land Use Over the Amazon Region: Current and Future Variability and Trends. **Frontiers in Earth Science**, v. 6, n. December, p. 1–21, 2018.

MARENGO, J. A. et al. Extreme Drought in the Brazilian Pantanal in 2019–2020: Characterization, Causes, and Impacts. **Frontiers in Water**, v. 3, 23 fev. 2021.

MARENGO, J. A. et al. Increased climate pressure on the agricultural frontier in the Eastern Amazonia–Cerrado transition zone. **Scientific Reports**, v. 12, n. 1, p. 1–10, 2022.

Mapbiomas - **Coleção 7 (1985-2021) da Série Anual de Mapas de Cobertura e Uso de Solo do Brasil.** Disponível em: https://plataforma.mapbiomas.org/map#coverage. Acesso em: 02 set 2022.

MORGAN, W. T. et al. Non-deforestation drivers of fires are increasingly important sources of aerosol and carbon dioxide emissions across Amazonia. **Scientific Reports**, v. 9, n. 1, p. 1–15, 2019.

NIKITENKO, A. A. et al. The Analysis of OCO-2 Satellite Measurements of CO_2 in the Vicinity of Russian Cities. **Atmospheric and Oceanic Optics**, v. 33, n. 6, p. 650–655, 2020.

NISBET, E. G. et al. Very Strong Atmospheric Methane Growth in the 4 Years 2014–2017: Implications for the Paris Agreement. **Global Biogeochemical Cycles**, v. 33, n. 3, p. 318–342, 1 mar. 2019.

NOBRE, C. A. et al. Land-use and climate change risks in the amazon and the need of a novel sustainable development paradigm. **Proceedings of the National Academy of Sciences of the United States of America**, v. 113, n. 39, p. 10759–10768, 2016.

O'DELL, C. W. et al. The ACOS CO_2 retrieval algorithm – Part 1: Description and validation against synthetic observations. **Atmospheric Measurement Techniques**, v. 5, n. 1, p. 99–121, jan. 2012.

OGUMA, H. et al. First observations of CO_2 absorption spectra recorded in 2005 using an airship-borne FTS (GOSAT TANSO–FTS BBM) in the SWIR spectral region. **International Journal of Remote Sensing**, v. 32, n. 24, p. 9033–9049, 2011.

PARAZOO, N. C. et al. Interpreting seasonal changes in the carbon balance of southern Amazonia using measurements of XCO_2 and chlorophyll fluorescence from GOSAT. **Geophysical Research Letters**, v. 40, n. 11, p. 2829–2833, 2013.

PARKER, R.; BOESCH, H. **University of Leicester GOSAT Proxy XCH_4 v9.0**. Centre for Environmental Data Analysis.

PARKER, R. et al. Methane observations from the Greenhouse Gases Observing SATellite: Comparison to ground-based TCCON data and model calculations. **Geophysical Research Letters**, v. 38, n. 15, ago. 2011.

PARKER, R. J. et al. Assessing 5 years of GOSAT Proxy XCH_4; data and associated uncertainties. **Atmospheric Measurement Techniques**, v. 8, n. 11, p. 4785–4801, nov. 2015.

PONTES-LOPES, A. et al. Drought-driven wildfire impacts on structure and dynamics in a wet Central Amazonian Forest. **Proceedings of the Royal Society B: Biological Sciences**, v. 288, n. 1951, 2021.

QGIS DEVELOPMENT TEAM. QGIS ***Geographic Information System*** (version 3.8).Open Source Geospatial Foundation, , 2019. Available in: <http://qgis.org/.> Access on: March 12 2022.

R CORE TEAM. A Language and Environment for Statistical Computing**. R Foundation for Statistical Computing**, Vienna, Austria., 2022

RIBEIRO, P. J. J.; CHRISTENSEN, O. F.; DIGGLE, P. J. **geoR** and geoRglm : Software for Model-Based Geostatistics. Proceedings of the 3rd International Workshop on Distributed Statistical Computing (DSC 2003), n. Dsc, p. 1–16, 2003.

ROSS, A. N. et al. First satellite measurements of carbon dioxide and methane emission ratios in wildfire plumes. **Geophysical Research Letters**, v. 40, n. 15, p. 4098–4102, ago. 2013.

ROSSI, F. S. et al. Carbon dioxide spatial variability and dynamics for contrasting land uses in central Brazil agricultural frontier from remote sensing data. **Journal of South American Earth Sciences**, v. 116, p. 103809, 2022.

SAATCHI, S. et al. Detecting vulnerability of humid tropical forests to multiple stressors. **One Earth**, v. 4, n. 7, p. 988–1003, 2021.

SAUNOIS, M. et al. The global methane budget 2000-2017. **Earth System Science Data**, v. 12, n. 3, p. 1561–1623, 15 jul. 2020.

SILVA, C. H. L. et al. Deforestation-induced fragmentation increases forest fire occurrence in central Brazilian Amazonia. **Forests**, v. 9, n. 6, 2018.

TEODORO, P. E. et al. Twenty-year impact of fire foci and its relationship with climate variables in Brazilian regions**. Environmental Monitoring and Assessment**, v. 194, n. 2, 2022.

TRANGMAR, B. B.; YOST, R. S.; UEHARA, G. Application of Geostatistics to Spatial Studies of Soil Properties. In: BRADY, N. C (Ed.). **Advances in Agronomy. Academic Press**, 1986. v. 38p. 45–94.

TUNNICLIFFE, R. L. et al. Quantifying sources of Brazil's CH_4 emissions between 2010 and 2018 from satellite data. **Atmospheric Chemistry and Physics**, v. 20, n. 21, p. 13041–13067, 2020.

WAN, Z., HOOK, S., & HULLEY, G. **MOD11A2 MODIS/Terra** land surface temperature/emissivity 8-day L3 global 1km SIN grid V006. Nasa Eosdis Land Processes Daac.

WEBB, A. J. et al. CH_4 concentrations over the Amazon from GOSAT consistent with in situ vertical profile data. **Journal of Geophysical Research**, v. 121, n. 18, p. 11,006-11,020, 2016.

WEBSTER, R. AND OLIVER, M. A. **Statistical methods in soil and land resource survey**. 1. ed. Oxford: Oxford University Press (OUP), 1990.

WECHT, K. J. et al. Spatially resolving methane emissions in California: constraints from the CalNex aircraft campaign and from present (GOSAT, TES) and future (TROPOMI, geostationary) satellite observations. **Atmospheric Chemistry and Physics**, v. 14, n. 15, p. 8173–8184, ago. 2014.

WILSON, C. et al. Large and increasing methane emissions from Eastern Amazonia derived from satellite data, 2010--2018. **Atmospheric Chemistry and Physics Discussions**, v. 2020, p. 1–38, 2020.

YIN, S. et al. Analyzing temporo-spatial changes and the distribution of the CO_2 concentration in Australia from 2009 to 2016 by greenhouse gas monitoring satellites. **Atmospheric Environment**, v. 192, n. October 2017, p. 1–12, 2018.

ZEMP, D. C. et al. Self-amplified Amazon Forest loss due to vegetation-atmosphere feedbacks. **Nature Communications**, v. 8, n. 1, p. 14681, 2017.

CHAPTER 4: FINAL CONSIDERATIONS

Understanding the temporal dynamics and spatial distribution of GHG concentrations and their relationships with biophysical variables allow efforts to be directed to monitoring the main sources and sinks of these gases in the Amazon. Thus, the use of remote sensing tools helps to monitor such aspects on a much larger scale, allowing for example to fill gaps associated with the absence of in situ data, justified both by the extensive territorial dimension of the biome and also by the need for strategies to combat and prevent fires for the biome.

Therefore, the results obtained in this study, according to the chapter, showed a trend of growth of CO_2 and CO (April), just as there was also an increase in FRP (April and July), in addition to the correlation and regression analysis between XCO_2 and fires in the Amazon biome, thus validating the hypotheses of the present study. On the other hand, it did not find a relationship between fire foci and CH_4 concentrations, considering the temporality between the variables.

In the third chapter of this study, a pattern of spatial distribution of CH_4 with a strong correlation with the terrestrial biophysical variable - SMAP (soil moisture), mainly in the dry period (May to October) became evident. In addition to being related to the occurrences of fire foci, unlike the temporal distribution, this indicates that the understanding of temporal concentrations of methane are possibly more associated with flooded environments.

Considering our results, it becomes possible to direct strategic policies to combat the occurrences of fire foci and face climate change. In the same way that the results can feed a platform with data on the concentration of Gases (XCO_2, XCH_4 and XCO), the condition of the vegetation (SIF and EVI), and the biophysical variables (soil moisture, temperature, and precipitation) while establishing efficient strategies to mitigate GHG emissions. At the same time, it reinforces the need to continue future research on the concentrations of GHGs, especially CH_4, due to the greater impact on terrestrial radiative forcing, in relation to CO_2, in addition to elucidating a greater understanding of the possible sinks and source in the Amazon biome.

Finally, with new research in portions of the Amazon region, considering that reducing the spatial resolution of the GHG monitoring sensors will facilitate the understanding of which regions are most affected by the fire foci number. Similarly, and which regions are the most GHG emitters. Therefore, this will contribute to a better

understanding of the sources and sinks of these gases.

APPENDICES

Appendix A. Supplementary material for chapter 2

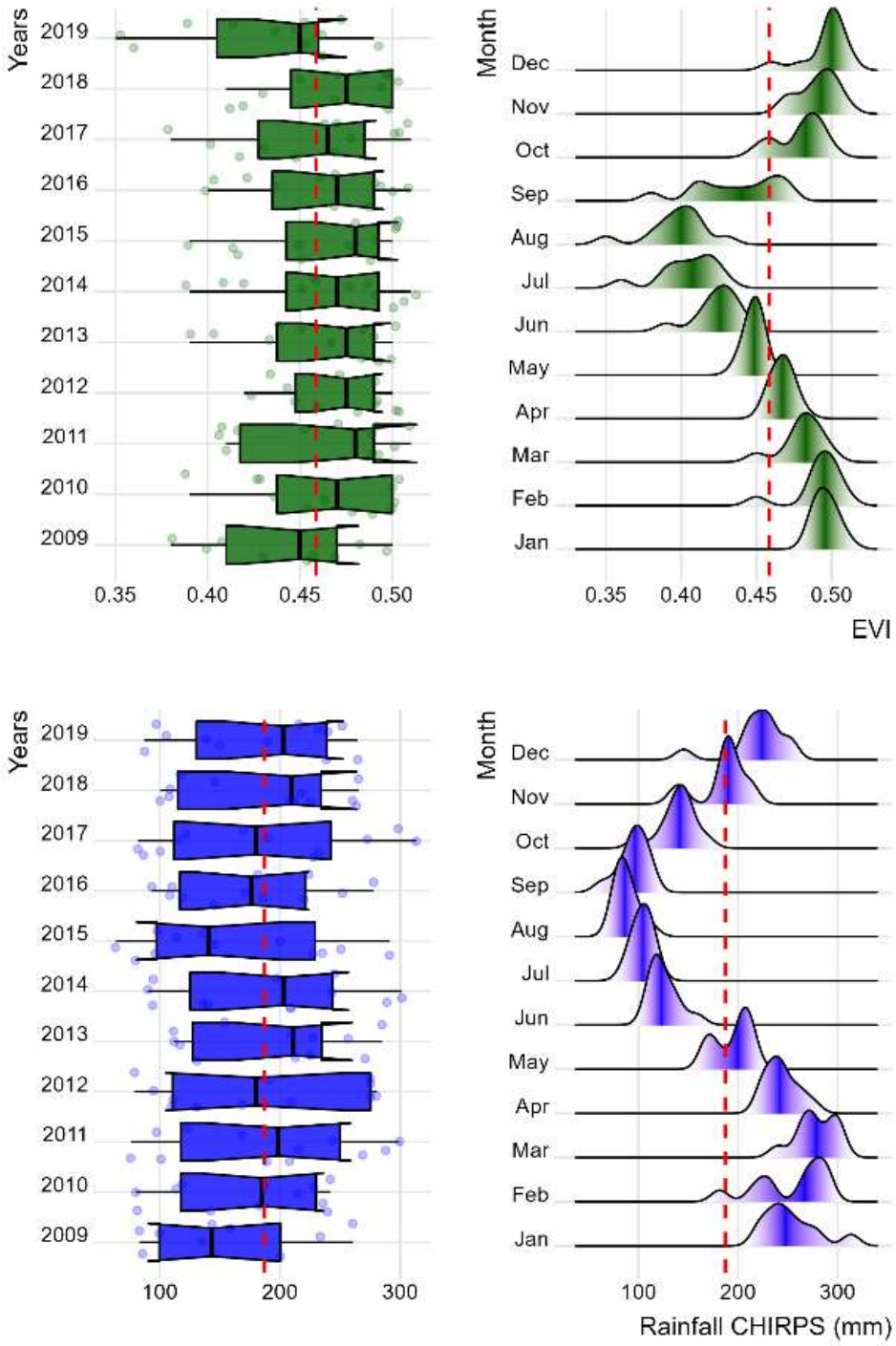

Figure 2.A1. Distribution of variables of Enhanced Vegetation Index (EVI) and Rainfall with the annual and monthly averages for the Amazon biome. EVI data was obtained by the Moderate Resolution Imaging Spectroradiometer (Huete et al., 2002). Rainfall data was obtained by the Climate Hazards Group Infrared Precipitation with Stations (CHIRPS; FINK et al., 2015).

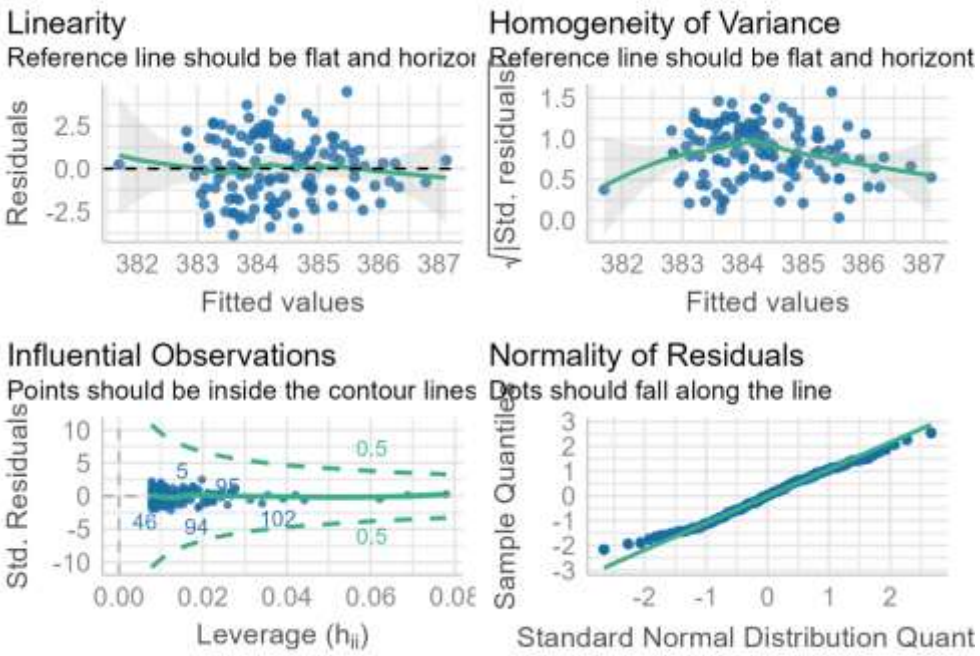

Figure 2.A2. Plot of residuals versus XCO_2 GOSAT (ppm) level x, homoscedasticity test, Leverage test, residual qqplot.

Table S1. Trend analysis of the annual averages of XCO MERRA (ppb), XCO_2 GOSAT (ppm), XCH_4 GOSAT (ppb), SIF755 GOSAT (W m^{-2} μm^{-1} sr^{-1}), EVI – MODIS, Rainfall – CHIRPS (mm), FRP – MODIS (MW) and Fire foci number – MODIS for Biome Amazon in the period from 2009 to 2019

Variables	Mann Kendall test		
	z-value	p-value	Interpretation
XCO MERRA	0.311	0.755	Reject H_0
XCO_2 GOSAT	-0.311	0.755	Reject H_0
XCH_4 GOSAT	0.779	0.436	Reject H_0
SIF GOSAT	-0.311	0.745	Reject H_0
EVI - MODIS	-0.234	0.815	Reject H_0
Rainfall - CHIRPS	0.778	0.436	Reject H_0
FRP - MODIS	0.778	0.437	Reject H_0
Fire foci - MODIS	0.156	0.876	Reject H_0

Table S2. Trend analysis of the monthly averages of XCO MERRA (ppb), XCO_2 GOSAT (ppm), XCH_4 GOSAT (ppb), SIF755 GOSAT (W m^{-2} μm^{-1} sr^{-1}), EVI – MODIS, Rainfall – CHIRPS (mm), FRP – MODIS (MW) and Fire foci number – MODIS for Biome Amazon in the period from 2009 to 2019

Months	Variables	Mann Kendall test		
		z-value	p-value	Interpretation
January	XCO MERRA	0.178	0.858	Reject H_0
	XCO_2 GOSAT	-1.167	0.243	Reject H_0
	XCH_4 GOSAT	-0.179	0.858	Reject H_0
	SIF GOSAT	-1.623	0.105	Reject H_0
	EVI - MODIS	0.001	0.999	Reject H_0
	Rainfall - CHIRPS	-0.715	0.474	Reject H_0
	FRP - MODIS	0.272	0.785	Reject H_0
	Fire foci - MODIS	0.358	0.674	Reject H_0
February	XCO MERRA	1.073	0.263	Reject H_0
	XCO_2 GOSAT	0.179	0.858	Reject H_0
	XCH_4 GOSAT	2.146	0.052	Reject H_0
	SIF GOSAT	-1.181	0.343	Reject H_0
	EVI - MODIS	0.386	0.699	Reject H_0
	Rainfall - CHIRPS	-0.716	0.474	Reject H_0
	FRP - MODIS	0.537	0.592	Reject H_0
	Fire foci - MODIS	1.252	0.211	Reject H_0
March	XCO MERRA	1.082	0.211	Reject H_0
	XCO_2 GOSAT	-0.716	0.474	Reject H_0
	XCH_4 GOSAT	2.325	0.057	Reject H_0
	SIF GOSAT	1.082	0.279	Reject H_0
	EVI - MODIS	-1.978	0.058	Reject H_0
	Rainfall - CHIRPS	-0.179	0.858	Reject H_0
	FRP - MODIS	2.147	0.052	Reject H_0
	Fire foci - MODIS	1.789	0.071	Reject H_0
April	**XCO MERRA**	**2.803**	**0.005**	**Accept H_0**
	XCO_2 GOSAT	**2.647**	**0.008**	**Accept H_0**
	XCH_4 GOSAT	0.001	0.998	Reject H_0
	SIF GOSAT	-1.335	0.182	Reject H_0

	EVI - MODIS	-0.318	0.751	Reject H_0
	Rainfall - CHIRPS	-0.934	0.350	Reject H_0
	FRP - MODIS	**2.958**	**0.003**	**Accept H_0**
	Fire foci - MODIS	2.024	0.059	Reject H_0
May	XCO MERRA	2.803	0.050	Reject H_0
	XCO_2 GOSAT	2.6469	0.049	Reject H_0
	XCH_4 GOSAT	0.001	0.996	Reject H_0
	SIF GOSAT	-1.335	0.182	Reject H_0
	EVI - MODIS	-1.532	0.125	Reject H_0
	Rainfall - CHIRPS	-0.934	0.350	Reject H_0
	FRP - MODIS	2.958	0.050	Reject H_0
	Fire foci - MODIS	2.031	0.049	Reject H_0
June	XCO MERRA	-1.713	0.087	Reject H_0
	XCO_2 GOSAT	-0.311	0.755	Reject H_0
	XCH_4 GOSAT	-0.778	0.436	Reject H_0
	SIF GOSAT	0.703	0.482	Reject H_0
	EVI - MODIS	-1.136	0256	Reject H_0
	Rainfall - CHIRPS	-0.156	0.876	Reject H_0
	FRP - MODIS	-0.467	0.640	Reject H_0
	Fire foci - MODIS	1.713	0.087	Reject H_0
July	XCO MERRA	-0.934	0.350	Reject H_0
	XCO_2 GOSAT	-0.623	0.533	Reject H_0
	XCH_4 GOSAT	-0.467	0.651	Reject H_0
	SIF GOSAT	0.783	0.433	Reject H_0
	EVI - MODIS	-0.635	0.525	Reject H_0
	Rainfall - CHIRPS	-0.467	0.640	Reject H_0
	FRP - MODIS	**2.491**	**0.013**	**Accept H_0**
	Fire foci - MODIS	2.024	0.052	Reject H_0
August	XCO MERRA	-1.099	0.276	Reject H_0
	XCO_2 GOSAT	-0.390	0.696	Reject H_0
	XCH_4 GOSAT	-0.778	0.436	Reject H_0
	SIF GOSAT	1.640	0.101	Reject H_0
	EVI - MODIS	0.080	0.936	Reject H_0
	Rainfall - CHIRPS	1.099	0.276	Reject H_0
	FRP - MODIS	0.156	0.876	Reject H_0
	Fire foci - MODIS	0.778	0.436	Reject H_0
September	XCO MERRA	0.156	0.876	Reject H_0
	XCO_2 GOSAT	-0.156	0.876	Reject H_0
	XCH_4 GOSAT	0.001	0.999	Reject H_0
	SIF GOSAT	2.349	0.049	Reject H_0
	EVI - MODIS	0.864	0.387	Reject H_0
	Rainfall - CHIRPS	0.934	0.350	Reject H_0
	FRP - MODIS	0.547	0.584	Reject H_0
	Fire foci - MODIS	0.001	0.995	Reject H_0
October	XCO MERRA	1.868	0.062	Reject H_0
	XCO_2 GOSAT	0.623	0.533	Reject H_0
	XCH_4 GOSAT	-0.467	0.640	Reject H_0
	SIF GOSAT	-0.948	0.343	Reject H_0
	EVI - MODIS	0.002	0.992	Reject H_0
	Rainfall - CHIRPS	0.156	0.876	Reject H_0

	FRP - MODIS	0.001	0.997	Reject H_0
	Fire foci - MODIS	-1.090	0.276	Reject H_0
November	XCO MERRA	1.246	0.213	Reject H_0
	XCO_2 GOSAT	-0.778	0.436	Reject H_0
	XCH_4 GOSAT	-0.156	0.876	Reject H_0
	SIF GOSAT	-1.253	0.210	Reject H_0
	EVI - MODIS	-2.436	0.049	Reject H_0
	Rainfall - CHIRPS	0.934	0.350	Reject H_0
	FRP - MODIS	-0.311	0.755	Reject H_0
	Fire foci - MODIS	-0.779	0.436	Reject H_0
December	XCO MERRA	1.401	0.162	Reject H_0
	XCO_2 GOSAT	1.401	0.161	Reject H_0
	XCH_4 GOSAT	0.001	0.999	Reject H_0
	SIF GOSAT	-0.311	0.755	Reject H_0
	EVI - MODIS	0.183	0.855	Reject H_0
	Rainfall - CHIRPS	0.0001	0.9991	Reject H_0
	FRP - MODIS	-1.640	0.101	Reject H_0
	Fire foci - MODIS	-0.467	0.640	Reject H_0

Table S3. Entire Amazon Biome changing point detection of the average monthly for XCO, XCO_2 and FRP in the period from 2009 to 2019.

Months	Variables	Pettit's test	
		p-value	Change-point (year)
April	XCO MERRA	0.046	2014
	XCO_2 GOSAT	0.045	2014
	FRP - MODIS	0.042	2014
July	FRP - MODIS	0.045	2014

Appendix B. Supplementary material for chapter 3

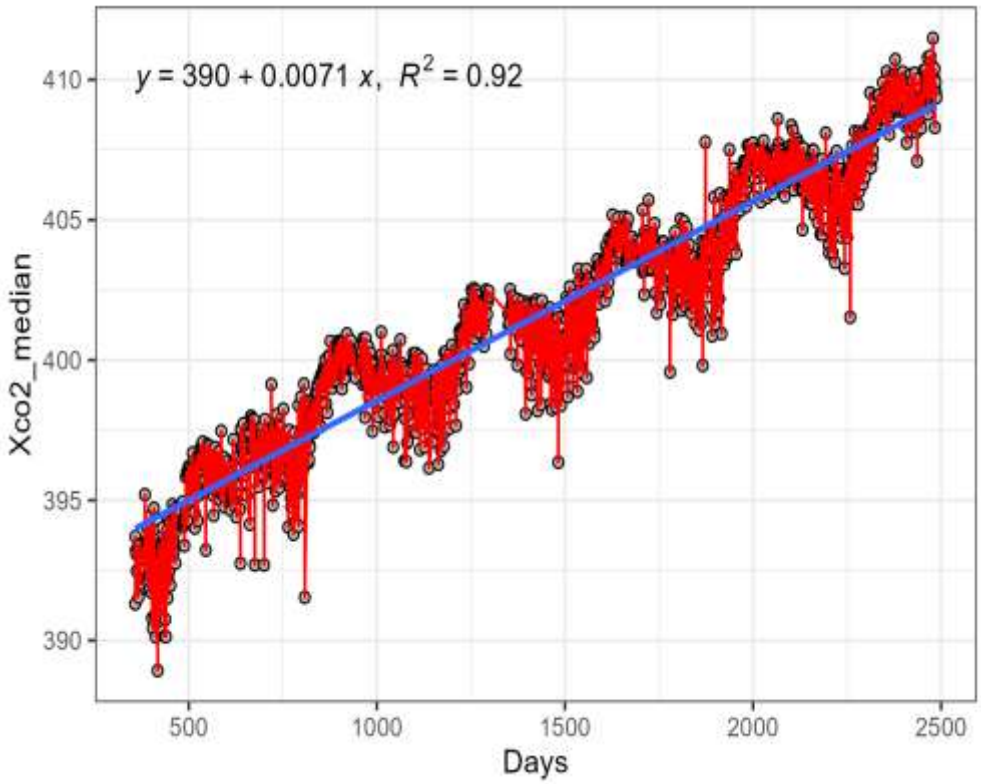

Figure 3.A1. The monotonic trend of XCO_2 concentration in the atmosphere of the Amazon biome for the time series from 2015 to 2020.

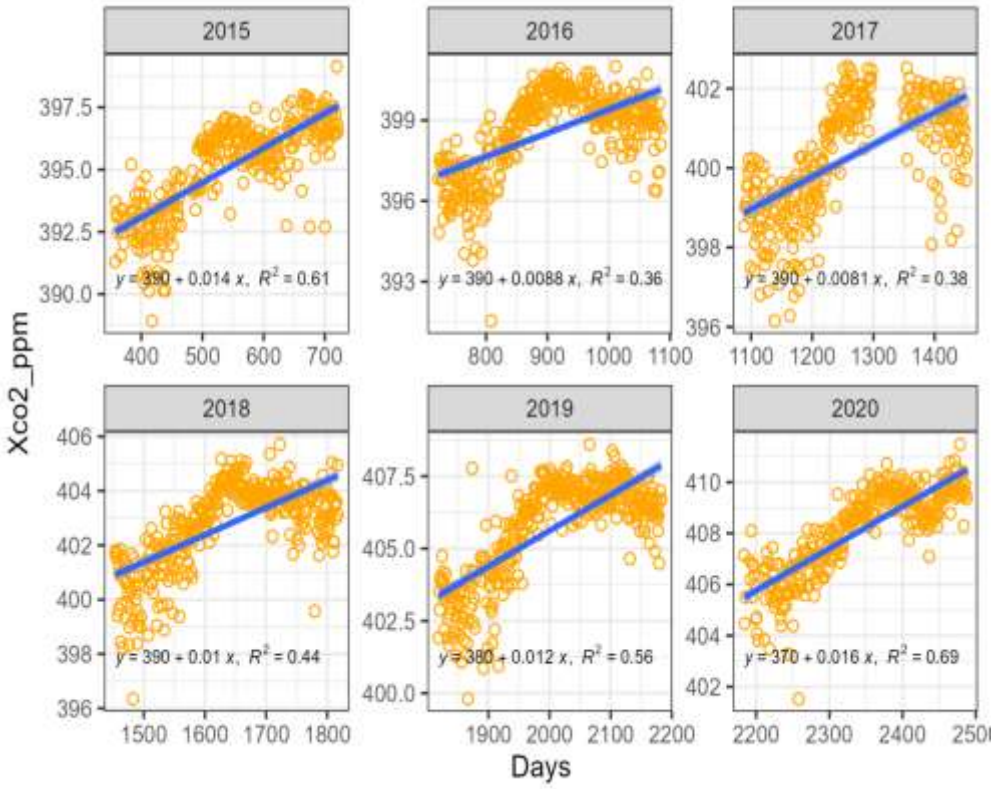

Figure 3.A2. Linear regression of XCO_2 (OCO-2) for time series from 2015 to 2020.